The CXTFIT Code for Estimating Transport Parameters from Laboratory or Field Tracer Experiments

Version 2. 0

by

N. Toride, F. J. Leij, and M. Th. van Genuchten

Research Report No. 137

August 1995

U. S. SALINITY LABORATORY
AGRICULTURAL RESEARCH SERVICE
U. S. DEPARTMENT OF AGRICULTURE
RIVERSIDE, CALIFORNIA

DISCLAIMER

This report documents version 2.0 of CXTFIT, a computer program for estimating solute transport parameters from observed concentrations (the inverse problem) or for predicting solute concentrations (the direct problem) using the convection-dispersion equation as the transport model. CXTFIT 2.0 is a public domain code, and as such may be used and copied freely. The code has been verified against a large number of test cases. However, no warranty is given that the program is completely error-free. If you do encounter problems with the code, find errors, or have suggestions for improvement, please contact one of the authors' at

U. S. Salinity Laboratory
USDA, ARS
450 West Big Springs Road
Riverside, CA 92507-46 17

Phone (909) 369-4850
Fax (909) 342-4964
e-mail titan@citrus.ucr.edu

'The senior author may be reached at: Dept. of Agricultural Sciences, Saga Univ., Saga 840, Japan. Phone: +81-952-24-5191; Fax: +81-952-22-6274; E-mail: nobuo@cc.saga-u.ac.jp.

ABSTRACT

N. Toride, F. J. Leij, and M. Th. van Genuchten. The CXTFIT Code for Estimating Transport Parameters from Laboratory or Field Tracer Experiments, Version 2.0, Research Report No. 137, U. S. Salinity Laboratory, USDA, ARS, Riverside, CA.

Successful predictions of the fate and transport of solutes in the subsurface hinges on the availability of accurate transport parameters. We modified and updated the CXTFIT code of **Parker and van Genuchten** [1984b] for estimating solute transport parameters using a nonlinear least-squares parameter optimization method. The program may be used to solve the inverse problem by fitting mathematical solutions of theoretical transport models, based upon the convection-dispersion equation (CDE), to experimental results. This approach allows parameters in the transport models to be quantified. The program may also be used to solve the direct or forward problem to determine the concentration as a function of time and/or position. Three different one-dimensional transport models are included: (i) the conventional CDE; (ii) the chemical and physical nonequilibrium CDE; and (iii) a stochastic stream tube model based upon the local-scale CDE with equilibrium or nonequilibrium adsorption. The two independent stochastic parameters in the stream-tube model are the pore-water velocity, v, and either the dispersion coefficient, D, the distribution coefficient, K_d, or the nonequilibrium rate parameter, a. These pairs of stochastic parameters were described with a bivariate lognormal probability density function (pdf). Examples are given on how transport parameters may be determined from laboratory or field tracer experiments for several types of initial and boundary conditions, as well as different zero-order production profiles. A detailed description is provided of the computer program, including the subroutines used to evaluate the analytical solutions for optimizing model parameters. Input and output files for all major problems are included in this manual.

Keywords: Solute transport, parameter estimation, convection-dispersion equation, analytical solutions, nonequilibrium transport, stochastic transport, stream tube model.

TABLE OF CONTENTS

LIST OF FIGURES

LIST OF TABLES

LIST OF SYMBOLS

a	constant in Goldstein's J-function (Table 3.4)
A	area of a field [L^2]
A_k	auxiliary functions for the nonequilibrium BVP (eqs. 3.21-3.24, $k = 1,2$)
b	constant in Goldstein's J-function (Table 3.4)
c	volume-averaged or resident concentration of the liquid phase [ML^{-3}]
c_o	characteristic concentration for dimensionless parameters used in Tables 2.1 and 3.1 [ML^{-3}]
$c_o(t)$	time-dependent input concentration (eq. 4.6) [ML^{-3}]
$c_i(x)$	position-dependent initial concentration (eq. 4.5) [ML^{-3}]
C_k^B	dimensionless concentration of phase k for the BVP ($k = 1,2$)
C_f	dimensionless flux-averaged concentration (eq. 2.13)
C or C_r	dimensionless resident concentration
$C_i(Z)$	dimensionless initial concentration (eq. 2.8)
C_k^I	dimensionless concentration of phase k for the IVP ($k = 1,2$)
C_T	dimensionless total resident concentration (eqs. 2.12 or 3.12)
$C_o(T)$	dimensionless time dependent input concentration (eq. 2.9)
C_k^P	dimensionless concentration of phase k for the PVP ($k = 1,2$)
CV	coefficient of variation (eq. 4.12)
D	dispersion coefficient [L^2T^{-1}]
D_m	dispersion coefficient of the mobile liquid phase [L^2T^{-1}]
erfc(t)	complementary error function; $\mathrm{erfc}(t) = \dfrac{2}{\sqrt{\pi}} \displaystyle\int_0^t e^{-u^2} du$
f	fraction of exchange sites assumed to be at equilibrium for the two-site model (eq. 3.1); fraction of adsorption sites that equilibrates with the mobile liquid phase for the two-region model (eq. 3.3)
$f(\eta)$	probability density function (pdf) for η (either D, K_d, or α) defined by eq. 4.15
$f(v,\eta)$	joint probability density function (pdf) for v and η as defined by eq. 4.8
$f(Z,T)$	travel time probability density function for the nonequilibrium CDE defined by eq. 3.15
f_i	input concentrations for the BVP (eq. 2.19; $i = 1,2,...,n$)
G_i^E	auxiliary functions for equilibrium transport (Table 2.3, $i = 1,2$)
G_1^N	auxiliary functions for nonequilibrium transport (Table 3.3)
$H_i(\tau,T)$	auxiliary expressions with Bessel functions for nonequilibrium transport (Table 3.4; $i = 0,1$)
I_0, I_1	modified Bessel function of orders zero and one, respectively

J	Goldstein's J-function (Table 3.4)
J_w	volumetric water flux density [LT^{-1}]
K_d	distribution coefficient for linear adsorption [$M^{-1}L^3$]
L	characteristic length (Tables 2.1 and 3.1) [L]
m_B	amount of mass added to unit area of solution phase (eq. 2.16b or 4.22) [ML^{-2}]
m_I	amount of mass present per unit soil area for a Dirac initial distribution (eq. 2.24b or 4.23) [ML^{-2}]
M_B	dimensionless amount of applied solute for a Dirac input (eq. 2.16a or 3.16)
M_I	dimensionless amount of solute present per unit soil area for a Dirac initial distribution (eq. 2.24a or 3.33)
p	variable in nonequilibrium solution for exponential input function (eq. 3.30a)
P	Peclet number (Tables 2.1 and 3.1) [-]
q	variable in nonequilibrium solution for exponential input function (eq. 3.30b)
R	retardation factor (eq. 2.4, Tables 2.1 and 3.1) [-]
s	concentration of the adsorbed phase [MM^{-1}]
t	time [T]
T	dimensionless time (Tables 2.1 and 3.1)
T_i	dimensionless times for multiple pulse input (eq. 2.19; $i = 1,2,...,n$)
U_i	initial concentrations for the IVP (eq. 2.26; $i = 1,2,...,n$)
v	average pore-water velocity [LT^{-1}]
$Var[...]$	variance (eqs. 4.20 or 4.21)
x	distance [L]
Y_v, Y_η	variables in lognormal distribution (eq. 4.10)
Z	dimensionless distance (Tables 2.1 and 3.1)
Z_i	dimensionless distances for stepwise initial or production distribution (eq. 2.26 or 2.31; $i = 1,2,...,n$)
$Z_{k,i}$	dimensionless distances for stepwise production distribution in phase k during nonequilibrium transport (eq. 3.36; $k = 1,2$; $i = 1,2,...,n$)

Greek

α	first-order kinetic rate coefficient (eq. 3.1-3.4) [T^{-1}]
β	dimensionless variable for partitioning in nonequilibrium transport models (Table 3.1)
γ	zero-order production term (eq. 2.6) [$ML^{-3}T^{-1}$]
γ^E	dimensionless zero-order production terms for equilibrium transport (Table 2.1)
γ_i	dimensionless production constants for the PVP (eq. 2.31; $i = 1,2,...,n$)
γ_k	dimensionless zero-order production terms for nonequilibrium transport (Table 3.1)
$\gamma_{k,i}$	dimensionless production constants for the PVP in phase k (eq. 3.45; $k = 1,2$; $i = 1,2,...,n$)
γ_ℓ	zero-order production term for the liquid phase (eqs. 3.1 and 4.1; Table 3.1) [$ML^{-3}T^{-1}$]
$\gamma_{\ell,m}, \gamma_{\ell,im}$	zero-order production term for the mobile and immobile liquid phases, respectively (Table 3.1) [$ML^{-3}T^{-1}$]
γ_s	zero-order production term for the adsorbed phase (eq. 4.2) [$MM^{-1}T^{-1}$]
$\gamma_{s,e}$	zero-order production term for the equilibrium adsorbed phase (eq. 3.1) [$MM^{-1}T^{-1}$]
$\gamma_{s,k}$	zero-order production term for the kinetically adsorbed phase (eq. 3.2) [$MM^{-1}T^{-1}$]
$\gamma_{s,m}$	zero-order production term for the mobile adsorbed phase (eq. 3.3) [$ML^{-3}T^{-1}$]
$\gamma_{s,m}, \gamma_{s,im}$	zero-order production term for the immobile adsorbed phase (eq. 3.4) [$ML^{-3}T^{-1}$]
$\Gamma(n)$	Gamma function; $\Gamma(n) = \int_0^\infty u^{n-1} e^{-u} du$
Γ_i^E	auxiliary functions for equilibrium transport (Table 2.2; $i = 1,2$)
Γ_i^N	auxiliary functions for nonequilibrium transport (Table 3.2; $i = 1,2$)
δ	Dirac delta function (eq. 2.16 or 2.24)
θ	volumetric water content (eq. 2.1) [L^3L^{-3}]
θ_m, θ_{im}	volumetric water contents of mobile and immobile liquid phases (eq. 3.3 and 3.4; $\theta = \theta_m + \theta_{im}$) [$L^3L^{-3}$]
λ	dispersivity eq. 4.25 [L]
λ^B	dimensionless constant for exponential input (eqs. 2.21 and 3.25)
λ^I	dimensionless constant for exponential initial distribution (eqs. 2.28 and 3.39)
λ^P	dimensionless constant for exponential production profile (eq. 2.35)
λ_k^P	dimensionless constant for exponential production profile in phase k (eq. 3.49; $k = 1,2$)
μ_v, μ_η	mean of logtransformed v and η (D, K_d, or α), respectively
μ	first-order decay coefficient (eq. 2.5) [T^{-1}]
μ^E	dimensionless first-order decay coefficient for equilibrium transport (Table 2.1)
μ_k	dimensionless first-order decay coefficient for phase k (Table 3.1; $k = 1,2$)
$\mu_{\ell,m}, \mu_{\ell,im}$	first-order decay coefficients for the mobile and immobile liquid phases, respectively (eqs. 3.3 and 3.4) [T^{-1}]

μ_ℓ	first-order decay coefficient for the liquid phase (eq. 3.1) [T^{-1}]
μ_s	first-order decay coefficient for the adsorbed phase (eq. 4.2) [T^{-1}]
$\mu_{s,m}, \mu_{s,im}$	first-order decay coefficients for the mobile and immobile adsorbed phases, respectively (eqs. 3.3 and 3.4) [T^{-1}]
$\mu_{s,e}, \mu_{s,k}$	first-order decay coefficient for phase with equilibrium and kinetic adsorption, respectively (eqs. 3.1 and 3.2) [T^{-1}]
ρ_b	bulk density (2.1) [ML^{-3}]
$\rho_{v\eta}$	correlation coefficient between Y_v and Y_η (eq. 4.11; $\eta = D$, K_d, or α)
σ_v, σ_η	standard deviation of the logtransform of v and η, respectively (eq. 4.9; $\eta = D$, K_d, or α)
ϕ_m	fraction of mobile water (Table 3.5) [-]
Φ_k	auxiliary functions in solution for nonequilibrium transport involving an exponential input (eqs. 3.28 and 3.29; $k = 1,2$)
ψ_i^E	auxiliary functions for equilibrium transport (Table 2.2; $i = 1,2$)
ψ_i^N	auxiliary functions for nonequilibrium transport (Table 3.2; $i = 1,2$)
ω	dimensionless mass transfer coefficient (Table 3.1)

Subscripts

D	stochastic dispersion coefficient
e	equilibrium
f	flux-averaged
im	immobile phase
k	kinetic
Kd	stochastic distribution coefficient
ℓ	liquid phase
m	mobile phase
r	resident (volume averaged)
s	adsorbed phase
T	total (resident)
v	stochastic pore-water velocity
α	stochastic first-order kinetic rate coefficient
η	stochastic transport parameter (D, K_d, or α)
1	phase 1 (equilibrium phase)
2	phase 2 (nonequilibrium phase)

Superscripts

B   boundary value problem

E   equilibrium

I   initial value problem

N   nonequilibrium

P   production value problem

Special Symbols

$<...>$ ensemble average (eq. 4.11)

$\hat{\ }$ field-scale concentration defined by (eq. 4.16)

Abbreviations

CDE   convection-dispersion equation

BTC   breakthrough curve

BVP   boundary value problem

EC   electrical conductivity

IVP   initial value problem

pdf   probability density function

PVP   production value problem

TDR   time-domain reflectometry

1. INTRODUCTION

The fate and movement of dissolved substances in soils and groundwater has generated considerable interest out of concern for the quality of the subsurface environment. The behavior of solutes over relatively long spatial and temporal scales has to be assessed with the help of theoretical models since it is usually not feasible to carry out experimental studies over sufficiently long distances and/or time periods. Mathematical models are often used to predict solute concentrations before management strategies are implemented. Advances in software and hardware now permit the simulation of subsurface transport using sophisticated mathematical models. Unfortunately, it is generally diicult to obtain reliable values for transport parameters such as the pore-water velocity, the retardation factor, the dispersion coefficient, and degradation or production parameters.

The program CXTFIT 2.0 may be used to estimate parameters in several models for transport during steady one-dimensional flow by fitting the parameters to observed laboratory or field data obtained from solute displacement experiments. The inverse problem is solved by minimizing an objective function, which consists of the sum of the squared differences between observed and fitted concentrations. The objective function is minimized using a nonlinear least-squares inversion method according to *Marquardt*

to predict solute distributions versus time and/or space for specified model parameters.

CXTFIT 2.0 is an extension and update of an earlier version program published more than ten years ago by *Parker and van Genuchten* [1984b]. The new CXTFIT, version 2.0, again uses the convection-dispersion equation, but with a greater number of analytical solutions to various initial, boundary, and production value problems. The nonequilibrium transport models now contains also terms for zero-order production and first-order decay. Considerably more attention is being paid to the use of stream tube models for simulating transport in heterogenous fields, thus reflecting the growing popularity of stochastic approaches for modeling field-scale solute transport. A bivariate lognormal probability density function is used to quantify stochastic flow and either stochastic dispersion, adsorption, or nonequilibrium solute transfer. Solute concentrations across the field can be in the resident mode or in two different types of flux-averaged modes.

This report serves to document the CXTFIT 2.0 computer program. Equilibrium transport according to the convection-dispersion equation (CDE) is reviewed in Chapter 2. The mathematical

problem is first stated, and solutions for the initial value problem (IVP), the boundary value problem (BVP), and the production value problem (PVP) are listed. The program may be used to estimate the pore-water velocity (v), the dispersion coefficient (D), the retardation factor (R), the first-order degradation coefficient (μ), and/or the zero-order production coefficient (γ) from observed concentration distributions versus time and/or distance. Nonequilibrium transport is discussed in Chapter 3 in terms of alternative physical and chemical nonequilibrium models. Solutions of the (bimodal) dimensionless nonequilibrium transport equation are presented for the same cases as for equilibrium transport. In addition to v, $\boldsymbol{D, R,} \mu,$ and $\gamma,$ the coefficient of partitioning between the equilibrium and nonequilibrium phases (β) and the mass transfer coefficient (ω) for transfer between the two phases can now be fitted as well. Chapter 4 describes the stream tube model as a relatively simple conceptualization of solute transport in heterogeneous fields. Transport in each stream tube (the local scale) is described with the CDE as an initial or a boundary value problem. Pairs of stochastic parameters, one always being v, are used in solutions of the CDE. Transport at the field scale is subsequently modeled by averaging the local concentrations.

Chapter 5 provides details about the numerical evaluation of some of the analytical functions, including the numerical integration procedures. This chapter also gives an outline of the parameter estimation procedure. Chapter 6 serves as user's guide for the program. This chapter lists all available transport models and gives instructions on how to solve the inverse problem. All possible variables in the input file are documented in terms of separate blocks. The blocks pertain to model selection, solution of the inverse problem definition of transport parameters, stipulation of boundary, initial, as well as production conditions, and specification of times and positions for which the direct problem is to be solved. Examples of input and output files are also provided. The examples are those given on the diskette accompanying this manual. Finally, Chapter 7 illustrates the use of CXTFIT 2.0 for several forward and inverse problems.

2. DETERMINISTIC EQUILIBRIUM CDE

2.1. Transport Model

The convection-dispersion equation (CDE) for one-dimensional transport of reactive solutes, subject to adsorption, first-order degradation, and zero-order production, in a homogeneous soil, is written as

$$\frac{\partial}{\partial t}\left(\theta c_r + \rho_b s\right) = \frac{\partial}{\partial x}\left(\theta D \frac{\partial c_r}{\partial x} - J_w c\right) - \theta \mu_\ell c_r - \rho_b \mu_s s + \theta \gamma_\ell(x) + \rho_b \gamma_s(x) \tag{2.1}$$

where c_r is the volume-averaged or resident concentration of the liquid phase (ML^{-3}), s is the concentration of the adsorbed phase (MM^{-1}), D is the dispersion coefficient ($L^2 T^{-1}$), θ is the volumetric water content ($L^3 L^{-3}$), J_w is the volumetric water flux density (LT^{-1}), ρ_b is the soil bulk density (ML^{-3}), μ_ℓ and μ_s are first-order decay coefficients for degradation of the solute in the liquid and adsorbed phases, respectively (T^{-1}); γ_ℓ ($ML^{-3}T^{-1}$) and γ_s ($MM^{-1}T^{-1}$) are zero-order production terms for the liquid and adsorbed phases, respectively; x is distance (L), and t is time (T). We assume that μ cannot be negative. Note that the production functions are given as a function of distance.

Solute adsorption by the solid phase is described with a linear isotherm as

$$s = K_d c_r \tag{2.2}$$

where K_d is an empirical distribution constant ($M^{-1}L^3$). Using (2.2) and assuming steady-state flow in a homogeneous soil, (2.1) may be rewritten as

$$R\frac{\partial c_r}{\partial t} = D\frac{\partial^2 c_r}{\partial x^2} - v\frac{\partial c_r}{\partial x} - \mu c_r + \gamma(x) \tag{2.3}$$

where v ($= J_w/\theta$) is the average pore-water velocity, R is the retardation factor given by

$$R = 1 + \frac{\rho_b K_d}{\theta} \tag{2.4}$$

and μ and γ are combined first- and zero-order rate coefficients:

$$\mu = \mu_\ell + \frac{\rho_b K_d \mu_s}{\theta} \tag{2.5}$$

$$\gamma(x) = \gamma_\ell(x) + \frac{\rho_b \gamma_s(x)}{\theta} \tag{2.6}$$

3

Note that when the first-order degradation coefficients in the liquid (μ_ℓ) and adsorbed (μ_s) phases are identical, (2.5) reduces to $\mu = \mu_\ell R$ (Section 4.1).

Table 2.1 lists the dimensionless parameters that allow (2.3) to be written in reduced form as

$$R\frac{\partial C_r}{\partial T} = \frac{1}{P}\frac{\partial^2 C_r}{\partial Z^2} - \frac{\partial C_r}{\partial Z} - \mu^E C_r + \gamma^E(Z) \tag{2.7}$$

where C_r is the reduced volume-averaged solute concentration, P is the Peclet number, μ^E is a first-order decay coefficient ($= L\mu/v$), γ^E is a zero-order production coefficient for equilibrium transport ($= L\gamma/vc_o$), and Z and T are the dimensionless space and time variables, respectively.

Table 2.1. Dimensionless Parameters for the Equilibrium CDE†

Parameters	T	Z	P	R	C	μ^E	γ^E
Expressions	$\dfrac{vt}{L}$	$\dfrac{x}{L}$	$\dfrac{vL}{D}$	$1 + \dfrac{\rho_b K_d}{\theta}$	$\dfrac{c}{c_o}$	$\dfrac{L(\theta\mu_\ell + \rho_b K_d \mu_s)}{\theta v}$	$\dfrac{L(\theta\gamma_\ell + \rho_b \gamma_s)}{\theta v c_o}$

† c_o and L represent a characteristic concentration and length, respectively.

2.2. Analytical Solutions

Solutions of the CDE will be presented in terms of the above dimensionless parameters. Dimensional solutions can be easily obtained by substituting the parameters listed in Table 2.1 back into the dimensionless solutions.

Resident Concentration

Analytical solutions of (2.7) are included in CXTFIT 2.0 for relatively simple initial and boundary conditions. The general initial condition is given by

$$C_r(Z,0) = C_i(Z) \tag{2.8}$$

where C_i is the initial concentration as a function of Z. Either a first- or a third-type condition is used for the inlet boundary, i.e.,

$$C_r(0,T) = C_o(T) \tag{2.9a}$$

4

or

$$C_r(0,T) - \frac{1}{P}\frac{\partial C_r(0,T)}{\partial Z} = C_o(T)$$ (2.9b)

where C_o is the input concentration as a function of T. The third-type boundary condition (2.9b) in terms of dimensional parameters is given as

$$vc_r(0,t) - D\frac{\partial c_r(0,t)}{\partial x} = vc_o(t)$$ (2.10)

where $c_o(t)$ represents a dimensional concentration that depends on real time, t. We will present solutions for both first- and third-type inlet conditions. Note that a third-type inlet condition is to be preferred for most transport scenarios since it conserves mass if we ignore dispersion outside the soil [*van Genuchten and Parker*, 1984; *Parker and van Genuchten*, 1984a; *van Genuchten and Parker*, 1994].

The outlet condition for an effectively semi-infinite system is given by

$$\frac{\partial C_r}{\partial Z}(\infty,T) = 0$$ (2.11a)

Although no "correct" outlet condition can probably be formulated for finite systems [*Parlange et al.*, 1992], a zero concentration gradient is often used for a finite system of length L:

$$\frac{\partial C_r}{\partial Z}(1,T) = 0$$ (2.11b)

This condition is based on the assumption that the concentration is macroscopically continuous at the outlet and that no dispersion occurs outside the soil [*Danckwerts*, 1953; *Wehner and Wilhelm*, 1956]. Solutions for an infinite outlet condition can be applied to the finite region $0 \le x \le L$ by making the assumption that upstream solute concentrations are not affected by the outlet boundary [*Parker and van Genuchten*, 1984a]. All solutions in this report are based on the infinite outlet condition (2.11a).

In addition to the resident solution concentration, we define the total resident concentration as the amount of solute per unit volume of soil solution:

$$C_T = R C_r$$ (2.12)

Flux-averaged Concentration

The injection and detection modes for several solute displacement experiments may require the

5

use of flux-averaged or flowing concentrations in the mathematical model [*Kreft and Zuber*, 1978; *Parker and van Genuchten,* 1984a]. Flux-averaged concentrations are defined as the ratio of the solute and water fluxes; they occur, for example, if a solute breakthrough curve is determined from effluent samples. The specification of the type of concentration is discussed in Chapter 7.

For transport according to the CDE, the flux-averaged concentration can be obtained from the resident concentration using the transformation:

$$C_f = C_r - \frac{1}{P} \frac{\partial C_r}{\partial Z} \tag{2.13}$$

where the subscript f refers to a flux-averaged concentration. Expressions for C_f are easily derived by substituting the solution for C_r for a third-type inlet condition into (2.13). We may drop the subscript of C if the difference between the two concentration modes is immaterial or if it is clear that we refer to a resident concentration.

Superposition

Since the governing equations and the initial and boundary conditions are linear in C, the superposition principle — as explained, for example, in *Farlow* [1982] -- may be used to express the analytical solution as the sum of three independent subproblems involving a boundary value problem (BVP), an initial value problem (IVP), and a production value problem (PVP). The overall solution can then be written as

$$C(Z,T) = C^B(Z,T) + C^I(Z,T) + C^P(Z,T) \tag{2.14}$$

where the superscripts B, I and P denote the boundary, initial, and production value problems, respectively. We first present the general solution to each subproblem, subsequently we give several specific solutions.

2.2.1. Boundary Value Problem (BVP)

General Solution

The general solution of the BVP is given by

$$C^B(Z,T) = \int_0^T C_o(T-\tau)\, \Gamma_1^E(Z,\tau)\, d\tau \tag{2.15}$$

where the auxiliary function Γ_1^E is defined in Table 2.2. Note that Γ_1^E is identical for C_f and C_r if a first-type inlet condition is used. General expression (2.15) will be used to obtain specific solutions for an input concentration, $C_o(T)$, given by Dirac delta, multiple pulse, and exponential functions.

Specific Solution

1. **Dirac Delta Input.** For instantaneous solute application, $C_o(T)$ may be written as

$$C_o(T) = M_B\, \delta(T) \tag{2.16a}$$

where $\delta(T)$ is the Dirac delta (unit impulse) function, and M_B is a dimensionless amount of applied solute. A dimensional Dirac delta input may be given by

$$c_o(t) = \frac{m_B}{v}\, \delta(t) \tag{2.16b}$$

where $\delta(t)$ is a Dirac function with respect to t (T^{-1}), and m_B is the total amount of mass added to a unit area of the soil liquid phase (ML^{-2}). The dimensional and dimensionless Dirac inlet conditions are related as $\delta(T) = L\delta(t)/v$, with $M_B = m_B/(Lc_o)$. The following properties of the Dirac delta function were used to evaluate the general solution:

$$\int_0^\infty \delta(t)\, dt = 1 \tag{2.17a}$$

and, for any continuous function $G(t)$,

$$\int_0^\infty \delta(t)\, G(t)\, dt = G(0) \tag{2.17b}$$

$$\int_0^\infty \delta(t-a)\, G(t)\, dt = G(a) \tag{2.17c}$$

7

Substitution of (2.16a) into (2.15) leads to

$$C^B(Z,T) = M_B \Gamma_1^E(Z,T) \qquad (2.18)$$

This solution is sometimes referred to as the travel time probability density function (pdf) for the equilibrium CDE [*Jury and Roth*, 1990].

2. Multiple Pulse Input Conditions. The input concentration for a series of successive applications of rectangular (constant) solute pulses, as illustrated in Figure 2.1, can be expressed as

$$C_o(T) = f_i \qquad T_i \le T < T_{i+1}$$
$$(i=1,2,...,n \; ; \; T_1=0 \text{ and } T_{n+1} \to \infty) \qquad (2.19)$$

where f_i ($i = 1,2,...,n$) is constant. The analytical solution for this case may be written as the following sum of the solutions for the individual pulses:
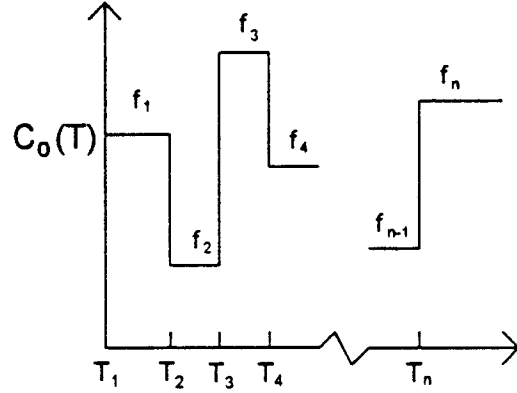
Figure 2.1. Multiple pulse input.

$$C^B(Z,T) = \sum_{j=1}^{i} (f_j - f_{j-1}) \, G_1^E(Z,T-T_j;\mu^E) \qquad (i = 1,2,...,n; f_o = 0) \qquad (2.20)$$

where $G_1^E(Z,T;\mu^E)$ is listed in Table 2.3. Note that the formulations for $G_1^E(Z,T;\mu^E)$ for $\mu^E = 0$ and $\mu^E \ne 0$ are different [*van Genuchten and Alves*, 1982].

3. Exponential Input Function. The exponential input concentration function is given by

$$C_o(T) = f_1 + f_2 \exp(-\lambda^B T) \qquad (2.21)$$

where f_1, f_2, and λ^B are constants. Substitution of (2.21) into (2.15), and integration, yields

$$C^B(Z,T) = f_1 \, G_1^E(Z,T;\mu^E) + f_2 \exp(-\lambda^B T) G_1^E(Z,T;\mu^E - R\lambda^B) \qquad (2.22)$$

where $G_1^E(Z,T;\Omega)$ is again given in Table 2.3. In this solution, a distinction needs to be made between $\Omega = 0$ (i.e., $\mu^E = R\lambda^B$) and $\Omega \ne 0$. Furthermore, when $\lambda^B > (\mu^E + P/4)/R$, it is necessary to evaluate the general expression for $G_1^E(Z,T)$ numerically since the parameter u in Table 2.3 becomes complex. CXTFIT 2.0 internally selects the appropriate expression for $G_1^E(Z,T)$.

2.2.2. Initial Value Problem (IVP)

General Solution

The general solution of the IVP is given by

$$C^I(Z,T) = \int_0^\infty C_i(\eta) \Gamma_2^E(Z,\eta,T) d\eta \qquad (2.23)$$

where $\Gamma_2^E(Z,\eta,\tau)$ is listed in Table 2.2. Specific solutions of the IVP are obtained for the same type of $C_i(Z)$ functions as for $C_o(T)$ in the BVP as discussed in the previous section, i.e., Dirac delta, stepwise, and exponential initial distributions.

Specific Solution

1. *Dirac Delta Initial Distribution.* When all of the solute is initially located at position $Z = Z_1$, the initial concentration distribution $C_i(Z)$ may be written as

$$C_i(Z) = M_I \delta(Z - Z_1) \qquad (2.24a)$$

where $\delta(Z)$ is the Dirac delta function, and M_I is a relative amount of solute in the liquid phase. For a dimensional distance, x, the Dirac initial condition may be given by

$$c_i(x) = \frac{m_I}{\theta} \delta(x - x_1) \qquad (2.24b)$$

where $\delta(x)$ is the Dirac function with respect to x [L^{-1}], and m_I is the amount of mass initially present in the liquid phase per unit area of soil [ML^{-2}] at $x = x_1$. The total amount of mass per unit soil area is given by $m_I R$. Dimensional and dimensionless initial conditions are related according to $\delta(Z) = L\delta(x)$ with $M_I = m_I/(\theta L c_o)$. Substitution of (2.24a) into (2.23) yields

$$C^I(Z,T) = M_I \Gamma_2^E(Z,Z_1,T) \qquad (2.25)$$

Notice that for a third-type inlet condition, the resident concentration according to (2.25) for $Z_1 = 0$ in (2.24a) — i.e., solutes reside initially at the soil surface — is identical to solution (2.18) for the BVP with a Dirac input since $\Gamma_1^E(Z,T) = \Gamma_2^E(Z,Z_1=0,T)$ in Table 2.2.

9

2. _Stepwise Initial Distribution._ A stepwise initial concentration distribution, consisting of n step functions, may be written in the form where

$$C_i(Z) = U_i \qquad Z_i \leq Z < Z_{i+1}$$

$$(i=1,2,...,n; \ Z_1 = 0 \text{ and } Z_{n+1} \to \infty) \qquad (2.26)$$

U_i is a constant. Figure 2.2 shows an example of such a stepwise initial concentration distribution. The analytical solution can again be written as the sum of solutions of the IVP for a single pulse:

where ψ_1^E is listed in Table 2.2 [cf. A5 and A6
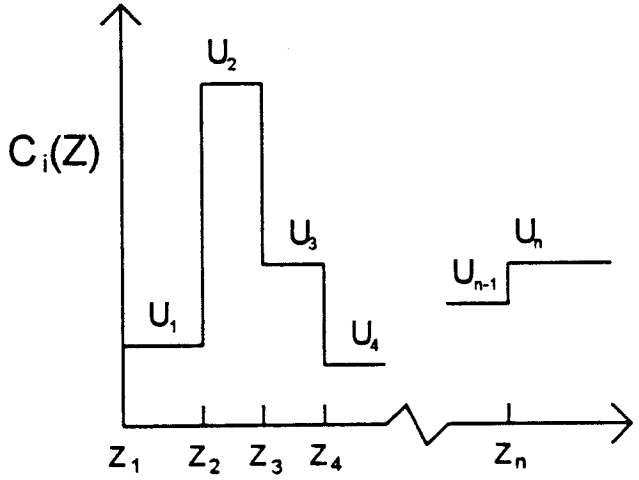
Figure 2.2. Stepwise initial distribution.

$$C^I(Z,T) = \sum_{i=1}^{n} (U_i - U_{i-1}) \ \psi_1^E(Z,T;Z_i) \qquad (2.27)$$

$$(i = 1,2,...,n; U_0 = 0)$$

of _van Genuchten and Alves_, 1982]. For a uniform initial concentration (i.e., $n = 1$; $C_i = U_1$ for $0 \leq Z < \infty$), the expression for C_f is identical to that of C_r for a first-type inlet condition [_Parker and van Genuchten_, 1984b; _Toride et al._, 1993a, 1993b].

3. _Exponential Initial Distribution._ The IVP can also be solved for an initial condition that changes exponentially with distance:

$$C_i(Z) = U_1 + U_2 \exp(-\lambda^I Z) \qquad (2.28)$$

where U_1, U_2, and λ^I are constants. The specific solution for this condition is given by [cf. A7 and A8 of _van Genuchten and Alves_, 1982]:

$$C^I(Z,T) = U_1 \ \psi_1^E(Z,T;0) + U_2 \ \psi_2^E(Z,T;\lambda^I) \qquad (2.29)$$

where ψ_1^E and ψ_2^E are listed in Table 2.2.

2.2.3. Production Value Problem (PVP)

General Solution

The solution for a depth-dependent production, $\gamma(Z)$, is [*Lindstrom and Boersma*, 1989]:

$$C^P(Z,T) = \frac{1}{R} \int_0^T \int_0^\infty \gamma^E(\eta) \, \Gamma_2^E(Z,\eta,\tau) \, d\eta \, d\tau \qquad (2.30)$$

where Γ_2^E is listed in Table 2.2. This solution is quite similar as (2.23) for the IVP. Specific solutions of the PVP for stepwise and exponential profiles can be obtained by integrating with respect to time.

Specific Solution

1. *Stepwise Production Profile.* Solute production having a distribution of n distinct steps is given as

$$\gamma^E(Z) = \gamma_i \qquad Z_i \le Z < Z_{i+1} \quad (i = 1,2,...,n \, ; \, Z_1 = 0 \text{ and } Z_{n+1} \to \infty) \qquad (2.31)$$

where γ_i is a constant. Inserting (2.31) into (2.30) and integrating with respect to η yields

$$C^P(Z,T) = \frac{1}{R} \int_0^T \sum_{i=1}^n (\gamma_i - \gamma_{i-1}) \psi_1^E(Z,\tau; Z_i) \, d\tau \qquad (i=1,2,...,n \, ; \gamma_0 = 0) \qquad (2.32)$$

where the expression for ψ_1^E is given in Table 2.2. For uniform solute production throughout the soil profile ($n = 1$), (2.32) reduces to

$$C^P(Z,T) = \frac{\gamma_1}{R} \int_0^T \psi_1^E(Z,\tau; Z_1 = 0) \, d\tau \qquad (2.33)$$

This expression can be readily integrated by parts. If $\mu^E \neq 0$, the concentration as a result of uniform solute production becomes [cf. A5 and A6 of *van Genuchten and Alves*, 1982]:

$$C^P(Z,T) = \frac{\gamma_1}{\mu^E} \left[1 - \psi_1^E(Z,T;0) - G_1^E(Z,T;\mu^E) \right] \qquad (2.34)$$

where ψ_1^E and $G_1^E(Z,T)$ are given in Tables 2.2 and 2.3, respectively. For $\mu^E = 0$, the solution is [cf. B5 and B6 of *van Genuchten and Alves*, 1982]:

11

$$C^P(Z,T) = \gamma_1 \, G_2^E(Z,T) / R \qquad\qquad (2.3\,5)$$

where $G_2^E(Z,T)$ is given in Table 2.3.

2. *Exponential Production Profile.* Solute production can be expressed as an exponential function in a manner similar as for the IVP:

$$\gamma^E(Z) = \gamma_1 + \gamma_2 \exp\left(-\lambda^P Z\right) \qquad\qquad (2.36)$$

where γ_1, γ_2, and λ^P are constants. The solution is now given by

$$C^P(Z,T) = \frac{1}{R} \int_0^T \gamma_1 \, \psi_1^E(Z,\tau;0) + \gamma_2 \, \psi_2^E(Z,\tau;\lambda^P) \, d\tau$$

$$= \begin{cases} \dfrac{\gamma_1}{\mu^E}\left[1 - \psi_1^E(Z,T;0) - G_1^E(Z,T;\mu^E)\right] & (\mu^E > 0) \\[2ex] \qquad + \dfrac{\gamma_2}{R} \displaystyle\int_0^T \psi_2^E(Z,\tau;\lambda^P) d\tau & \\[3ex] \dfrac{\gamma_1}{R} G_2^E(Z,T) + \dfrac{\gamma_2}{R} \displaystyle\int_0^T \psi_2^E(Z,\tau;\lambda^P) d\tau & (\mu^E = 0) \end{cases} \qquad (2.37)$$

where ψ_1^E and ψ_2^E are given in Table 2.2, while $G_1^E(Z,T,\Omega)$ and $G_2^E(Z,T)$ are defined in Table 2.3.

Table 2.2. Expressions for Γ^E and ψ^E in the Solutions for the Resident and Flux-Averaged Concentrations of the Equilibrium CDE

Function	Resident Concentration, C_r		Flux-averaged Concentration, C_f
	First-Type	Third-Type	
$\Gamma_1^E(Z,\tau)$	$\exp\left(-\frac{\mu^E\tau}{R}\right)\sqrt{\frac{RPZ^2}{4\pi\tau^3}}\exp\left[-\frac{P(RZ-\tau)^2}{4R\tau}\right]$	$\exp\left(-\frac{\mu^E\tau}{R}\right)\left\{\sqrt{\frac{P}{\pi R\tau}}\exp\left[-\frac{P(RZ-\tau)^2}{4R\tau}\right] - \frac{P}{2R}\exp(PZ)\,\text{erfc}\left(\frac{RZ+\tau}{\sqrt{4R\tau/P}}\right)\right\}$	$\exp\left(-\frac{\mu^E\tau}{R}\right)\sqrt{\frac{RPZ}{4\pi\tau^3}}\exp\left[-\frac{P(RZ-\tau)^2}{4R\tau}\right]$
$\Gamma_2^E(Z,\eta,\tau)$	$\exp\left(-\frac{\mu^E\tau}{R}\right)\sqrt{\frac{RP}{4\pi\tau}}\left\{\exp\left[-\frac{P[R(\eta-Z)+\tau]^2}{4R\tau}\right] - \exp(PZ)\exp\left[-\frac{P[R(\eta+Z)+\tau]^2}{4R\tau}\right]\right\}$	$\exp\left(-\frac{\mu^E\tau}{R}\right)\left\{\sqrt{\frac{RP}{4\pi\tau}}\exp\left[-\frac{P[R(\eta-Z)+\tau]^2}{4R\tau}\right] + \sqrt{\frac{RP}{4\pi\tau}}\exp(PZ)\exp\left[-\frac{P[R(\eta+Z)+\tau]^2}{4R\tau}\right] - \frac{P}{2}\exp(PZ)\,\text{erfc}\left[\frac{R(\eta+Z)+\tau}{\sqrt{4R\tau/P}}\right]\right\}$	$\exp\left(-\frac{\mu^E\tau}{R}\right)\sqrt{\frac{RP}{4\pi\tau}} \times \left\{\left[1-\frac{R(\eta-Z)+\tau}{2\tau}\right]\exp\left[-\frac{P[R(\eta-Z)+\tau]^2}{4R\tau}\right] - \left[1-\frac{R(\eta+Z)+\tau}{2\tau}\right]\exp(PZ)\exp\left[-\frac{P[R(\eta+Z)+\tau]^2}{4R\tau}\right]\right\}$
$\psi_1^E(Z,\tau,Z_i)$	$\exp\left(-\frac{\mu^E\tau}{R}\right)\left\{1-\frac{1}{2}\text{erfc}\left[\frac{R(Z-Z_i)-\tau}{\sqrt{4R\tau/P}}\right] - \frac{1}{2}\exp(PZ)\,\text{erfc}\left[\frac{R(Z+Z_i)+\tau}{\sqrt{4R\tau/P}}\right]\right\}$	$\exp\left(-\frac{\mu^E\tau}{R}\right)\left\{1-\frac{1}{2}\text{erfc}\left[\frac{R(Z-Z_i)-\tau}{\sqrt{4R\tau/P}}\right] - \sqrt{\frac{P\tau}{\pi R}}\exp\left[PZ-\frac{P[R(Z+Z_i)+\tau]^2}{4R\tau}\right] + \frac{1}{2}\left[1+P(Z+Z_i)+\frac{P\tau}{R}\right]\exp(PZ)\,\text{erfc}\left[\frac{R(Z+Z_i)+\tau}{\sqrt{4R\tau/P}}\right]\right\}$	$\frac{1}{2}\exp\left(-\frac{\mu^E\tau}{R}\right)\left\{2-\text{erfc}\left[\frac{R(Z-Z_i)-\tau}{\sqrt{4R\tau/P}}\right] - \exp(PZ) \times \text{erfc}\left[\frac{R(Z+Z_i)+\tau}{\sqrt{4R\tau/P}}\right] - \sqrt{\frac{R}{\pi P\tau}}\exp\left[-\frac{P[R(Z-Z_i)-\tau]^2}{R\tau}\right] + \sqrt{\frac{R}{\pi P\tau}}\exp(PZ)\exp\left[-\frac{P[R(Z+Z_i)+\tau]^2}{4R\tau}\right]\right\}$
$\psi_2^E(Z,\tau,\lambda)$	$\frac{1}{2}\exp\left(-\frac{\mu^E\tau}{R}+\frac{\lambda^2\tau}{RP}+\frac{\lambda\tau}{R}-\lambda Z\right) \times \left\{2-\text{erfc}\left[\frac{RZ-(1+2\lambda/P)\tau}{\sqrt{4R\tau/P}}\right] + \exp(PZ+2\lambda Z)\,\text{erfc}\left[\frac{RZ+(1+2\lambda/P)\tau}{\sqrt{4R\tau/P}}\right]\right\}$	$\exp\left(-\frac{\mu^E\tau}{R}+\frac{\lambda^2\tau}{RP}+\frac{\lambda\tau}{R}-\lambda Z\right)\left\{1-\frac{1}{2}\text{erfc}\left[\frac{RZ-(1+2\lambda/P)\tau}{\sqrt{4R\tau/P}}\right] + \frac{1}{2}\left(1+\frac{P}{\lambda}\right)\exp(PZ+2\lambda Z)\,\text{erfc}\left[\frac{RZ+(1+2\lambda/P)\tau}{\sqrt{4R\tau/P}}\right] - \frac{P}{2\lambda}\exp\left(-\frac{\mu^E\tau}{R}+PZ\right)\text{erfc}\left[\frac{RZ+\tau}{\sqrt{4R\tau/P}}\right]\right\}$	$\frac{1}{2}\left(1+\frac{\lambda}{P}\right)\exp\left(-\frac{\mu^E\tau}{R}+\frac{\lambda^2\tau}{RP}+\frac{\lambda\tau}{R}-\lambda Z\right) \times \left\{2-\text{erfc}\left[\frac{RZ-(1+2\lambda/P)\tau}{\sqrt{4R\tau/P}}\right] + \exp(PZ+2\lambda Z)\,\text{erfc}\left[\frac{RZ+(1+2\lambda/P)\tau}{\sqrt{4R\tau/P}}\right]\right\}$

Table 2.3. Expressions for $G^E(Z,T)$ in the Solutions for the Resident and Flux-Averaged Concentrations

G^E	C_r $\quad$ C_f First-Type	C_r Third-Type
General $G_1^E(Z,T;\Omega)$†	$\displaystyle\int_0^T \exp\left(-\frac{\Omega\tau}{R}\right)\frac{Z}{\tau}\sqrt{\frac{RP}{4\pi\tau}}\ \exp\left[-\frac{P(RZ-\tau)^2}{4R\tau}\right]d\tau$	$\displaystyle\int_0^T \exp\left(-\frac{\Omega\tau}{R}\right)\left\{\sqrt{\frac{P}{\pi R\tau}}\ \exp\left[-\frac{P(RZ-\tau)^2}{4R\tau}\right]\right.$ $\left.-\frac{P}{2R}\exp(PZ)\ \mathrm{erfc}\left(\frac{RZ+\tau}{\sqrt{4R\tau/P}}\right)\right\}d\tau$
for $\Omega=0$ $G_1^E(Z,T;0)$	$\displaystyle\frac{1}{2}\mathrm{erfc}\left(\frac{RZ-T}{\sqrt{4RT/P}}\right)+\frac{1}{2}\exp(PZ)\,\mathrm{erfc}\left(\frac{RZ+T}{\sqrt{4RT/P}}\right)$	$\displaystyle\frac{1}{2}\mathrm{erfc}\left(\frac{RZ-T}{\sqrt{4RT/P}}\right)+\sqrt{\frac{P}{\pi R}}\exp\left[-\frac{P(RZ-T)^2}{4RT}\right]$ $\displaystyle-\frac{1}{2}\left(1+PZ+\frac{PT}{R}\right)\exp(PZ)\,\mathrm{erfc}\left(\frac{RZ+T}{\sqrt{4RT/P}}\right)$
for $\Omega\neq0$ $(\Omega>-P/4)$ $G_1^E(Z,T;\Omega)$	$\displaystyle\frac{1}{2}\exp\left[\frac{P(1-u)Z}{2}\right]\mathrm{erfc}\left(\frac{RZ-uT}{\sqrt{4RT/P}}\right)$ $\displaystyle+\frac{1}{2}\exp\left[\frac{P(1+u)Z}{2}\right]\mathrm{erfc}\left(\frac{RZ+uT}{\sqrt{4RT/P}}\right)$	$\displaystyle\frac{1}{1+u}\exp\left[\frac{P(1-u)Z}{2}\right]\mathrm{erfc}\left(\frac{RZ-uT}{\sqrt{4RT/P}}\right)$ $\displaystyle+\frac{1}{1-u}\exp\left[\frac{P(1+u)Z}{2}\right]\mathrm{erfc}\left(\frac{RZ+uT}{\sqrt{4RT/P}}\right)$ $\displaystyle-\frac{2}{1-u^2}\exp\left[PZ+\frac{P(1-u^2)T}{4R}\right]\mathrm{erfc}\left(\frac{RZ+T}{\sqrt{4RT/P}}\right)$
	with $\quad u=\sqrt{1+\dfrac{4\Omega}{P}}$	
$G_2^E(Z,T)$	$\displaystyle T+\frac{RZ-T}{2}\mathrm{erfc}\left(\frac{RZ-T}{\sqrt{4RT/P}}\right)$ $\displaystyle-\frac{RZ+T}{2}\exp(PZ)\,\mathrm{erfc}\left(\frac{RZ+T}{\sqrt{4RT/P}}\right)$	$\displaystyle T+\frac{1}{2}\left(RZ-T+\frac{R}{P}\right)\mathrm{erfc}\left(\frac{RZ-T}{\sqrt{4RT/P}}\right)$ $\displaystyle-\sqrt{\frac{PT}{4\pi R}}\left(RZ+T+\frac{2R}{P}\right)\exp\left[-\frac{P(RZ-T)^2}{4RT}\right]$ $\displaystyle+\left[\frac{T}{2}-\frac{R}{2P}+\frac{P(RZ+T)^2}{4R}\right]\exp(PZ)\,\mathrm{erfc}\left(\frac{RZ+T}{\sqrt{4RT/P}}\right)$

† The integrals in $G_1^E(Z,T;\Omega)$ are evaluated numerically for $\Omega>-P/4$.

14

3. DETERMINISTIC NONEQUILIBRIUM CDE

3.1. Transport Model

Solute transport in the subsurface is affected by a variety of chemical and physical nonequilibrium processes [*Nielsen et al.*, 1986; *Aharoni and Sparks*, 1991]. Chemical nonequilibrium may occur as a result of kinetic adsorption while physical nonequilibrium is caused by a heterogeneous flow regime. Chemical nonequilibrium models consider adsorption on some (or none) of the adsorption sites to be instantaneous, while adsorption on the remaining sites is governed by first-order kinetics [*Selim et al.*, 1976; *Cameron and Klute*, 1977]. In contrast, physical nonequilibrium is often modeled by using a two-region (dual-porosity) type formulation. The medium contains two distinct mobile (flowing) and immobile (stagnant) liquid regions [*Coats and Smith*, 1964; *van Genuchten and Wierenga*, 1976]; mass transfer between the two regions is modeled as a first-order process.

Although the chemical and physical nonequilibrium CDE are based on different concepts, they can be put into the same dimensionless form for conditions of linear adsorption and steady-state water flow [*Nkedi-Kizza et al.*, 1984; *van Genuchten and Wagenet*, 1989]. We will first present the formulations of the two-site and two-region models, followed by both general and specific solutions of the nonequilibrium CDE (cf. Chapter 2).

3.1.1. Two-Site Nonequilibrium Transport

The two-site nonequilibrium model makes a distinction between type-1 (equilibrium) and type-2 (first-order kinetic) adsorption sites [*van Genuchten and Wagenet*, 1989]. For steady-state flow in a homogeneous soil, transport of a linearly adsorbed solute is given by

$$
\left(1 + \frac{f\rho_b K_d}{\theta}\right)\frac{\partial c}{\partial t} = D\frac{\partial^2 c}{\partial x^2} - v\frac{\partial c}{\partial x} - \frac{\alpha \rho_b}{\theta}\left[(1-f)K_d c - s_k\right]
$$
$$
- \mu_\ell c - \frac{f\rho_b K_d \mu_{s,e} c}{\theta} + \gamma_\ell(x) + \frac{f\rho_b \gamma_{s,e}(x)}{\theta}
\tag{3.1}
$$

$$
\frac{\partial s_k}{\partial t} = \alpha\left[(1-f)K_d c - s_k\right] - \mu_{s,k} s_k + (1-f)\gamma_{s,k}(x)
\tag{3.2}
$$

where α is a first-order kinetic rate coefficient (T^{-1}), f is the fraction of exchange sites that are always

15

at equilibrium, and the subscripts e and *k* refer to equilibrium and kinetic adsorption sites, respectively. Equations (3.1) and (3.2) use the customary first-order rate expression for describing kinetic adsorption on type-2 sites. The two-site adsorption model reduces to the one-site fully kinetic adsorption model if *f* = 0 (only type-2 sites are present). The one-site model is used in Section 4.2 in the stream-tube formulation for field transport.

3.1.2. **Two-Region Nonequilibrium Transport**

The two-region transport model assumes that the liquid phase can be partitioned into mobile (flowing) and immobile (stagnant) regions. Solute exchange between the two liquid regions is modeled as a first-order process. The two-region solute transport model is given by [see also van *Genuchten and Wagenet,* 1989]:

$$(\theta_m + f\rho_b K_d)\frac{\partial c_m}{\partial t} = \theta_m D_m \frac{\partial^2 c_m}{\partial x^2} - J_w \frac{\partial c_m}{\partial x} - \alpha(c_m - c_{im})$$

$$- (\theta_m \mu_{\ell,m} + f\rho_b K_d \mu_{s,m})c_m + \theta_m \gamma_{\ell,m}(x) + f\rho_b \gamma_{s,m}(x)$$

(3.3)

$$[\theta_{im} + (1-f)\rho_b K_d]\frac{\partial c_{im}}{\partial t} = \alpha(c_m - c_{im}) - [\theta_{im}\mu_{\ell,im} + (1-f)\rho_b K_d \mu_{s,im}]c_{im}$$

$$+ \theta_{im}\gamma_{\ell,im}(x) + (1-f)\rho_b \gamma_{s,im}(x)$$

(3.4)

where the subscripts *m* and *im* refer to the mobile and immobile liquid regions, respectively, $J_w = v\theta$ $= v_m \theta_m$ is the volumetric water flux density (LT^{-1}), *f* represents the fraction of adsorption sites that equilibrates with the mobile liquid phase, and α is again a first-order mass transfer coefficient (T^{-1}) governing the rate of solute exchange between the mobile and immobile liquid regions. Note that θ is equal to $\theta_m + \theta_{im}$.

16

3.1.3. Dimensionless Transport Equations

If we employ the dimensionless parameters listed in Table 3.1, the two-site and two-region models reduce to the same dimensionless form [see also **Nkedi-Kizza et al.,** 1984]:

$$\beta R\frac{\partial C_1}{\partial T} = \frac{1}{P}\frac{\partial^2 C_1}{\partial Z^2} - \frac{\partial C_1}{\partial Z} - \omega(C_1 - C_2) - \mu_1 C_1 + \gamma_1(Z) \tag{3.5}$$

$$(1 - \beta)R\frac{\partial C_2}{\partial T} = \omega(C_1 - C_2) - \mu_2 C_2 + \gamma_2(Z) \tag{3.6}$$

where the subscripts 1 and 2 refer to equilibrium and nonequilibrium sites, respectively; β is a partitioning coefficient, and ω is a dimensionless mass transfer coefficient. Table 3.1 defines the various dimensionless parameters for the one-site ($f = 0$) and two-site adsorption models, as well as for the two-region model. We further assume that ω and μ cannot be negative. Note that P is defined as $D = \theta_m D_m/\theta$ for the two-region model (Table 3.1). In CXTFIT 2.0, v $(= \theta_m v_m/\theta)$ and D are used as input parameters instead of v_m and D_m. **Also** note that β for the two-region model represents the fraction of mobile water, $\phi_m (= \theta_m/\theta)$ if the solute is nonreactive.

3.2. Analytical Solutions

Similar mathematical conditions as for the equilibrium model can be formulated also for the nonequilibrium problem [*Toride et al,* 1993a]. If the same initial condition is used for the equilibrium and nonequilibrium phase, we can write the general initial condition for the dimensionless nonequilibrium transport model as

$$C_1(Z, 0) = C_2(Z, 0) = C_i(Z) \tag{3.7}$$

The condition at the inlet is again given by'either a first- or a third-type condition, i.e.,

$$C_1(0, T) = C_o(T) \tag{3.8a}$$

or

$$C_1(0, T) - \frac{1}{P}\frac{\partial C_1(0, T)}{\partial Z} = C_o(T) \tag{3.8b}$$

while the invoked outlet condition is

$$\frac{\partial C_1}{\partial Z}(\infty, T) = 0 \tag{3.9}$$

17

Table 3.1. Dimensionless Parameters for the Nonequilibrium CDE†

Parameter	One-Site‡	Two-Site	Two-Region*
T	$\dfrac{vt}{L}$	$\dfrac{vt}{L}$	$\dfrac{vt}{L}$
Z	$\dfrac{x}{L}$	$\dfrac{x}{L}$	$\dfrac{x}{L}$
P	$\dfrac{vL}{D}$	$\dfrac{vL}{D}$	$\dfrac{v_m L}{D_m} = \dfrac{vL}{D}$
R	$1 + \dfrac{\rho_b K_d}{\theta}$	$1 + \dfrac{\rho_b K_d}{\theta}$	$1 + \dfrac{\rho_b K_d}{\theta}$
β	$\dfrac{1}{R}$	$\dfrac{\theta + f\rho_b K_d}{\theta + \rho_b K_d}$	$\dfrac{\theta_m + f\rho_b K_d}{\theta + \rho_b K_d}$
ω	$\dfrac{\alpha(R-1)L}{v}$	$\dfrac{\alpha(1-\beta)RL}{v}$	$\dfrac{\alpha L}{\theta v}$
C_1	$\dfrac{c}{c_o}$	$\dfrac{c}{c_o}$	$\dfrac{c_m}{c_o}$
C_2	$\dfrac{s_k}{K_d c_o}$	$\dfrac{s_k}{(1-f)K_d c_o}$	$\dfrac{c_{im}}{c_o}$
μ_1	$\dfrac{L\mu_\ell}{v}$	$\dfrac{L(\theta\mu_\ell + f\rho_b K_d \mu_{s,e})}{\theta v}$	$\dfrac{L(\theta_m \mu_{\ell,m} + f\rho_b K_d \mu_{s,m})}{\theta v}$
μ_2	$\dfrac{L(R-1)\mu_s}{v}$	$\dfrac{L(1-f)\rho_b K_d \mu_{s,k}}{\theta v}$	$\dfrac{L(\theta_{im}\mu_{\ell,im} + (1-f)\rho_b K_d \mu_{s,im})}{\theta v}$
γ_1	$\dfrac{L\gamma_\ell}{vc_o}$	$\dfrac{L(\theta\gamma_\ell + f\rho_b \gamma_{s,e})}{\theta v c_o}$	$\dfrac{L(\theta_m \gamma_{\ell,m} + f\rho_b \gamma_{s,m})}{\theta v c_o}$
γ_2	$\dfrac{L\rho_b \gamma_{s,k}}{\theta v c_o}$	$\dfrac{L(1-f)\rho_b \gamma_{s,k}}{\theta v c_o}$	$\dfrac{L(\theta_{im}\gamma_{\ell,im} + (1-f)\rho_b \gamma_{s,im})}{\theta v c_o}$

† c_o and L represent a characteristic concentration and length, respectively.
‡ The one-site model is obtained by setting $f = 0$ in the two-site model.
* $D = \theta_m D_m / \theta_m$

18

Because of the linearity of the problem in terms of C, the solution can again be obtained as the sum of independent solutions for a boundary value problem (BVP), an initial value problem (IVP), and a production value problem (PVP), hence:

$$C_1(Z,T) = C_1^B(Z,T) + C_1^I(Z,T) + C_1^P(Z,T) \tag{3.10}$$

$$C_2(Z,T) = C_2^B(Z,T) + C_2^I(Z,T) + C_2^P(Z,T) \tag{3.11}$$

Analytical solutions of (3.5) and (3.6) subject to (3.7) through (3.9) can be derived using Laplace transforms [*Lindstrom and Narasimhan*, 1973; *Lindstrom and Stone*, 1974; *Lindstrom*, 1976]. Details of the solution process are outlined by *Toride et al.* [1993a], and will not be reported here.

We will follow the same approach as in Chapter 2 by first presenting the general solution and subsequently giving several specific solutions. Expressions for the resident concentration, obtained for both a first- and a third-type inlet condition, and the flux-averaged concentration are provided. Solutions for the nonequilibrium CDE can be readily reduced to those for the equilibrium CDE by first assuming $\omega = 0$ and subsequently setting $\beta = 1$ [*Toride et al.*, 1993a]. The nonequilibrium solutions are given in terms of auxiliary expressions listed in Tables 3.2 and 3.3; these functions are similar to those in Tables 2.2 and 2.3 except for the nonequilibrium parameter β.

Effluent concentrations obtained from column displacement experiments are usually viewed to represent flux-averaged equilibrium concentrations, $C_{1,f}$. Resident concentrations, on the other hand, are typically obtained from core samples. Current measurement techniques are inadequate for distinguishing the equilibrium and nonequilibrium phases of the resident concentration (this is particularly true for the two-region model where a further partitioning of the liquid phase is needed). Usually the total resident concentration, C_T, is measured:

$$C_T = \beta R C_{1,r} + (1-\beta) R C_{2,r} \tag{3.12}$$

i.e., the total amount of solute in phases 1 and 2 per unit volume of soil solution at a given point in time and space [*Parker and Valocchi*, 1986].

3.2.1. Boundary Value Problem (BVP)

General solution

Concentrations as a result of an arbitrary input function, $C_o(T)$, can be expressed as

$$C_1^B(Z,T) = \int_0^T C_o(T-\tau) f(Z,\tau) d\tau \tag{3.13}$$

$$C_2^B(Z,T) = \frac{\omega}{(1-\beta)R} \int_0^T C_1^B(Z,\tau) \exp\left[-\frac{(\omega+\mu_2)(T-\tau)}{(1-\beta)R} \right] d\tau \tag{3.14}$$

where

$$f(Z,T) = \Gamma_1^N(Z,T) \exp\left(-\frac{\omega T}{\beta R} \right) + \frac{\omega}{R} \int_0^T \sqrt{\frac{\tau}{\beta(1-\beta)(T-\tau)}} \; \Gamma_1^N(Z,\tau) \; H_1(\tau,T) \; d\tau \tag{3.15}$$

with $\Gamma_1^N(Z,\tau)$ given in Table 3.2 and where the superscript refers to the nonequilibrium solution. Furthermore, $H_1(\tau,T)$ is given in Table 3.4 with I, as the modified Bessel function of order one. Below we give specific solutions for cases where $C_o(T)$ in (3.8) is described by a Dirac delta, a multiple pulse, and an exponential function.

Specific Solution

1. *Dirac Delta Input Function.* The inlet condition for a Dirac delta function is (cf. (2.16a)):

$$C_o(T) = M_B \delta(T) \tag{3.16}$$

Substitution of (3.16) into the general solutions leads to the following specific solutions:

$$C_1^B(Z,T) = M_B f(Z,T) \tag{3.17}$$

$$C_2(Z,T) = \frac{M_B \omega}{(1-\beta)R} \int_0^T \Gamma_1^N(Z,\tau) \; H_0(\tau;T) \; dr \tag{3.18}$$

where the nonequilibrium travel time pdf, $f(Z,T)$, is given by (3.15) $\Gamma_1^N(Z,\tau)$ can be found in Table 3.2, and $H_0(\tau,T)$ is given in Table 3.4 with I_0 as the modified Bessel function of order zero.

20

2. Multiple Pulse Input Conditions. The input concentration for a series of successive applications of rectangular solute pulses, as illustrated in Figure 2.1, is

$$C_o(T) = f_i \qquad T_i \le T < T_{i+1} \quad (i=1,2,...,n; \; T_1 = 0 \text{ and } T_{n+1} \to \infty) \tag{3.19}$$

where f_i denotes again an arbitrary constant. The superposition principle allows the solution to be written as the sum of the equilibrium ($k = 1$) and nonequilibrium ($k = 2$) concentrations resulting from a single pulse input as published by, for example, *Lindstrom and Stone* [1974]:

$$C_k^B(Z,T) = \sum_{j=1}^{i} (f_j - f_{j-1}) A_k(Z, T - T_j) \qquad (i = 1, 2, ..., n, \; k = 1, 2; f_o = 0) \tag{3.20}$$

with

$$A_1(Z,T) = \int_0^T \Gamma_1^N(Z,\tau) \exp\left[-\frac{\omega \mu_2 \tau}{(\omega + \mu_2)\beta R}\right] J(a,b) d\tau \tag{3.21}$$

$$A_2(Z,T) = \frac{\omega}{\omega + \mu_2} \int_0^T \Gamma_1^N(Z,\tau) \exp\left[-\frac{\omega \mu_2 \tau}{(\omega + \mu_2)\beta R}\right] [1 - J(b,a)] d\tau \tag{3.22}$$

where Goldstein's J-function, $J(a,b)$, and a and b are given in Table 3.4.

The following alternative expression can be obtained for $A_k(Z,T)$ by partial integration of (3.21) [see *De Smedt and Wierenga*, 1979; *Toride et al.*, 1993a]:

$$A_1(Z,T) = G_1^N\left(Z,T; \mu_1 + \frac{\omega\mu_2}{\omega+\mu_2}\right) \exp\left[-\frac{\omega^2 T}{(\omega + \mu_2)\beta R}\right]$$

$$+ \frac{\omega}{R} \int_0^T G_1^N\left(Z,\tau; \mu_1 + \frac{\omega\mu_2}{\omega+\mu_2}\right) \exp[-a-b] \tag{3.23}$$

$$\cdot \left[\frac{\omega}{(\omega+\mu_2)\beta} I_0[\, 2\sqrt{ab}\,] + \sqrt{\frac{\tau}{\beta(1-\beta)-\tau}} \; I_1[\, 2\sqrt{ab}\,]\right] d\tau$$

$$A_2(Z,T) = \frac{\omega}{(1-\beta)R} \cdot \int_0^T G_1^N\left(Z,\tau; \mu_1 + \frac{\omega\mu_2}{\omega+\mu_1}\right) \exp[-a-b]$$

$$\cdot \left[I_0[\, 2\sqrt{ab}\,] + \frac{\omega}{\omega+\mu_2} \sqrt{\frac{(1-\beta)(T-\tau)}{\beta\tau}} \; I_1[\, 2\sqrt{ab}\,]\right] d\tau \tag{3.24}$$

where $G_1^N(Z,T;\Omega)$ is given in Table 3.3. CXTFIT always assumes that $\mu_1 + \omega\mu_2/(\omega+\mu_2) \geq 0$, which is consistent with earlier assumptions that μ_1 and $\mu_2 \geq 0$. Differentiating the solutions for a single step input (i.e., $A_1(Z,T)$ and $A_2(Z,T)$) with respect to T yields the travel time pdf (cf. (3.17) and (3.18)) [*De Smedt and Wierenga,* 1979].

*3. **Exponential Input Function.*** The exponential input function is given by

$$C_o(T) = f_1 + f_2 \exp(-\lambda^B T) \tag{3.25}$$

where $f_1, f_2,$ and λ^B are constants. As described by *Leij et al.* [1993], an approximate solution for this exponential input can be derived by using the series expansion of the zero-order modified Bessel function [9.6.12 of *Abramowitz and Stegun,* 1970]:

$$C_1^B(Z,T) = f_1 A_1(Z,T) + f_2 \exp(-\lambda^B T)\, G_1^N\!\left(Z,T; \mu_1 + \omega + \frac{\beta R p q}{\lambda^B - q} - \beta R\lambda^B\right)$$
$$- f_2 \exp(-qT) \int_0^T \Gamma_1^N(Z,\tau)\exp\!\left[-\frac{\tau}{\beta R}(\omega - \beta R q)\right]\Phi_1(\tau)\,d\tau \tag{3.26}$$

$$C_2^B(Z,T) = f_1 A_2(Z,T) + \frac{\omega f_2}{(1-\beta)R}\left\{\frac{\exp(-qT)}{\lambda^B - q}\, G_1^N\!\left(Z,T; \mu_1 + \omega + \frac{\beta R p q}{\lambda^B - q} - \beta R q\right)\right.$$
$$- \frac{\exp(-\lambda^B T)}{\lambda^B - q}\, G_1^N\!\left(Z,T; \mu_1 + \omega + \frac{\beta R p q}{\lambda^B - q} - \beta R\lambda^B\right)$$
$$\left.- f_2 \exp(-qT)\int_0^T \Gamma_1^N(Z,\tau)\exp\!\left[-\frac{\tau}{\beta R}(\omega - \beta r q)\right]\Phi_2(\tau)\,d\tau\right\} \tag{3.27}$$

with

$$\Phi_1(\tau) = \sum_{n=1}^{\infty} \frac{(pq\tau)^n}{n!}\left[\sum_{k+1}^{n}\left(\frac{-1}{\lambda^B - q}\right)^k \frac{(T-\tau)^{n-k}}{(n-k)!}\right] \tag{3.28}$$

$$\Phi_2(\tau) = \sum_{n=1}^{\infty} \frac{(pq\tau)^n}{n!}\left[\sum_{k+1}^{n}\left(\frac{-1}{\lambda^B - q}\right)^k \frac{(T-\tau)^{n-k+1}}{(n-k+1)(n-k)!}\right] \tag{3.29}$$

and

$$p = \frac{a}{\tau} = \frac{\omega^2}{(\omega+\mu_2)\beta R}\ , \qquad q = \frac{b}{T-\tau} = \frac{\omega+\mu_2}{(1-\beta)R} \tag{3.30a,b}$$

The auxiliary functions $A_1(Z,T)$ and $A_2(Z,T)$ are given by (3.21) and (3.22), respectively. In analogy to the equilibrium solution of the BVP for an exponential input (cf. (2.22)), the parameter u in

$G_1^N(Z,T)$ can be complex for large x^p. A convergent solution is usually obtained for a maximum n value of 25. The solution is less appropriate for relatively large values of the product pq and/or T.

3.2.2. Initial Value Problem (IVP)

General Solution

The general solution of the IVP is

$$C_1^I(Z,T) = \exp\left(-\frac{\omega T}{\beta R}\right) \int_0^\infty C_i(\eta)\Gamma_2^N(Z,\eta,T)\,d\eta$$

$$+ \frac{\omega}{\beta R}\int_0^T \left(H_0(\tau;T) + \sqrt{\frac{\beta\tau}{(1-\beta)(T-\tau)}}\, H_1(\tau;T) \right) \int_0^\infty C_i(\eta)\Gamma_2^N(Z,\eta,\tau)\,d\eta\,d\tau \tag{3.31}$$

$$C_2^I(Z,T) = C_i(Z)\exp\left[-\frac{(\omega+\mu_2)T}{(1-\beta)R}\right]$$

$$+ \frac{\omega}{(1-\beta)R}\int_0^T \left(H_0(\tau;T) + \sqrt{\frac{(1-\beta)(T-\tau)}{\beta\tau}}\, H_1(\tau;T) \int_0^\infty C_i(\eta)\Gamma_2^N(Z,\eta,\tau)d\eta \right) d\tau \tag{3.32}$$

where $\Gamma_2^N(Z,\eta,\tau)$ is listed in Table 3.2, and $H_0(\tau,T)$ and $H_1(\tau,T)$ are given in Table 3.4. Specific solutions will again be presented for a Dirac delta, stepwise and an exponential initial distribution. These solutions are obtained by substituting the initial profile $C_i(Z)$ into (3.31) and (3.32), followed by integration with respect to η (cf. Section 2.2.2).

Specific Solution

1. Dirac Delta Initial Distribution. If solutes are initially located at $Z = Z_1$, the initial concentration $C_i(Z)$ is written as

$$C_i(Z) = M_I\,\delta(Z-Z_1) \tag{3.33}$$

where $\delta(Z)$ is a Dirac delta function, and M_I is the dimensionless amount of solutes initially placed at $Z = Z_1$. The corresponding dimensional initial condition is given by (2.24b). After substituting (3.33) into (3.31) and (3.32), the dimensionless concentrations of phases 1 and 2 become

$$C_1^I(Z,T) = \exp\left(-\frac{\omega T}{\beta R}\right) \ \Gamma_2^N(Z,Z_1,T)$$

$$+ \frac{\omega}{\beta R} \int_0^T \left(H_0(\tau;T) + \sqrt{\frac{\beta \tau}{(1-\beta)(T-\tau)}} H_1(\tau;T) \right) \Gamma_2^N(Z,Z_1,\tau) \, d\tau \qquad (3.34)$$

$$C_2^I(Z,T) = C_i(Z) \exp\left[-\frac{(\omega+\mu_2)T}{(1-\beta)R}\right]$$

$$+ \frac{\omega}{(1-\beta)R} \int_0^T \left(H_0(\tau;T) + \sqrt{\frac{(1-\beta)(T-\tau)}{\beta \tau}} H_1(\tau;T) \right) \Gamma_2^N(Z,Z_1,\tau) \, d\tau \qquad (3.35)$$

In contrast with the equilibrium CDE, the above solution for a Dirac initial condition at $Z_1 = 0$ differs from the solution for the Dirac input (i.e., (3.17) and (3.18)).

2. Stepwise Initial Distribution.

The stepwise initial distribution is given by

$$C_i(Z) = U_i \qquad Z_i \leq Z < Z_{i+1} \quad (i=1,2,\ldots,n; Z_1=0 \text{ and } Z_{n+1} \to \infty) \qquad (3.36)$$

where U_i denotes an arbitrary constant (cf. Figure 2.2). The solution of the IVP for this case is

$$C_1^I(Z,T) = \exp\left(-\frac{\omega T}{\beta R}\right) \sum_{i=1}^n (U_i - U_{i-1}) \psi_1^N(Z,T;Z_i)$$

$$+ \frac{\omega}{\beta R} \int_0^T \left(H_0(\tau;T) + \sqrt{\frac{\beta \tau}{(1-\beta)(T-\tau)}} H_1(\tau;T) \right) \sum_{i=1}^n (U_i - U_{i-1}) \psi_1^N(Z,\tau;Z_i) d\tau \qquad (3.37)$$

$$C_2^I(Z,T) = C_i(Z) \exp\left[-\frac{(\omega+\mu_2)T}{(1-\beta)R}\right] + \frac{\omega}{(1-\beta)R} \int_0^T \left(H_0(\tau,T) + \sqrt{\frac{(1-\beta)(T-\tau)}{\beta \tau}} H_1(\tau,T) \right)$$

$$\cdot \sum_{i=1}^n (U_i - U_{i-1}) \psi_1^N(Z,\tau;Z_i) \ d\tau \qquad\qquad (i=1,2,\ldots,n; U_0 = 0) \qquad (3.38)$$

where ψ_1^N is listed in Table 3.2.

3. *Exponential Initial Distribution.* The exponential initial condition is given by

$$C_i(Z) = U_1 + U_2 \exp(-\lambda^I Z) \tag{3.39}$$

where U_1, U_2, and λ^I are constants. The specific solutions for this condition are

$$C_1^I(Z,T) = \exp\left(-\frac{\omega T}{\beta R}\right)\left[U_1\,\psi_1^N(Z,T;0) + U_2\,\psi_2^N(Z,T;\lambda^I)\right]$$

$$+ \frac{\omega}{\beta R}\int_0^T \left(H_0(\tau;T) + \sqrt{\frac{\beta\tau}{(1-\beta)(T-\tau)}}H_1(\tau;T)\right)\left[U_1\,\psi_1^N(Z,\tau;0) + U_2\psi_2^N(Z,\tau;\lambda^I)\right]d\tau \tag{3.40}$$

$$C_2^I(Z,T) = C_i(Z)\exp\left[-\frac{(\omega+\mu_2)T}{(1-\beta)R}\right] + \frac{\omega}{(1-\beta)R}\int_0^T \left(H_0(\tau;T)\right.$$

$$\left. + \sqrt{\frac{(1-\beta)(T-\tau)}{\beta\tau}}H_1(\tau;T)\right)\left[U_1\,\psi_1^N(Z,\tau;0) + U_2\,\psi_2^N(Z,\tau;\lambda^I)\right]d\tau \tag{3.41}$$

where ψ_1^N and ψ_2^N are listed in Table 3.2, and $H_0(\tau,T)$ and $H_1(\tau,T)$ are given in Table 3.4.

3.2.3. Production Value Problem (PVP)

General Solution

As outlined in the Appendix of *Toride et al.* [1993a], the general solution for the equilibrium concentration in case of production profiles $\gamma_1(Z)$ and $\gamma_2(Z)$ can be written as

$$C_1^P(Z,T) = \frac{1}{\beta R}\int_0^T \exp\left[-\frac{\omega\mu_2\tau}{(\omega+\mu_2)\beta R}\right]J(a,b)\int_0^\infty\left(\gamma_1(\eta) + \frac{\omega}{\omega+\mu_2}\gamma_2(\eta)\right)$$

$$\cdot\,\Gamma_2^N(Z,\eta,\tau)\,d\eta\;d\tau - \frac{1}{\beta R}\int_0^T H_0(\tau;T)\int_0^\infty\frac{\omega}{\omega+\mu_2}\gamma_2(\eta)\,\Gamma_2^N(Z,\eta,\tau)\,d\eta\,d\tau \tag{3.42}$$

Two cases need to be distinguished for the solution of phase 2, viz. $\omega+\mu_2 > 0$ and $\omega = \mu_2 = 0$. For the special case that $\omega = \mu_2 = 0$, we have the simple solution

$$C_2^P(Z,T) = \frac{\gamma_2(Z)T}{(1-\beta)R} \tag{3.43}$$

whereas for $\omega+\mu_2 > 0$ the nonequilibrium (phase 2) concentration is given by

$$C_2^P(Z,T) = \frac{\gamma_2(Z)}{\omega+\mu_2}\left\{1-\exp\left[-\frac{(\omega+\mu_2)T}{(1-\beta)R}\right]\right\} + \frac{\omega}{\beta R(\omega+\mu_2)}\int_0^T \exp\left[-\frac{\omega\mu_2\tau}{(\omega+\mu_2)\beta R}\right]$$

$$\cdot [1-J(b,a)]\int_0^\infty\left(\gamma_1(\eta)+\frac{\omega}{\omega+\mu_2}\gamma_2(\eta)\right)\Gamma_2^N(Z,\eta,\tau)\,d\eta\,d\tau \qquad (3.44)$$

$$-\frac{1}{\beta R}\int_0^T\sqrt{\frac{\beta(T-\tau)}{(1-\beta)\tau}}\,H_1(\tau;T)\int_0^\infty\frac{\omega}{\omega+\mu_2}\gamma_2(\eta)\,\Gamma_2^N(Z,\eta,\tau)\,d\eta\,d\tau$$

where Γ_2^N, which is the same as for the IVP, is listed in Table 3.2 and $H_0(\tau,T)$, $H_1(\tau,T)$, and $J(a,b)$ is again given in Table 3.4. Specific solutions for stepwise and exponential distributions for the production profiles, $\gamma_1(Z)$ and $\gamma_2(Z)$, are given below for $\omega+\mu > 0$. In case $\omega+\mu = 0$, the concentration for phase 1 can be readily obtained from (3.42) (cf. (2.30)), whereas a specific solution for phase 2 can be obtained by substituting the production profile into (3.44).

Specific Solution

1. Stepwise Production Profile. The production distribution for n distinct steps is given as

$$\gamma_1(Z) = \gamma_{1,i} \qquad Z_{1,i}\le Z<Z_{1,i+1} \quad (i=1,2,\ldots,n;\ Z_{1,1}=0\ \text{and}\ Z_{1,n+1}\to\infty) \qquad (3.45)$$

$$\gamma_2(Z) = \gamma_{2,j} \qquad Z_{2,j}\le Z<Z_{2,j+1} \quad (j=1,2,\ldots,m;\ Z_{2,1}=0\ \text{and}\ Z_{2,n+1}\to\infty) \qquad (3.46)$$

where $\gamma_{1,i}$, $\gamma_{2,j}$, $Z_{1,i}$, and $Z_{2,j}$ are constants. For a single step ($n=1$, $m=1$), the production is uniform throughout the soil profile. Inserting (3.45) and (3.46) into the general solution and subsequent integration with respect to η yields

$$C_1^P(Z,T) = \frac{1}{\beta R}\int_0^T\exp\left[-\frac{\omega\mu_2\tau}{(\omega+\mu_2)\beta R}\right]J(a,b)\sum_{i=1}^n(\gamma_{1,i}-\gamma_{1,i-1})\psi_1^N(Z,\tau;Z_{1,i})\,d\tau$$

$$+\frac{\omega}{\beta R(\omega+\mu_2)}\int_0^T\left\{\exp\left[-\frac{\omega\mu_2\tau}{(\omega+\mu_2)\beta R}\right]J(a,b)-H_0(\tau,T)\right\} \qquad (3.47)$$

$$\cdot\sum_{j=1}^m(\gamma_{2,j}-\gamma_{2,j-1})\,\psi_1^N(Z,\tau;Z_{2,j})\,d\tau$$

$$C_2^P(Z,T) = \frac{\gamma_2(Z)}{\omega+\mu_2}\left\{1-\exp\left[-\frac{(\omega+\mu_2)T}{(1-\beta)R}\right]\right\}$$

$$+\frac{\omega}{\beta R(\omega+\mu_2)}\int_0^T\left\{\exp\left[-\frac{\omega\mu_2\tau}{(\omega+\mu_2)\beta R}\right][1-J(b,a)]\sum_{i=1}^n(\gamma_{1,i}-\gamma_{1,i-1})\psi_1^N(Z,\tau;Z_{1,i})\right.$$

$$+\left[\frac{\omega}{\omega+\mu_2}\exp\left(-\frac{\omega\mu_2\tau}{(\omega+\mu_2)\beta R}\right)[1-J(b,a)]-\sqrt{\frac{\beta(T-\tau)}{(1-\beta)\tau}}H_1(\tau;T)\right]$$

$$\left.\cdot\sum_{j=1}^m(\gamma_{2,j}-\gamma_{2,j-1})\,\psi_1^N(Z,\tau;Z_{2,j})\right\}d\tau \qquad (i=1,2,...,n;\ \gamma_{1,0}=\gamma_{2,0}=0)$$

(3.48)

where ψ_1^N is listed in Table 3.2.

2. Exponential Production Profile.

The depth-dependent production terms are given by:

$$\gamma_k(Z) = \gamma_{k,1} + \gamma_{k,2}\exp(-\lambda_k^P Z) \qquad (k=1,2)$$

(3.49)

where γ_{k1}, γ_{k2}, and λ_k^P are constants. The concentrations are now given by

$$C_1^P(Z,T) = \frac{1}{\beta R}\int_0^T\exp\left[-\frac{\omega\mu_2\tau}{(\omega+\mu_2)\beta R}\right]J(a,b)$$

$$\cdot[\gamma_{1,1}\,\psi_1^N(Z,\tau;0)+\gamma_{1,2}\,\psi_2^N(Z,\tau;\lambda_1^P)]\,d\tau$$

$$+\frac{\omega}{\beta R(\omega+\mu_2)}\int_0^T\left\{\exp\left[-\frac{\omega\mu_2\tau}{(\omega+\mu_2)\beta R}\right]J(a,b)-H_0(\tau,T)\right\}$$

$$\cdot[\gamma_{2,1}\,\psi_1^N(Z,\tau;0)+\gamma_{2,2}\,\psi_2^N(Z,\tau;\lambda_2^P)]\,d\tau$$

(3.50)

$$C_2^P(Z,T) = \frac{\gamma_2(Z)}{\omega+\mu_2}\left\{1-\exp\left[-\frac{(\omega+\mu_2)T}{(1-\beta)R}\right]\right\}+\frac{\omega}{\beta R(\omega+\mu_2)}\int_0^T\left\{\exp\left[-\frac{\omega\mu_2\tau}{(\omega+\mu_2)\beta R}\right]\right.$$

$$\cdot[1-J(b,a)][\gamma_{1,1}\,\psi_1(Z,\tau;0)+\gamma_{1,2}\,\psi_2(Z,\tau;\ \lambda_1^P)]$$

$$+\left[\frac{\omega}{\omega+\mu_2}\exp\left(-\frac{\omega\mu_2\tau}{(\omega+\mu_2)\beta R}\right)[1-J(b,a)]-\sqrt{\frac{\beta(T-\tau)}{(1-\beta)\tau}}H_1(\tau,T)\right]$$

$$\left.\cdot[\gamma_{2,1}\,\psi_1(Z,\tau;0)+\gamma_{2,2}\,\psi_2(Z,\tau;\lambda_2^P)]\right\}d\tau$$

(3.51)

27

Table 3.2. Expressions for Γ^N and ψ^N in the Solutions for the Resident and Flux-Averaged Concentrations of the Nonequilibrium CDE

Function	Resident Concentration, C_r		Flux-averaged Concentration, C_f
	First-Type	Third-Type	
$\Gamma_1^N(Z,\tau)$	$\exp\left(-\dfrac{\mu_1\tau}{\beta R}\right)\dfrac{Z}{\tau}\sqrt{\dfrac{\beta RP}{4\pi\tau}}\exp\left[-\dfrac{P(\beta RZ-\tau)^2}{4\beta R\tau}\right]$	$\exp\left(-\dfrac{\mu_1\tau}{\beta R}\right)\left\{\sqrt{\dfrac{P}{\pi\beta R\tau}}\exp\left[-\dfrac{P(\beta RZ-\tau)^2}{4\beta R\tau}\right]\right.$ $\left.-\dfrac{P}{2\beta R}\exp(PZ)\;\text{erfc}\left[\dfrac{\beta RZ+\tau}{\sqrt{4\beta R\tau/P}}\right]\right\}$	$\exp\left(-\dfrac{\mu_1\tau}{\beta R}\right)\dfrac{Z}{\tau}\sqrt{\dfrac{\beta RP}{4\pi\tau}}\exp\left[-\dfrac{P(\beta RZ-\tau)^2}{4\beta R\tau}\right]$
$\Gamma_2^N(Z,\eta,\tau)$	$\exp\left(-\dfrac{\mu_1\tau}{\beta R}\right)\sqrt{\dfrac{\beta RP}{4\pi\tau}}\left\{\exp\left[-\dfrac{P[\beta R(\eta-Z)+\tau]^2}{4\beta R\tau}\right]\right.$ $\left.-\exp(PZ)\exp\left[-\dfrac{P[\beta R(\eta+Z)+\tau]^2}{4\beta R\tau}\right]\right\}$	$\exp\left(-\dfrac{\mu_1\tau}{\beta R}\right)\left\{\sqrt{\dfrac{\beta RP}{4\pi\tau}}\exp\left[-\dfrac{P[\beta R(\eta-Z)+\tau]^2}{4\beta R\tau}\right]\right.$ $+\sqrt{\dfrac{\beta RP}{4\pi\tau}}\exp(PZ)\exp\left[-\dfrac{P[\beta R(\eta+Z)+\tau]^2}{4\beta R\tau}\right]$ $\left.-\dfrac{P}{2}\exp(PZ)\,\text{erfc}\left[\dfrac{\beta R(\eta+Z)+\tau}{\sqrt{4\beta R\tau/P}}\right]\right\}$	$\exp\left(-\dfrac{\mu_1\tau}{\beta R}\right)\sqrt{\dfrac{\beta RP}{4\pi\tau}}\left\{\left[1-\dfrac{\beta R(\eta-Z)+\tau}{2\tau}\right]\right.$ $\times\exp\left[-\dfrac{P[\beta R(\eta-Z)+\tau]^2}{4\beta R\tau}\right]$ $\left.+\left[\dfrac{\beta R(\eta+Z)-\tau}{2\tau}\right]\exp\left[PZ-\dfrac{P[\beta R(\eta+Z)+\tau]^2}{4\beta R\tau}\right]\right\}$
$\psi_1^N(Z,\tau;Z_i)$	$\exp\left(-\dfrac{\mu_1\tau}{\beta R}\right)\left\{1-\dfrac{1}{2}\text{erfc}\left[\dfrac{\beta R(Z-Z_i)-\tau}{\sqrt{4\beta R\tau/P}}\right]\right.$ $\left.-\dfrac{1}{2}\exp(PZ)\,\text{erfc}\left[\dfrac{\beta R(Z+Z_i)+\tau}{\sqrt{4\beta R\tau/P}}\right]\right\}$	$\exp\left(-\dfrac{\mu_1\tau}{\beta R}\right)\left\{1-\dfrac{1}{2}\text{erfc}\left[\dfrac{\beta R(Z-Z_i)-\tau}{\sqrt{4\beta R\tau/P}}\right]\right.$ $-\sqrt{\dfrac{P\tau}{\pi\beta R}}\exp\left[PZ-\dfrac{P[\beta R(Z+Z_i)+\tau]^2}{4\beta R\tau}\right]$ $\left.+\dfrac{1}{2}\left[1+P(Z+Z_i)+\dfrac{P\tau}{\beta R}\right]\exp(PZ)\text{erfc}\left[\dfrac{\beta R(Z+Z_i)+\tau}{\sqrt{4\beta R\tau/P}}\right]\right\}$	$\exp\left(-\dfrac{\mu_1\tau}{\beta R}\right)\left\{1-\dfrac{1}{2}\text{erfc}\left[\dfrac{\beta R(Z-Z_i)-\tau}{\sqrt{4\beta R\tau/P}}\right]\right.$ $-\dfrac{1}{2}\exp(PZ)\,\text{erfc}\left[\dfrac{\beta R(Z+Z_i)+\tau)}{\sqrt{4\beta R\tau/P}}\right]$ $+\sqrt{\dfrac{\beta R}{4\pi P\tau}}\times\left[\exp\left(PZ-\dfrac{P[\beta R(Z+Z_i)+\tau]^2}{4\beta R\tau}\right)\right.$ $\left.\left.-\exp\left(-\dfrac{P[\beta R(Z-Z_i)-\tau]^2}{4\beta R\tau}\right)\right]\right\}$
$\psi_2^N(Z,\tau;\lambda)$	$\dfrac{1}{2}\exp\left(-\dfrac{\mu_1\tau}{\beta R}+\dfrac{\lambda^2\tau}{\beta RP}+\dfrac{\lambda\tau}{\beta R}-\lambda Z\right)$ $\times\left\{2-\text{erfc}\left[\dfrac{\beta RZ-(1+2\lambda/P)\tau}{\sqrt{4\beta R\tau}}\right]\right.$ $\left.+\exp(PZ+2\lambda Z)\text{erfc}\left[\dfrac{\beta RZ+(1+2\lambda/P)\tau}{\sqrt{4\beta R\tau}}\right]\right\}$	$\exp\left(-\dfrac{\mu_1\tau}{\beta R}+\dfrac{\lambda^2\tau}{\beta RP}+\dfrac{\lambda\tau}{\beta R}-\lambda Z\right)\left\{1-\dfrac{1}{2}\text{erfc}\left[\dfrac{\beta RZ-(1+2\lambda/P)\tau}{\sqrt{4\beta R\tau/P}}\right]\right.$ $+\dfrac{1}{2}\left(1+\dfrac{P}{\lambda}\right)\exp(PZ+2\lambda Z)\,\text{erfc}\left[\dfrac{\beta RZ+(1+2\lambda/P)\tau}{\sqrt{4\beta R\tau}}\right]\right\}$ $\left.-\dfrac{P}{2\lambda}\exp\left(-\dfrac{\mu_1\tau}{\beta R}+PZ\right)\text{erfc}\left[\dfrac{\beta RZ+\tau}{\sqrt{4\beta R\tau/P}}\right]\right\}$	$\dfrac{1}{2}\left(1+\dfrac{\lambda}{P}\right)\exp\left(-\dfrac{\mu_1\tau}{\beta R}+\dfrac{\lambda^2\tau}{\beta RP}+\dfrac{\lambda\tau}{\beta R}-\lambda Z\right)$ $\times\left\{2-\text{erfc}\left[\dfrac{\beta RZ-(1+2\lambda/P)\tau}{\sqrt{4\beta R\tau/P}}\right]\right.$ $\left.+\exp(PZ+2\lambda Z)\,\text{erfc}\left[\dfrac{\beta RZ+(1+2\lambda/P)\tau}{\sqrt{4\beta R\tau/P}}\right]\right\}$

28

Table 3.3. Expressions for $G^N(Z,T)$ in the Solutions for the Resident
and Flux-Averaged Concentrations

G^N	C_r or C_f First-Type	C_r Third-Type
General† $G_1^N(Z,T;\Omega)$	$\displaystyle\int_0^T \exp\left(-\frac{\Omega\tau}{\beta R}\right)\frac{Z}{\tau}\sqrt{\frac{\beta RP}{4\pi\tau}}\exp\left[-\frac{P(\beta RZ-\tau)^2}{4\beta R\tau}\right]d\tau$	$\displaystyle\int_0^T \exp\left(-\frac{\Omega\tau}{\beta R}\right)\left\{\sqrt{\frac{P}{\pi\beta R\tau}}\exp\left[-\frac{P(\beta RZ-\tau)^2}{4\beta R\tau}\right]\right.$ $\left.-\frac{P}{2\beta R}\exp(PZ)\,\mathrm{erfc}\left[\frac{\beta RZ+\tau}{\sqrt{4\beta R\tau/P}}\right]\right\}d\tau$
for $\Omega=0$ $G_1^N(Z,T;0)$	$\displaystyle\frac{1}{2}\mathrm{erfc}\left[\frac{\beta RZ-T}{\sqrt{4\beta RT/P}}\right]+\frac{1}{2}\exp(PZ)\,\mathrm{erfc}\left[\frac{\beta RZ+T}{\sqrt{4\beta RT/P}}\right]$	$\displaystyle\frac{1}{2}\mathrm{erfc}\left[\frac{\beta RZ-T}{\sqrt{4\beta RT/P}}\right]+\sqrt{\frac{P}{\pi\beta R}}\exp\left[-\frac{P(\beta RZ-T)^2}{4\beta RT}\right]$ $-\frac{1}{2}\left(1+PZ+\frac{PT}{\beta R}\right)\exp(PZ)\,\mathrm{erfc}\left[\frac{\beta RZ+T}{\sqrt{4\beta RT/P}}\right]$
for $\Omega\neq0$ $(\Omega>-P/4)$ $G_1^N(Z,T;\Omega)$	$\displaystyle\frac{1}{2}\exp\left[\frac{P(1-u)Z}{2}\right]\mathrm{erfc}\left[\frac{\beta RZ-uT}{\sqrt{4\beta RT/P}}\right]$ $+\frac{1}{2}\exp\left[\frac{P(1+u)Z}{2}\right]\mathrm{erfc}\left[\frac{\beta RZ+uT}{\sqrt{4\beta RT/P}}\right]$	$\displaystyle\frac{1}{1+u}\exp\left[\frac{P(1-u)Z}{2}\right]\mathrm{erfc}\left[\frac{\beta RZ-uT}{\sqrt{4\beta RT/P}}\right]$ $+\frac{1}{1-u}\exp\left[\frac{P(1+u)Z}{2}\right]\mathrm{erfc}\left[\frac{\beta RZ+uT}{\sqrt{4\beta RT/P}}\right]$ $-\frac{2}{1-u^2}\exp\left[PZ+\frac{P(1-u^2)T}{4\beta R}\right]\mathrm{erfc}\left[\frac{\beta RZ+T}{\sqrt{4\beta RT/P}}\right]$

$$\text{with}\quad u=\sqrt{1+\frac{4\Omega}{P}}$$

† The integral in the general expression of $G_1^N(Z,T;\Omega)$ is evaluated numerically for $\Omega>-P/4$.

Table 3.4. Expressions for $H(\tau,T)$ and Goldstein's J-function, $J(a,b)$

Function	Expression
$H_0(\tau,T)$	$\exp\left[-\dfrac{\omega\,\tau}{\beta R} - \dfrac{(\omega+\mu_2)(T-\tau)}{(1-\beta)R}\right] I_0\left[\dfrac{2\omega}{R}\sqrt{\dfrac{(T-\tau)\tau}{\beta(1-\beta)}}\right]$
$H_1(\tau,T)$	$\exp\left[-\dfrac{\omega\,\tau}{\beta R} - \dfrac{(\omega+\mu_2)(T-\tau)}{(1-\beta)R}\right] I_1\left[\dfrac{2\omega}{R}\sqrt{\dfrac{(T-\tau)\tau}{\beta(1-\beta)}}\right]$
$J(a,b)$	$1 - \exp(-b)\int_0^a \exp(-\lambda)I_0[2\sqrt{b\lambda}]\ d\lambda$

with $a = \dfrac{\omega^2\tau}{(\omega+\mu_2)\beta R}$ and $b = \dfrac{(\omega+\mu_2)(T-\tau)}{(1-\beta)R}$

3.3. Degradation for the Nonequilibrium CDE

Thus far, no assumptions were made regarding the values of the degradation coefficients (i.e., $\mu_{s,e}$, $\mu_{s,k}$, $\mu_{\ell,m}$, $\mu_{\ell,im}$, $\mu_{s,m}$, $\mu_{s,im}$). For many actual transport problems it may not be possible to determine meaningful individual degradation parameters. The number of degradation pathways and associated coefficients can be reduced in several ways.

As outlined by van Genuchten and Wagenet [1989], one simplification is to assume that all rate coefficients are the same (e.g., for nuclear decay), i.e., $\mu_\ell = \mu_{s,e} = \mu_{s,k} \equiv \mu$ for the two-site model, or $\mu_{\ell,m} = \mu_{\ell,im} = \mu_{s,m} = \mu_{s,im} \equiv \mu$ for the two-region model. The dimensionless parameters, μ_1 and μ_2, for the two-site and the two-region models (cf. Table 3.1) reduce then to

$$\mu_1 = \beta R\,\psi, \qquad \mu_2 = (1-\beta)R\,\psi \qquad (3.52a,b)$$

where the dimensionless parameter, ψ, is defined as

$$\psi = \mu\,L/v \qquad (3.53)$$

An alternative simplification assumes negligible decay in the adsorbed phase. The assumption of exclusive decay in the liquid phase appears realistic for at least some pesticide-soil combinations [Weber and Cole, 1968; Moyer et al., 1972; Ogram et al., 1985]. The dimensionless degradation coefficients for the two-site model are now given by

$$\mu_1 = \psi_\ell, \qquad \mu_2 = 0 \qquad (3.54a,b)$$

where $\psi_\ell = \mu_\ell L/v$. It may also be possible that degradation occurs only in the adsorbed phase rather than the solution phase; an appropriate ψ_s is then defined from the corresponding μ_s.

Table 3.5 summarizes the expressions for μ_1 and μ_2 in terms of ψ for the most general case as well as for several limiting scenarios. We have furthermore assumed that the degradation coefficients for decay in the liquid or adsorbed phase are the same for both regions in the two-region model when degradation takes place exclusively in the liquid or adsorbed phase.

Table 3.5. Expressions for the Dimensionless Parameters μ_1 and μ_2 in (3.5) and (3.6)

	One-site model	Two-site model	Two-region model†
Independent degradations rates in liquid and adsorbed phases	$\mu_1 = \psi_\ell$ $\mu_2 = (R-1)\psi_s$	$\mu_1 = \psi_\ell + (\beta R - 1)\psi_{s,\ell}$ $\mu_2 = (1-\beta)R\,\psi_{s,k}$	$\mu_1 = \phi_m \psi_{\ell m} + (\beta R - \phi_m)\psi_{s,m}$ $\mu_2 = \phi_{im}\psi_{\ell im} + [(1-\beta)R - \phi_{im}]\psi_{s,im}$
Identical degradation in liquid and adsorbed phases	$\mu_1 = \psi$ $\mu_2 = (R-1)\psi$	$\mu_1 = \beta R\,\psi$ $\mu_2 = (1-\beta)R\,\psi$	$\mu_1 = \beta R\,\psi$ $\mu_2 = (1-\beta)R\,\psi$
No degradation in the adsorbed phase	$\mu_1 = \psi_\ell$ $\mu_2 = 0$	$\mu_1 = \psi_\ell$ $\mu_2 = 0$	$\mu_1 = \phi_m \psi_\ell$ $\mu_2 = \phi_{im}\psi_\ell$
No degradation in the liquid phase	$\mu_1 = 0$ $\mu_2 = (R-1)\psi_s$	$\mu_1 = (\beta R - 1)\psi_s$ $\mu_2 = (1-\beta)R\,\psi_s$	$\mu_1 = (\beta R - \phi_m)\psi_s$ $\mu_2 = [(1-\beta)R - \phi_{im}]\psi_s$

† $\phi_m = \theta_m/\theta$, $\phi_{im} = \theta_{im}/\theta$

4. STREAM TUBE MODEL FOR FIELD-SCALE TRANSPORT

4.1. Introduction

Traditional deterministic approaches based upon the convection-dispersion equation (CDE) for chemical transport and the Richards equation for water flow work relatively well for homogeneous soils and packed laboratory soil columns. However, most field soils are far from homogeneous, resulting in sometimes highly nonuniform flow and transport processes. Experimental investigations at the field scale have demonstrated the effects of heterogeneity on solute transport [e.g., *Biggar and Nielsen,* 1976; *Sudicky,* 1986]. A variety of stochastic modeling approaches have been employed to describe nonreactive solute transport in a heterogeneous flow field [e.g., *Dagan,* 1984; *Sposito and Barry,* 1987]. Recently, stochastic methods have also been used to study solute transport subject to equilibrium *[Kabala and Sposito,* 1991] or nonequilibrium adsorption [e.g., *Dagan and Cvetkovic,* 1993; *Bellin et al.,* 1993]. In these investigations, a transport equation in terms of a mean solute concentration across the field is formulated using the covariance functions of local-scale transport parameters. Unfortunately, it is usually not possible to determine a reliable statistical distribution for each parameter.

In a simplified approach to stochastic modeling, the field may be viewed as a series of independent vertical soil columns (cf. Figure 4.1). These columns are generally referred to as "stream tubes" *[Dagan,* 1993; *Jury and Roth,* 1990]. Local-scale transport in each stream tube is described deterministically assuming a convective or convective-dispersive model. Transport at the field scale may be modeled by viewing selected parameters in the convective or convective-dispersive model for each tube as realizations of a stochastic process. The mean solute concentration for an entire field is given by the ensemble average of the local concentrations in all stream tubes. At the field scale, the one-dimensional CDE (perfect mixing perpendicular to the flow direction) and the stream tube model (no mixing between tubes) constitute the limiting cases for solute transport [Jury *and Flühler,* 1992].

There are several ways in which the stream tube model has been used to quantify solute transport in heterogeneous soils. *Dagan and Bresler* [1979] and *Bresler and Dagan* [1979] described the downward movement of nonreactive solutes at the field scale assuming a lognormal distribution for

the saturated hydraulic conductivity. *Jury* [1982] used a so called convective lognormal transfer function model (CLT), which neglects local-scale dispersion. *Van der Zee and van Riemsdijk* [1986, 1987] applied the stream tube model to reactive solutes, while *Destouni and Cvetkovic [* 1991] introduced physical and chemical nonequilibrium in the local-scale transport model.

CXTFIT 2.0 allows the use of the stream tube model for a variety of transport scenarios. The analytical solutions of the equilibrium and nonequilibrium CDE as described in Chapters 2 and 3, will be used to model local-scale transport. Stochastic variables are the pore water velocity, v, in combination with either the dispersion coefficient, D, the distribution coefficient for linear adsorption, K_d or the fist-order rate coefficient for nonequilibrium adsorption, α. These three different pairs of random parameters are described with a bivariate lognormal joint probability density function (pdf). Further details can be found in *Tori& andLeij* [1995a]. The implications of describing the transport problem as an initial or as a boundary problem for the stream tube model were discussed by *Jury and Scotter [* 1994] and *Toride and Leij [* 1995b].
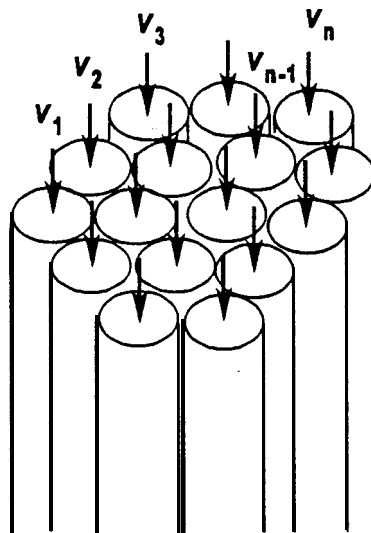
Fig. 4.1. Schematic illustration of the stream tube model.

4.2. Local-Scale Transport

We will describe solute transport at the local scale with the one-dimensional one-site chemical nonequilibrium CDE by setting f to zero in (3.1) and (3.2):

$$\frac{\partial c_r}{\partial t} = D\frac{\partial^2 c_r}{\partial x^2} - v\frac{\partial c_r}{\partial x} - \frac{\alpha \rho_b}{\theta}\left[K_d c_r - s\right] - \mu_l c_r + \gamma_l(x) \tag{4.1}$$

$$\frac{\partial s}{\partial t} = \alpha\left[K_d c_r - s\right] - \mu_s s + \gamma_s(x) \tag{4.2}$$

The subscript k is now dropped because there are no equilibrium adsorption sites. Furthermore, transport equations are given in dimensional form in this chapter. For equilibrium adsorption ($\alpha \to \infty$), the nonequilibrium CDE reduces to (cf. (2.3)):

$$R\frac{\partial c_r}{\partial t} = D\frac{\partial^2 c_r}{\partial x^2} - v\frac{\partial c_r}{\partial x} - \mu c_r + \gamma(x) \tag{4.3}$$

where the retardation factor R was defined as

$$R = 1 + \frac{\rho_b K_d}{\theta} \tag{4.4}$$

and where μ and γ are given by (2.5) and (2.6), respectively. We will assume equal degradation rates in the liquid and adsorbed phases, i.e., $\mu = \mu_l R$.

The equilibrium and nonequilibrium CDEs were solved subject to the following general initial and boundary conditions (cf. Chapters 2 and 3):

$$c_r(x, 0) = c_i(x), \quad s(x, 0) = K_d c_i(x) \tag{4.5a,b}$$

$$v c_r(0, t) - \delta D\frac{\partial c_r(0, t)}{\partial x} = v c_o(t) \tag{4.6}$$

$$\frac{\partial c_r}{\partial x}(\infty, t) = 0 \tag{4.7}$$

in which $\delta = 0$ for a first-type and $\delta = 1$ for a third-type inlet condition. A flux-averaged concentration, c_f, can be obtained from c_r according to (2.13). The dimensionless solutions of the BVP, IVP, and PVP were previously presented in Chapters 2 and 3.

35

The solution of the local-scale transport equation depends exclusively on random transport parameters such as v, D, and K_d, once the independent variables t and x have been specified. For example, Figure 4.2a shows the solution, c_r, for the equilibrium CDE as a function of v and K_d at t = 5 d for a 2-d pulse input at $x = 100$ cm assuming $D = 20$ cm^2 d^{-1} and $\rho_b/\theta = 4$ g cm" (cf. (2.20)). The concentration is normalized using the input concentration, c_o. As K_d increases, the solute moves slower because of increased adsorption; a higher v is required for the solute to reach $x = 100$ cm at $t = 5$ d.

4.3 Field-Scale Transport

4.3.1. Bivariate Lognormal Distribution

The pairs of stochastic parameters in the local-scale model for transport in each stream tube are obtained from a bivariate lognormal joint probability density function (pdf). Because of their relatively low coefficient of variation, CV, the same values for θ and ρ_b are used for each stream tube. The joint pdfs of v, in conjunction with either D, K_d, or α, are written as $f(v,D)$, $f(v,K_d)$, and $f(v,\alpha)$, respectively. The general bivariate lognormal joint pdf is defined as [Spiegel, 1992; p. 118]:

$$f(v,\eta) = \frac{1}{2\pi\sigma_v\sigma_\eta v\eta\sqrt{1-\rho_{v\eta}^2}} \ \exp\left(-\frac{Y_v^2 - 2\rho_{v\eta}Y_vY_\eta + Y_\eta^2}{2(1-\rho_{v\eta}^2)}\right) \tag{4.8}$$

with

$$Y_v = \frac{\ln(v) - \mu_v}{\sigma_v} \ , \qquad Y_\eta = \frac{\ln(\eta) - \mu_\eta}{\sigma_\eta} \tag{4.9a,b}$$

$$\rho_{v\eta} = <Y_vY_\eta> = \int_0^\infty \int_0^\infty Y_vY_\eta f(v,\eta)\,dv\,d\eta \tag{4.10}$$

where η denotes D, K_d, or a (i.e., the second random parameter in addition to v), μ and σ are the mean and standard deviation of the log-transformed variable, and $\rho_{v\eta}$ is the correlation coefficient between Y_v and Y_η.
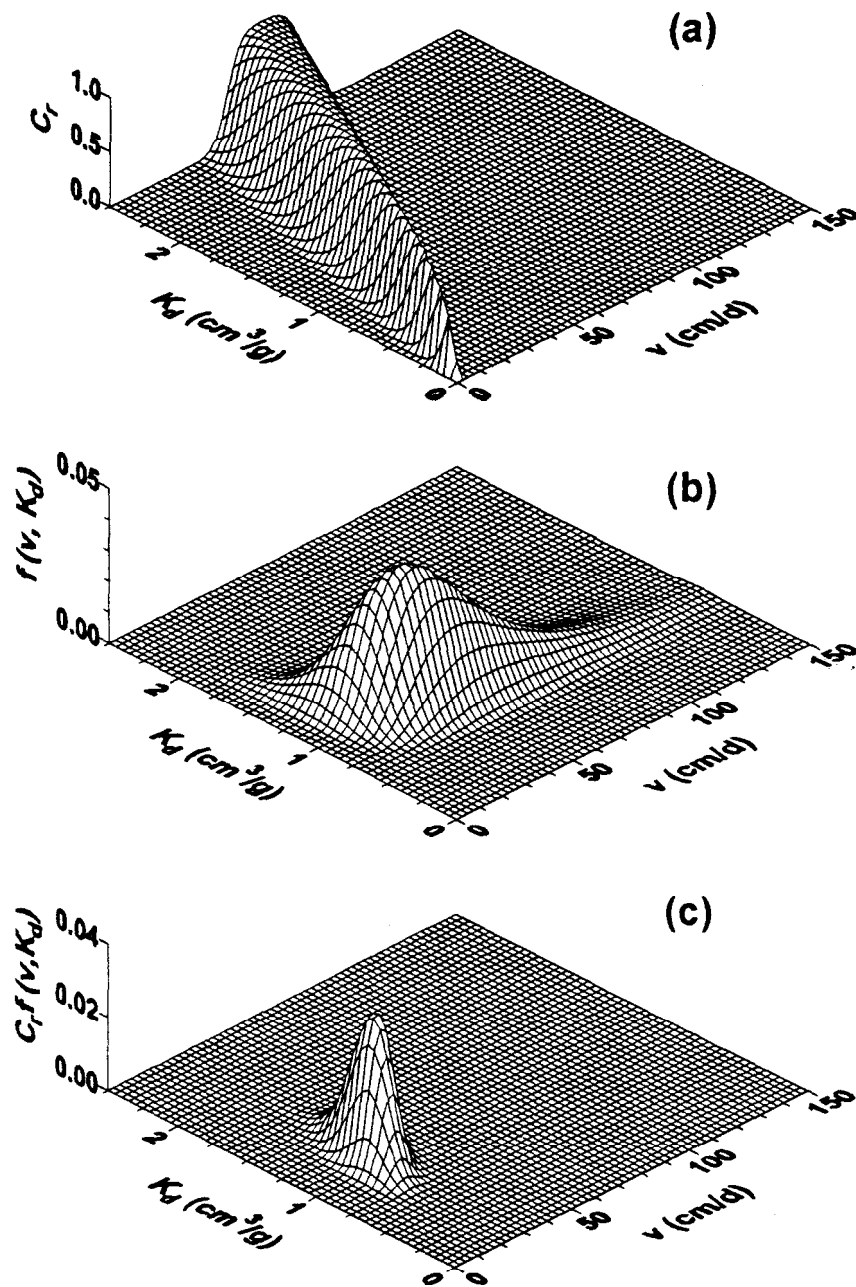
Fig. 4.2. Predicted resident concentrations according to the stream tube model:
(a) local-scale c_r as a function of v and K_d at $x = 100$ cm and $t = 5$ d;
(b) a bivariate lognormal pdf for $\rho_{vKd} = -0.5$; and
(c) expected c_r at x = 100 cm and $t = 5$ d.

The ensemble averages of v and η are given by *[Aitcheson and Brown,* 1963; p. S]:

$$<v> = \exp\left(\mu_v + \frac{1}{2}\sigma_v^2\right), \qquad <\eta> = \exp\left(\mu_\eta + \frac{1}{2}\sigma_\eta^2\right) \tag{4.11a,b}$$

with the coefficient of variation CV expressed as

$$CV(v) = \sqrt{\exp(\sigma_v^2) - 1}, \qquad CV(\eta) = \sqrt{\exp(\sigma_\eta^2) - 1} \tag{4.12a,b}$$

Figure 4.2b presents an example of a bivariate lognormal pdf for v and K_d with $<v> = 50$ cm d^{-1}, $\sigma_v = 0.2$ cm d^{-1}, $<K_d> = 1$ cm^3 g^{-1}, $\sigma_{Kd} = 0.2$ cm^3 g^{-1}, and $\rho_{vKd} = -0.5$. The distribution for v is skewed due to the relatively high standard deviation, σ_v, whereas the smaller σ_{Kd} results in a more symmetric distribution for K_d. The value for v tends to increase as K_d decreases.

The joint pdf given by (4.8) can be simplified for some special cases. When two parameters are uncorrelated, i.e., $\rho_{v\eta} = 0$, the joint pdf is the product of two single pdfs:

$$f(v, \eta) = f(v) \cdot f(\eta) \tag{4.13}$$

where the single lognormal distribution is given by

$$f(\eta) = \frac{1}{\sqrt{2\pi}\sigma_\eta \eta} \exp\left(-\frac{[\ln(\eta) - \mu_\eta]^2}{2\sigma_\eta^2}\right) \tag{4.14}$$

A perfect correlation, i.e., $\rho_{v\eta} = 1$ or -1, is the result of a complete dependency of the stochastic variables with $Y_\eta = Y_v$ and $Y_\eta = -Y_v$, respectively. Subsequent use of (4.11) yields

$$\eta(v) = \left(\frac{v}{<v>}\right)^{\frac{\rho_{v\eta}\sigma_\eta}{\sigma_v}} <\eta> \exp\left(\frac{\rho_{v\eta}}{2}\sigma_v\sigma_\eta - \frac{1}{2}\sigma_\eta^2\right) \tag{4.15}$$

In this case, the distributions of v and η are given by either $f(v)$ or $f(\eta)$. Figure 4.3 demonstrates the two cases of perfect correlation between v and K_d — the same values for the mean and standard deviation are used as in Figure 4.2b. For a perfect negative correlation K_d decreases as v increases, and vice versa.

Additional stochastic parameters can be included as long as only two of the parameters are independent. CXTFIT 2.0 can evaluate up to four stochastic parameters in this manner.
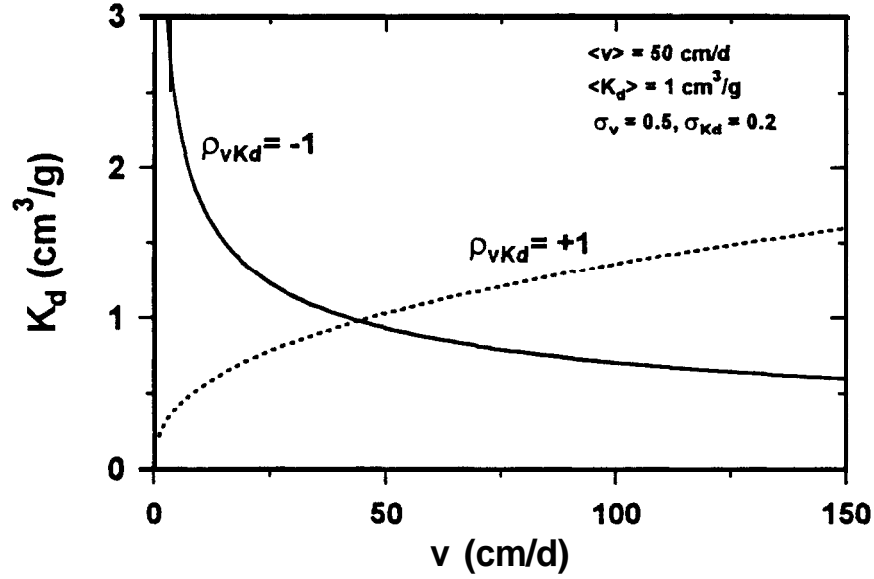
Fig. 4.3. Perfect positive and negative correlation for stochastic v and K_d.

4.3.2. **Field-Scale Mean Concentration**

Field-scale transport may be modeled by averaging the local-scale concentrations over all stream tubes. In case of weak stationarity and ergodicity of the random functions describing the stochastic parameters [cf. de *Marsily, 1986; Dagan,* 1989], the spatial average for the entire field is identical to the ensemble average:

$$<c(x,t)> = \frac{1}{A}\int_A c(x,t)\,dA = \int_0^\infty \int_0^\infty c(x,t;v,\eta)f(v,\eta)\,dv\,d\eta \qquad (4.16)$$

where A denotes the area of the field. The local concentration can be of the resident or flux-averaged type, in which case the corresponding ensemble averages are $<c_r>$ and $<c_f>$, respectively. The above assumptions of weak stationarity and ergodicity seem reasonable for our idealized pdfs.

The field-scale resident concentration, $\hat{c}_r$, which represents the resident concentration averaged over the entire horizontal plane as determined by a "sufficient" number of samples at a particular depth, is equal to the ensemble average, $<c_r>$, given by (4.16):

$$\hat{c}_r(x,t) = <c_r(x,t)> \qquad (4.17)$$

39

Figure 4.2c shows the product of the individual resident concentrations (Figure 4.2a) and the joint pdf(Figure 4.2b), such a product also appears in the integrand on the right-hand side of (4.16). The peak in Figure 4.2c suggests that stream tubes with $v \ll 20$ cm $\mathbf{d^{-1}}$ and $K_d \approx 1$ $\mathbf{cm^3\ g^{-1}}$ contribute the most to the field-scale mean concentration for the selected independent variables $(x = 100$ cm and $t = 5$ d). The total volume of the distribution in Figure 4.2c corresponds to the ensemble average $<c_r>$ which is equal to $\hat{c}_r$. The field-scale total resident concentration, $\hat{c}_T$, for nonequilibrium adsorption is obtained as the total solute amount per unit solution volume:

$$\hat{c}_T = \left\langle c_r + \frac{\rho_b s}{\theta} \right\rangle = \hat{c}_r + \frac{\rho_b}{\theta}<s>$$

(4.18)

For equilibrium adsorption (i.e., $s = K_d c_r$), (4.18) can be simplified to $\hat{c}_T = <Rc_r>$. Notice that $<Rc_r> \neq <R><c_r>$ for a stochastic K_d.

A field-scale flux-averaged concentration, $\hat{c}_f$, can be defined as the ratio of the mean solute and water fluxes in a similar manner as (4.16):

$$\hat{c}_f(x,t) = <vc_f> / <v> = \frac{1}{<v>} \int_0^\infty \int_0^\infty v c_f(x,t;v,\eta) f(v,\eta)\,dv\,d\eta$$

(4.19)

The solute flux for an entire field is given by A $\theta<v>\hat{c}_f$. Unlike the resident concentration, the ensemble and field-scale average of this flux-averaged concentration will generally be different (i.e., $\hat{c}_f \neq <c_f>$) since $<vc_f> \neq <v><c_f>$. Because local values for v are not easily obtained experimentally, estimates for $\hat{c}_f$ will be diicult to obtain. The pdf for the pore- water velocity, $f(v)$, may be estimated from either $\hat{c}_r$ or $<c_f>$. Once $f(v)$ is specified, $\hat{c}_f$ can be calculated subsequently.

Variations in the local resident or flux-averaged concentration between stream tubes across the horizontal plane (i.e., at a particular depth and time) can be characterized by its variance [*Bresler and Dagan,* 1981]:

$$\mathrm{Var}[c(x,t)] = \int_0^\infty \int_0^\infty [c(x,t) - <c(x,t)>]^2 f(v,\eta)\,did\,\eta = <c^2(x,t)> - <c(x,t)>^2$$

(4.20)

where c may denote either c_r or c_f. The variance corresponding to the field-scale flux-averaged concentration, $\hat{c}_f$, is expressed as

$$\text{Var}\left[\frac{vc_f(x,t)}{<v>}\right] = \frac{1}{<v>^2} \int_0^\infty \int_0^\infty [vc_f(x,t) - <vc_f(x,t)>]^2 f(v,\eta)\,dv\,d\eta$$

$$= \left[<v^2 c_f^2(x,t)> - <vc_f(x,t)>^2\right] \Big/ <v>^2$$

(4.21)

The variance for the adsorbed phase concentration s across the horizontal plane may be defined in a similar manner as (4.20) and (4.21).

4.4. Solute Application for the Stream Tube Model

A correct mathematical description of how the solute is applied at the surface is necessary for effective use of the stream tube model. We will present several possible formulations for the solute application depending upon whether each stream tube contains the same amount of solute, or the amount of solute in each stream tube is proportional to the local-scale pore-water velocity, v. Only a third-type inlet condition ($\delta=1$ in (4.6)) will be considered; similar results can be obtained for a first-type inlet condition.

Dirac-Type Application

The instantaneous application of solute to the surface of an initially solute-free soil profile, may be described as a boundary value problem (BVP) with $c_i = 0$ and $c_o(t)$:

$$c_o(t) = \frac{m_B}{v} \delta(t)$$

(4.22)

where $\delta(t)$ is the Dirac delta function [d^{-1}] and m_B is the amount of mass added to a unit area of the liquid phase in a stream tube [g cm^{-2}] (see also (2.16b)). The amount of mass added to a unit area of soil is given by θm_B where θ is the volumetric water content. When the solute is applied uniformly across the field during a fixed and short period of time, the amount of mass, m_B, added to each stream tube will be equal to $v<m_B>/<v>$, where $<m_B>$ is the mean of m_B for all tubes (see input parameter MASSST in Table 6.7).

The above scenario can also be described as an initial value problem (IVP) in which solutes are initially distributed uniformly across the soil surface, and solute-free water ($c_o(t) = 0$) is applied to the soil surface. The initial distribution is now described as

$$c_i(t) = \frac{m_I}{\theta}\,\delta(x) \qquad\qquad\qquad (4.23)$$

where $\delta(x)$ is the Dirac delta function [cm^{-1}], describing the initial solute spike at $x = 0$, and m_I is the amount of mass present per unit cross sectional soil area [g cm^{-2}] (see also (2.24b)). The same amount of solute, m_I, is present in all stream-tubes regardless of v.

Figure 4.4 illustrates the solute distribution between tubes for the BVP according to (4.22) and the IVP according to (4.23). Figure 4.5 demonstrates the effect of the two different solute applications on $\hat{c}_r$ predicted as a function of depth at $t = 1$ d (the concentrations are normalized by assuming $m_B/v = 1$). The same amount of nonreactive chemical ($R = 1$, $<m_B> = m_I/\theta$) is recovered in the soil profile, either applied at $x = 0$ for the BVP or present at $t = 0$ for the IVP. Additional parameters are: $<v> = 50$ cm d^{-1}, $<D> = 20$ cm^2 d^{-1}, and $\sigma_v = \sigma_D = 0.5$. Figure 4.5 shows that more solute remains near the surface for the IVP, while the BVP predicts somewhat faster downward movement since a larger fraction of solutes resides in stream tubes with a higher velocity as a result of the velocity dependent application. Although this example pertains to a Dirac delta function, similar differences between the boundary and initial value problems occur for other influent and initial solute concentration profiles.

The BVP will give identical results as the IVP if m_B is the same for each tube, regardless of the local v, as long as solute adsorption is instantaneous. The solutions for the BVP according to (4.22) and the IVP according to (4.23) are identical for the equilibrium CDE when $m_B = m_I/\theta$ (cf. (2.17) and (2.24)). However, this equality does not hold for nonequilibrium adsorption. The solutions of the nonequilibrium CDE for the BVP and IVP are different because of the kinetic desorption process (cf. (3.17) and (3.34)). We finally note that for the equilibrium CDE, the ensemble average of the flux-averaged concentration, $<c_f>$, for the BVP with variable m_B according to (4.22), is identical to the field-scale flux-averaged concentration, $\hat{c}_f$, for the IVP according to (4.23).
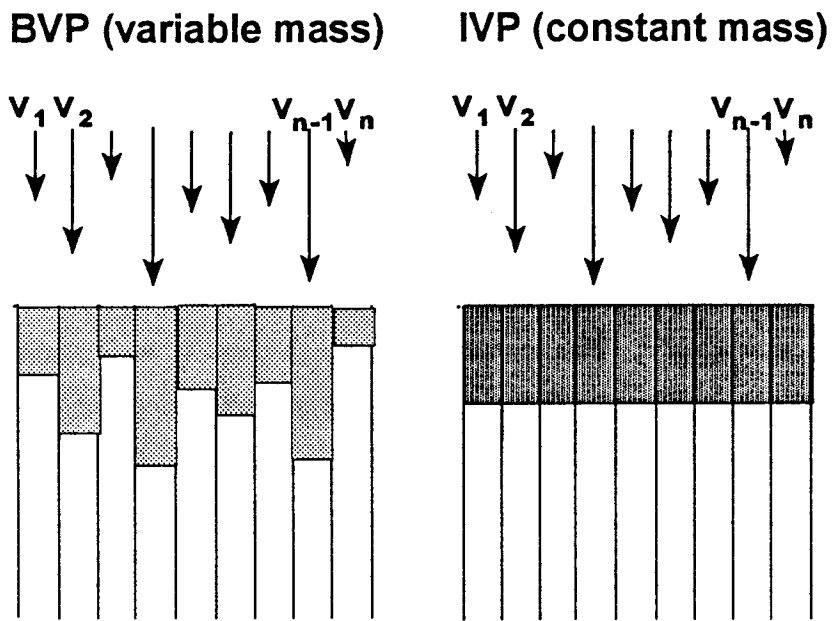
Fig. 4.4. Illustration of the solute distribution in stream tubes for variable and constant mass solute applications based on the BVP and IVP.
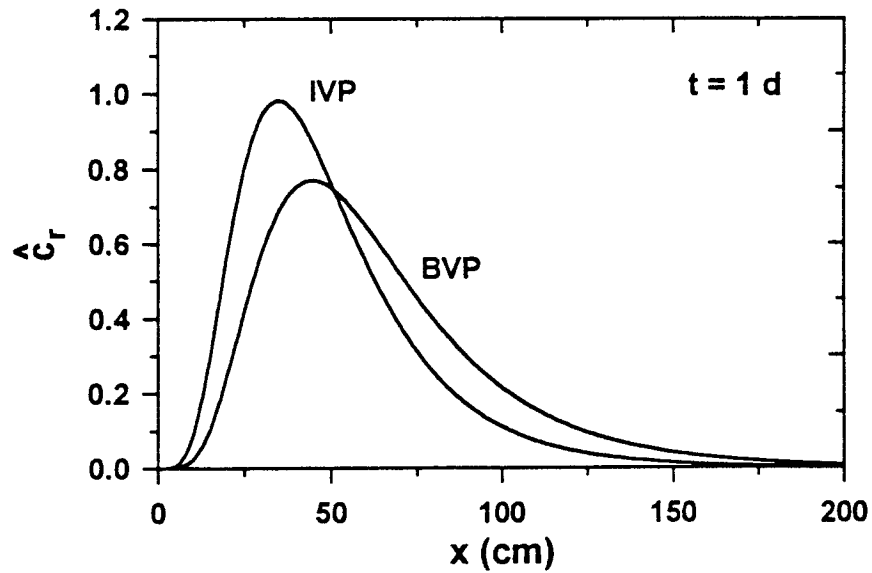
Fig. 4.5. Field-scale resident concentrations $(\hat{c}_r)$ versus depth as the result of instantaneous solute application to the surface described as a BVP or an IVP.

Pulse-Type Application

Following *Parker and van Genuchten* [1984b], we study the BVP involving a finite pulse input for the case of either a constant or variable application time for each tube. Consider a pulse-type solute application of **concentration** f_1 and application time t_2 (cf. Figure 2.1). If t_2 is constant for all stream tubes, the amount of solute in each tube, $m_B = f_1 t_2 v$, is directly proportional to the random velocity, v. The field-averaged mean, $<m_B>$, is given by $f_1 t_2 <v>$. However, the same amount of mass, m_B, can be delivered to each tube by setting the application time inversely proportional to the velocity, i.e., $t_2 = m_B/(f_1 v)$. This scenario, where both v and t_2 are random, may occur when solid chemicals are added uniformly across the field and leached subsequently by continuously applying solute-free water. The input concentration, f_1, is regarded as approximately constant since this concentration may be governed by the solubility of the chemical. Figure 4.6 schematically illustrates the solute distribution between tubes for a pulse input of constant and variable duration.

Figure 4.7 presents field-scale resident concentrations ($\hat{c}_r$) versus depth at $t = 3$ d as a result of a pulse-type solute application with a constant ($t_2 = 1$ d) and variable ($<t_2> = 1$ d) solute application time. The same amount of solute is applied to the entire field. The transport parameters for this example are the same as those used for Figure 4.5. Again, more solute remains near the surface for the constant mass injection. Since the amount of solute in stream tubes with a higher v is larger for the constant duration scenario, solute moves down faster in this case compared to the case of a variable solute application time.

We emphasize that the previous examples involving Dirac- and pulse-type applications are somewhat hypothetical since the stream tube model does not permit mixing between stream tubes. Redistribution between stream tubes is likely to establish an intermediate situation where the mass in each stream tube is not constant, but where differences between tubes are also not as large as for the constant duration case because of horizontal mixing. Some horizontal mixing will likely **also** occur at the surface.

Constant duration   **Variable duration**
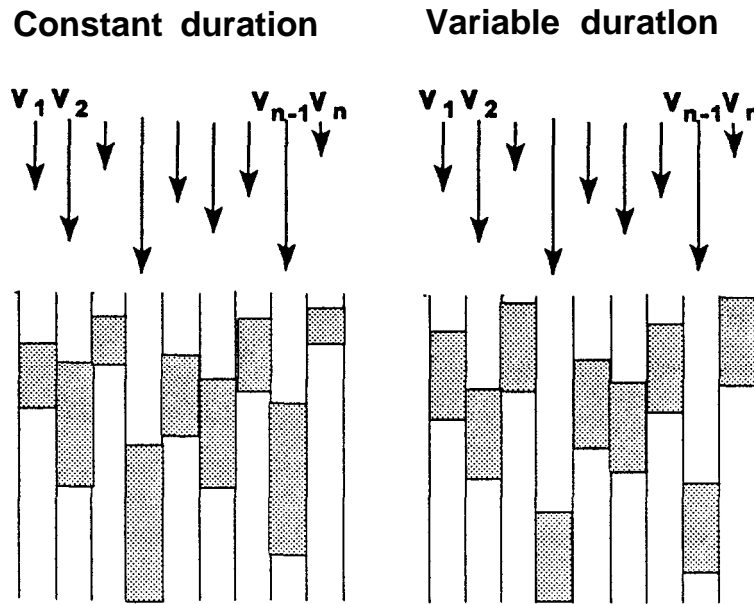
Fig. 4.6. Illustration of the solute distribution in stream tubes
after a pulse application of constant and variable duration.
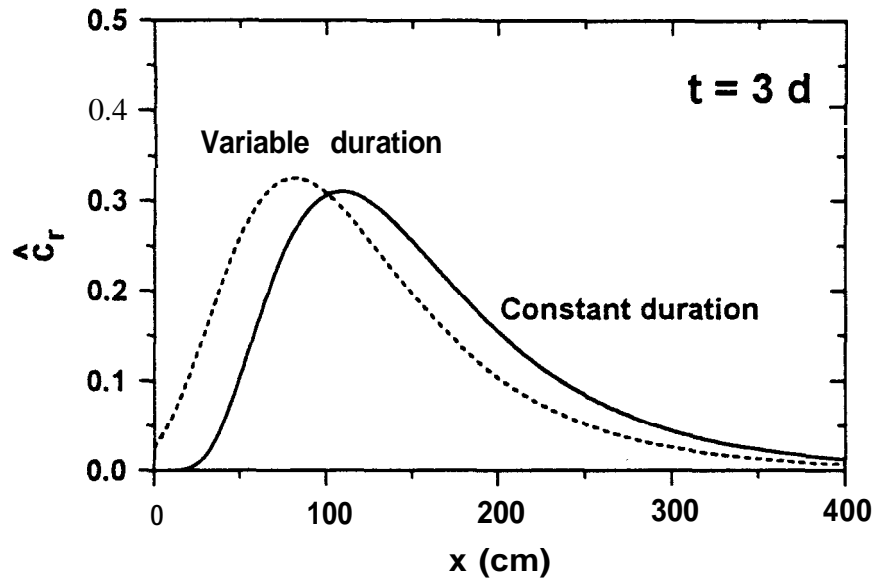
Fig. 4.7. Field-scale resident concentrations $(\hat{c}_r)$ versus depth as a result
of a pulse-type solute application of constant and variable duration.

4.5. Stream Tube Models in CXTFIT 2.0

CXTFIT 2.0 allows the use of the stream tube model using several analytical solutions of the CDE for local-scale transport, and with stochastic parameters described by the bivariate lognormal pdfs can be used, viz. $f(v, D)$, $f(v, K_d)$, and $f(v, a)$. Two additional stochastic parameters can be included provided that they are perfectly correlated with v (cf. (4.15)).

If v and D are stochastic, a positive correlation between them might be plausible as suggested by the widely used relationship for the dispersivity, $\lambda = D/v$. Substitution of $\eta = D$ into (4.15) for a perfect positive correlation, $\rho_{vD} = 1$, leads to

$$D(v) = \left(\frac{v}{<v>} \right)^{\frac{\sigma_D}{\sigma_v}} <D> \exp\left(\frac{1}{2}\sigma_v\sigma_D - \frac{1}{2}\sigma_D^{\,2} \right) \qquad (4.24)$$

In case $\sigma_v = a$,, the relationship between v and D can be simplified to

$$D(v) = <D> v \Big/ <v> \qquad (4.25)$$

This equation implies a constant dispersivity $\lambda = <D>/<v>$ for all stream tubes (cf. Eq.(60) of *Parker and van Genuchten* [1984b]).

A negative correlation between v and K_d may also be plausible since coarse-textured soils generally have a relatively high conductivity — and hence a high v — and a small K_d — and therefore a small R — whereas the opposite is true for fine-textured soils. When $\rho_{vKd} = -1$, the expression for K_d becomes (cf. (4.15)):

$$K_d(v) = \left(\frac{v}{<v>} \right)^{-\frac{\sigma_{Kd}}{\sigma_v}} <K_d> \exp\left(-\frac{1}{2}\sigma_v\sigma_{Kd} - \frac{1}{2}\sigma_{Kd}^{\,2} \right) \qquad \textit{(4.26)}$$

If, in addition, we assume that $\sigma_v = \sigma_{Kd}$, this expression may be written as

$$K_d(v) = <v><K_d> \exp\left(-\sigma_v^2\right) \Big/ v \qquad (4.27)$$

An overview of the five stream tube models in CXTFIT 2.0 will be given later in Table 6.1. The boundary (BVP), initial (IVP), and production (PVP) value problems in terms of the field-scale stream tube model foilow directly from the local-scale solution.

5. NUMERICAL EVALUATION

The FORTRAN program CXTFIT 2.0 was written to evaluate the one-dimensional analytical solutions that were discussed in Chapters 2 through 4. In this chapter we will provide background information on numerical procedures followed to solve the direct and inverse problems. First, the main program units of CXTFIT 2.0 are briefly reviewed. The numerical evaluation of the integrals and various special functions in the analytical solutions are discussed subsequently. The previous version of CXTFIT published by *Parker and van Genuchten* [1984b] was widely used to fit mathematical solutions to experimental results in order to estimate transport parameters. We have included several details of the estimation procedure, which is based on the Levenberg-Marquardt algorithm.

We note that all the information needed to use the program is given in Chapter 6. Detailed instructions for the preparation of the input file are presented in Section 6.2, while significant variables and arrays in CXTFIT 2.0 are listed in the Appendix. This Chapter 5 should be of special interest to readers who experience unexpected results due to errors in the evaluation of mathematical functions, or when trying to solve inverse problems.

5.1. Description of Program Units

CXTFIT 2.0 consists of a main program, 22 subroutines, and 27 functions. These subprograms are stored in nine source files. The executable program CXTFIT2 is obtained after compiling and linking. Table 5.1 presents a list of the source files and associated subprograms.

CXTFIT2. FOR

The program unit **Main** controls the input, output, and parameter optimization procedures. The subroutine **MATINV** performs matrix inversion for the least-squares analysis.

Table 5.1. Source files in CXTFIT 2.0

Source file	Subroutine and Function
CXTFIT2.FOR	Main, MATINV
DATA.FOR	DATAIN, CHECK, DATAOUT
MODEL.FOR	MODEL, DIRECT
DETCDE.FOR	DETCDE, BOUND, INITIAL, PRODUC
STOCDE.FOR	STOCDE, CON-PROV, CONPROY, LIMIT, XLNPROB, BLNPROB
FUNC 1 .FOR	CTTRAN, CBJ, CBAL, CBEXP, CBIN1, CBIN2, CIVP, C1PRO, C2PRO, CCO, CC1, CC2, CC3, CC4, CC5, PROW
FUNC2.FOR	DBEXP, EXF, EXPBIO, EXPBI1, PHI1, PHI2, GOLD,
INTEGRAL.FOR	ROMB, ROMB2, CHEBY, CHEBY2, CHEBYCON, CHEBYLOG, CHEBYLOG2
USER.FOR	CONST1, CONST2, CINPUT

DATA.FOR

Subroutine DATAIN reads data from the input file specified by the user. The data is verified with subroutine CHECK, which gives error messages for unacceptable input. The subroutine DATAOUT writes user-provided input data to the output file.

MODEL.FOR

Subroutine MODEL performs coefficient assignments and routes the execution to an appropriate subroutine for evaluation of a particular model. Subroutine DIRECT calculates the concentration for specific times and depths (i.e., the solution of the direct problem).

DETCDE.FOR

Subroutine DETCDE models deterministic transport according to the equilibrium and nonequilibrium CDE by adding the solutions for the BVP, IVP, and PVP. Subroutines BOUND, INITIAL, and PRODUC are used to calculate the specific solutions for the BVP, IVP, and PVP, respectively.

STOCDE.FOR

This file calculates concentrations and variances for stochastic transport. Subroutine **STOCDE** routes the execution. Function **CONPROV** is used for integration with respect to v, while the function **CONPROY** evaluates the integrand for other stochastic parameters. Subroutine **LIMIT** modifies the integration boundaries for the field-scale mean concentrations using the Newton-Raphson method. Subroutines **XLNPROB** and **BLNPROB** quantify the single and bivariate lognormal distributions, respectively.

FUNC1.FOR

This file evaluates many of the functions used in the analytical solutions for the equilibrium and nonequilibrium CDE. The integrands in the nonequilibrium CDE are determined by the functions: CTTRAN for (3.17) and (3.18), **CBJ** for (3.21) and (3.22), **CBAL** for (3.23) and (3.24), **CBEXP** for (3.26) and (3.27), CBIN1 for (3.13), CBIN2 for (3.14), **CIVP** for the IVP (i.e., (3.34), (3.35), (3.37), (3,38), (3.40), and (3.41)), C1PRO for (3.47) and (3.50), and C2PRO for (3.48) and (3.51). The functions listed in Tables 2.2, 2.3, 3.2, and 3.3 are evaluated as follows: CC0 for Γ_1^E or I',", **CC1** for G_1^E or G_1^N for $\Omega = 0$, **CC2** for ψ_1^E or ψ_1^N, **CC3** for ψ_2^E or ψ_2^N, **CC4** for G_1^E or G_1^N if $\Omega \neq 0$; **CC5** for Γ_2^E or Γ_2^N; and PROD0 for G_2^E.

FUNC2.FOR

The remaining functions in the analytical solutions are evaluated in FUNC2.FOR. The function **DBEXP** calculates the exponential function (exp), a (minimum) constraint of -100 is placed on the value of the argument. The function **EXF** evaluates the product of the exponential function (exp) and the complementary error function (erfc). **EXPBIO** and EXPBI1 are used to determine the product of the exponential function (exp) and the modified Bessel functions of order zero (I_0) and one (I_1), respectively (used in H_0 and H_1 as shown in Table 3.4). Functions **PHI1** and **PHI2** are used for exponential solute input to calculate Φ_1 in (3.28) and Φ_2 in (3.29). Goldstein's J-function (Table 3.4) is determined with the function GOLD, which appears in the BVP and PVP for the nonequilibrium CDE.

INTEGRAL.FOR

This file includes subroutines for numerical integration. Subroutines **ROMB** and ROMB2 perform a Romberg quadrature on a log-transformed interval for the field-scale mean concentration. Subroutines **CHEBY**, CHEBY2, and **CHEBYCON** use Gauss-Chebyshev quadrature to determine integrals in the solutions for the nonequilibrium CDE. Similarly, routines **CHEBYLOG** and CHEBYLOG2 carry out the integration on a log-transformed interval.

USER.FOR

USER.FOR contains subroutines that allow a user to change settings for the numerical integration or the input function. The default settings have been found to work well in most cases. Subroutine CONST1 includes parameters for the least-squares inversion method and Gauss-Chebyshev quadrature, while **CONST2** specifies parameters for Romberg quadrature. The user can specify an arbitrary input function with **CINPUT**.

5.2. Deterministic CDE

The analytical solutions described in Chapters 2 and 3 are evaluated in **DETER.FOR**. Several functions for evaluating these solutions are stored in FUNC1.FOR and FUNC2.FOR. The expressions for the equilibrium CDE (Table 2.2 and 2.3) are evaluated by setting $\beta = 1$ in the functions for the nonequilibrium CDE (Table 3.2 and 3.3).

The function **EXF**(A,B) defines the product of the exponential function (exp) and the complementary error function (erfc) *[van Genuchten and Alves,* 1982]:

$$\text{EXF}(A,B) = exp(A)\,\text{erfc}(B) \tag{5.1}$$

where

$$\text{erfc}(B) = \frac{2}{\sqrt{\pi}}\int_{B}^{\infty}\exp(-\tau^{2})d\tau \tag{5.2}$$

Two different approximations are used for **EXF**(A,B). For $0 \le B \le 3$ [see also (7.1.26) of *Abramowitz and Stegun,* 1970]

$$\text{EXF}(A,B) \approx \exp(A - B^2)(a_1\tau + a_2\tau^2 + a_3\tau^3 + a_4\tau^4 + a_5\tau^5) \tag{5.3}$$

where $\tau = 1/(1+0.3275911B)$, $a_1 = 0.254896$, $a_2 = -0.2844967$, $a_3 = 1.421414$, $a_4 = -1.453152$, and $a_5 = 1.061405$. For $B>3$ [(7.1.14) of *Abramowitz and Stegun*, 1970]:

$$\text{EXF}(A,B) \approx \frac{1}{\sqrt{\pi}}\exp(A-B^2)\Big/ (B+0.5/(B+1.0/(B+1.5/(B+2.0/(B+2.5/(B+1.0)))))) \tag{5.4}$$

The following relation is used for negative values of B:

$$\text{EXF}(A,B) = 2\exp(A) - \text{EXF}(A,-B) \tag{5.5}$$

The above approximations do not work well if the arguments A and/or B are small. Therefore, EXF(A,B) is set to zero for either of the following two conditions:

$$\begin{array}{cc} |A| > 170 & \\ B \le 0 & \end{array} \quad \text{or} \quad \begin{array}{c} |A - B^2| > 170 \\ B > 0 \end{array} \tag{5.6}$$

Evaluation of the function $G(Z,T;\Omega)$ listed in Tables 2.3 and 3.3 depends on the value of Ω. Note that for an exponential input involving a large λ^B, Ω in solution (2.21) can be less than $-P/4$. In this case the integral in the general expression for $G(Z,T;\Omega)$ will be evaluated using numerical integration.

The functions $H_0(\tau, T)$ and $H_1(\tau, T)$ in the solutions listed in Table 3.4 are evaluated with EXPBI0 and EXPBI1, respectively, using (9.8.1), (9.8.2), (9.8.3), and (9.8.4) of *Abramowitz and Stegun* [1970] with $Y = X/3.75$:

EXPBI0 $(X,Z) = e^Z I_0(X)$

$$= \begin{cases} e^Z(1.0 + 3.5156229\,Y^2 + 3.0899424\,Y^4 + 1.2067492\,Y^6 \\ \quad + 0.2659732\,Y^8 + 0.0360768\,Y^{10} + 0.0045813\,Y^{12}) \quad (-3.71 \le X \le 3.75) \\[2mm] e^{(Z+X)}/\sqrt{X}\,(0.39894228 + 0.01328592\,Y^{-1} + 0.00225319\,Y^{-2} \\ \quad - 0.00157565\,Y^{-3} + 0.00916281\,Y^{-4} - 0.02057706\,Y^{-5} \\ \quad + 0.02635537\,Y^{-6} - 0.01647633\,Y^{-7} + 0.00392377\,Y^{-8}) \quad (X \ge 3.75) \end{cases} \tag{5.7}$$

EXPBI1 $(X,Z) = e^Z I_1(X)$

$$= \begin{cases} X e^Z(0.5 + 0.87890594\,Y^2 + 0.51498869\,Y^4 + 0.15084934\,Y^6 \\ \quad + 0.02658733\,Y^8 + 0.00301532\,Y^{10} + 0.00032411\,Y^{12}) \quad (-3.71 \le X \le 3.75) \\[2mm] e^{(Z+X)}/\sqrt{X}\,(0.39894228 - 0.03988024\,Y^{-1} - 0.00362018\,Y^{-2} \\ \quad + 0.00163801\,Y^{-3} - 0.01031555\,Y^{-4} + 0.02282967\,Y^{-5} \\ \quad - 0.02895312\,Y^{-6} + 0.01787654\,Y^{-7} - 0.00420059\,Y^{-8}) \quad (X \ge 3.75) \end{cases} \tag{5.8}$$

Goldstein's *J*-function, given in Table 3.4, is evaluated with the function **GOLD**. Two approximations are used depending on the values of *a* and *b* [*van Genuchten*, 1981b]. For relatively small values of *a* and *b*, a series expansion of the Bessel function is integrated [*De Smedt and Wierenga*, 1979]. For $a \geq b$ with $k = 11 + 2b + 0.3a < 25$ we used

$$J(a,b) = \exp(-a-b) \sum_{n=0}^{k} \frac{b^n}{n!} \sum_{m=0}^{n} \frac{x^m}{m!} + E, \qquad |E| < \frac{b^{k+1}}{(k+1)!} \qquad (5.9)$$

where *E* is the error in the series expansion containing *k* terms, while for $a < b$ with $k = 11 + 2a + 0.3b < 25$ we used

$$J(a,b) = 1 - \exp(-a-b) \sum_{n=0}^{k} \frac{a^n}{n!} \sum_{m=0}^{n-1} \frac{b^m}{m!} + E, \qquad |E| < \frac{a^k}{k!} \qquad (5.10)$$

For larger values of *a* and *b*, *J*(*a*,*b*) is given by [*Goldstein*, 1953]

$$J(a,b) = \begin{cases} A + B & (a \geq b) \\ 1 - A + B & (a < b) \end{cases} \qquad (5.11)$$

where

$$A = \frac{\sqrt{a} + \sqrt{b}}{4(ab)^{1/4}} \operatorname{erfc}(\sqrt{z}) \qquad (5.12)$$

$$B = \frac{1}{2} \exp(-a-b) I_0(2\sqrt{ab}) + \frac{(a-b)e^{-z}}{4\sqrt{\pi}(ab)^{1/4}} \sum_{m=1}^{\infty} \frac{\alpha_m S_m(z)}{(16ab)^{m/2}} \qquad (5.13)$$

$$\alpha_m = \frac{\Gamma(m+1/2)}{\Gamma(1/2)m!} \qquad (5.14)$$

$$S_{m+1}(z) = \frac{\Gamma(m+1/2)}{\Gamma(1/2)m!} - z S_m(z) \qquad (5.15)$$

$$S_1(z) = 1 - \sqrt{\pi z}\, e^{z} \operatorname{erfc}(\sqrt{z}) \qquad (5.16)$$

$$z = (\sqrt{a} - \sqrt{b})^2 \qquad (5.17)$$

The integrals in the nonequilibrium solutions were evaluated with Gauss-Chebyshev quadrature

52

[e.g. Carnahan *et al.*, 1969; **Press et al.,** 1992]. Gauss-Chebyshev quadrature offers flexibility in terms of selecting the number of integration points. We obtained accurate results with 50 integration points for most cases (generally four to five significant digits). In some extreme cases, such as for very small ,B and Z or very large **T,** the results using 50 points may become inaccurate or incorrect. A greater number of integration points generally results in more accurate results at the expense of additional computer time. The latter effect is especially of concern when solving the inverse problem. The number of integration points, MM, can be changed in subroutine **CONST1.** The parameter ICHEB in subroutine **CONST1** controls the integration method. If ICHEB = 0, MM is constant at all times. If ICHEB = 1, the program evaluates the solutions twice, namely with MM and **2×MM** in the integration routine. The number of integration points is increased until the relative change in the solution becomes less than 0.1%. We suggest to use a set (ICHEB = 0) value of 75 for MM when solving the inversion problem whereas ICHEB = 1 and MM = 75 appear attractive selections for the direct problem.

An alternative method to achieve computational efficiency and accuracy is to narrow the integration interval. The integrand in (3.17) for a Delta input (i.e., f according to (3.15)) or in (3.20) for a pulse input, becomes negligible for small or large τ due to the exponential and complementary error functions in Γ_1^N. The modified lower (T1) and upper (T2) integration limits were obtained by restricting integration to the domain where the argument of exponential function exceeds -30:

$$\text{T1} = \beta RZ + \frac{60\beta R}{P}\left\{1 - \sqrt{1 + \frac{PZ}{30}}\right\} \tag{5.18}$$

$$\text{T2} = \beta RZ + \frac{60\beta R}{P}\left\{1 + \sqrt{1 + \frac{PZ}{30}}\right\} \tag{5.19}$$

The above modifications may significantly improve the computational efficiency without loss of accuracy, especially for large **T.**

The general solution of the deterministic BVP for an arbitrary input C_o is calculated by numerically evaluating convolution integrals (2.15) for the equilibrium CDE or (3.13) and (3.14) for the nonequilibrium CDE. The input function needs to be specified in function **CINPUT** in file USER.FOR (see also Chapter 6). Calculation of the solution should be relatively slow since a double integral is evaluated numerically.

5.3. Stochastic CDE

File **STOCDE.FOR** assigns local-scale parameters to each stream tube and evaluates field-scale averaged concentrations. The concentration in each stream tube is determined as described in section 5.2. Numerical integration required for the field-scale concentration and variance is carried out on in subroutines **ROMB** and ROMB2 on a log-transformed interval using up to 14th order Romberg quadrature. Since a lognormal pdf is used, log-transformation improves the efficiency and accuracy of the numerical integration, especially for a large standard deviation, σ. Similar to Gauss-Chebyshev quadrature, convergence is evaluated by comparing the integration for the kth and $k+1$ th order. The relative error criterion is set with variable STOPER. Convergence can usually be achieved for order $k \le 10$ with STOPER $= 5 \times 10^{-7}$ unless the local Peclet number, vx/D, is high. As with the deterrninisitc CDE, increasing the number of integration points will result in more accurate results at the expense of more computer time. The default upper limit for k is eight, with STOPER $= 5 \times 10$" for the evaluation of triple integrals (e.g., the stochastic nonequilibrium CDE with $\rho_{v\eta} \ne \pm 1$) or the solution of the inverse problem. The settings for Romberg quadrature are contained in subroutine CONST2, which appears in file USER.FOR.

To improve the computational efficiency, the upper and lower limits of integrals in the expressions for the field-scale concentration are restricted by excluding values for v and η that have a likelihood of occurrence of less than 1×10^{-7}. The integration limits are determined according to the Newton-Raphson method in subroutine LIMIT. For a large standard deviation, for example $\sigma = 2$ (CV = 732 %), the integration range may become too broad for numerical evaluation with this criterion.

5.4. Parameter Estimation

CXTFIT 2.0 estimates unknown model parameters using a nonlinear least-squares optimization approach based on the Levenberg-Marquardt method [Marquardt, 1963]. The inverse problem is solved by fitting an appropriate mathematical solution to observed concentration data. Most of the calculations for the least-squares analysis are carried out in the main program **(Main).** The model parameters are determined by minimizing an objective function (the sum of squared residuals, SSQ) defined as

$$SSQ \ (\mathbf{b}) \ = \ \sum_{i=1}^{N} \left[c(x_i) - f(x_i; \mathbf{b}) \right]^2 \tag{5.20}$$

where $\mathbf{b}$ represents the vector of unknowns containing M adjustable parameters b_j ($j = 1,...,M$), and c and f are the observed and fitted concentrations for the ith data point as obtained with the independent variable(s) x_i ($i = 1,...,N$). The inversion procedure in CXTFIT 2.0 is essentially the same as used in its precursors [*van Genuchten*, 1979; 1980; *Parker and van Genuchten*, 1984b], and hence will be reviewed here only briefly. The optimization routine is a simplification of the nonlinear least-squares curve-fitting program of *Meeter* [1966]. A detailed description of the method is given by *Press et al.* [1992].

When a model depends nonlinearly on a set of M unknown parameters b_j, minimization of (5.20) has to be carried out iteratively. At the rth iteration, the correction vector $\delta\mathbf{b}$ is evaluated according to the following linear equation:

$$(\mathbf{A}^r + \lambda^r \mathbf{I}) \ \delta\mathbf{b} \ = \ \mathbf{Q}^r \tag{5.21}$$

where

$$A_{kj} = \sum_{i=1}^{N} \frac{\partial f(x_i; \mathbf{b}^r)}{\partial b_k} \frac{\partial f(x_i; \mathbf{b}^r)}{\partial b_j} \qquad k = 1,...,M, \qquad j = 1,...,M \tag{5.22}$$

$$Q_j = \sum_{i=1}^{N} \frac{\partial f(x_i; \mathbf{b}^r)}{\partial b_j} \left[c(x_i) - f(x_i; \mathbf{b}^r) \right] \qquad j = 1,...,M \tag{5.23}$$

and λ^r is a nonnegative scalar (a Lagrangian multiplier), $\mathbf{I}$ is the unit matrix of order N, and the new trial vector is given by $\mathbf{b}^{r+1} = \mathbf{b}^r + \delta\mathbf{b}$. Notice that when λ is very large, $\mathbf{A} + \lambda\mathbf{I}$ becomes diagonally dominant, and (5.21) can be rewritten to

$$\delta b_j = \frac{1}{A_{jj}(1+\lambda)} Q_j \tag{5.24}$$

which is identical to the steepest descent method. On the other hand, when λ approaches zero, (5.21) converges to the Taylor series method (the Gauss-Newton method). Since a linear expansion of the Taylor method will be accurate only over a small region, the Levenberg-Marquardt method aims to gradually reduce λ as SSQ($\mathbf{b}$) reaches its minimum.

After an initial estimate for $\mathbf{b}$ is provided, "best-fit" parameters are determined as follows (most constants for the optimization are stored in subroutine **CONST1** of file **USER.FOR**):

(1) Compute **SSQ(b).**

(2) **Set** $\lambda = 0.001$ (= GA/GD in **CONSTl).**

(3) **Solve** (5.2 1) for $\delta\mathbf{b}$ and define a scale factor $\mu = 1$.

(4) Compute **SSQ(b+$\mu\delta$ b).**

(5) If **SSQ(b+$\mu\delta$ b) < SSQ(b),** decrease λ by a factor 10 (GD in **CONSTl),** update the trial vector $\mathbf{b} = \mathbf{b}+\mu\delta\,\mathbf{b}$, and go back to (3).

(6) If **SSQ(b+$\mu\delta$ b) ≥ SSQ(b),** evaluate the angle ϑ **between** the correction vector δ **b** and the steepest descent direction **Q**.

(7) If $\vartheta < 30°$, decrease μ by a factor 2, and return to (6).

(8) If $\vartheta \ge 30°$, increase λ by a factor 10, and return to (3).

The iteration stops when either of the following conditions is met:

(a) The relative change in each estimation parameter $(\mu\delta b_j /b_j)$ is less than the criterion STOPCR (default value is 0.0005 in **CONSTl).**

(b) The relative decrease in SSQ is less than 1.0×10^{-6} (= STSQ in CONSTl) for three successive iterations.

(c) SSQ decreases more than MIT times without meeting either condition (a) or (b) (MIT is defined in the input file).

(d) SSQ fails to decrease during 50 consecutive iterations (= MAXTRY in **CONSTl).**

The derivatives of the fitted concentrations ——based on the selected mathematical model ——with respect to parameter b_j *are* evaluated according to

$$\frac{\partial f(x_i; \mathbf{b})}{\partial b_j} \simeq \frac{f(x_i; b_,, \ldots (1+\Delta)b_j, \ldots b_M) - f(x_i; b_,, \ldots b_j, \ldots b_M)}{\Delta b_j} \qquad (5.25)$$

The current setting for A is 0.01 for all parameters (DERL in **CONSTl),** which we found to be appropriate for most cases. When b_j is very small or insensitive to changes in the fitted concentration, however, approximation (5.25) for the derivative may become inaccurate. The restriction $|\rho_{v\eta}| > 1\times10^{-5}$ is placed on the correlation between stochastic parameters in order to evaluate the derivative according to (5.25) for the parameter estimation involving stream tube models.

The iteration procedure sometimes converges to different local minima depending upon the initial estimate for **b, as will** be demonstrated in Table 7.2. It is essential to provide realistic initial estimates

of the parameters, as close to the global minimum as possible. Furthermore, CXTFIT 2.0 allows the use of maximum and minimum constraints on fitted parameters. When the new parameter value exceeds a specified maximum or minimum value during the iteration process, the value for the constraint is used for the next trial.

In addition to user-specified constraints, the program employs an internal constraint on β for the deterministic nonequilibrium CDE. Since the fraction of equilibrium adsorption **sites**, f, ranges from 0 to 1 for the two-site model (see Section 3. 1), the range of possible β values is

$$\frac{1}{R} \leq \beta < 1 \tag{5.26}$$

A similar range holds for the fraction of adsorption sites in the mobile **phase**, f, for the two-region model:

$$\frac{1}{R}\frac{\theta_m}{\theta} \leq \beta < \frac{1}{R}\left(\frac{\theta_m}{\theta} + \frac{\rho_b K_d}{e} \right) \tag{5.27}$$

A maximum constraint is also placed on ω, the constraint value for this parameter is defined by OMMAX in subroutine CONST1. We note that constrained parameter optimization often results in a slightly slower rate of convergence because of a loss in flexibility.

Finally, we recommend to generally carry out several estimation trials with and without constraints as well as with different initial estimates for **b. Also,** parameter optimization ("curve fitting") should never be used as a panacea for a mathematical model that does not reflect the underlying transport processes.

6. CXTFIT 2.0 USER'S GUIDE

The previous chapters provided a background of the solute transport models and of the numerical procedures to evaluate their analytical solutions. This chapter serves as a self-contained user manual for CXTFIT 2.0. First, the structure of CXTFIT 2.0 is outlined to give the user a quick overview of the different modeling options.   Second, the preparation of the input file is discussed. The input is provided in a modular fashion, by using a series of blocks. Readers may only have to read the text pertaining to the blocks for their specific application. Third, the structure of the input and output files used for examples in this report will be reviewed. Fourth, we will compare the differences in input format between the first version of CXTFIT [*Parker and* van *Genuchten,* 1984b] and the current CXTFIT 2.0.

6.1. Structure of CXTFIT 2.0

CXTFIT 2.0 contains three different one-dimensional transport models: (I) the conventional CDE; (ii) the chemical and physical nonequilibrium CDE; and (iii) a stochastic stream tube model based on the local-scale CDE. Five different versions of the stochastic model can be selected depending upon the type of adsorption present (equilibrium or nonequilibrium), and the type of random transport parameters. Table 6.1 lists the characteristics of all seven models in CXTFIT 2.0; the models are identified in the program by the parameter MODE. Deterministic transport can be modeled with the equilibrium (MODE = 1) and nonequilibrium (MODE = 2) CDEs.   The five versions of the stream tube model are: equilibrium (MODE = 3) and nonequilibrium (MODE = 4) adsorption with random v, D, and K_d (ρ_{vD} = 1); equilibrium (MODE = 5) and nonequilibrium (MODE = 6) adsorption with random v, D, and K_d (ρ_{vKd} = - 1); and nonequilibrium adsorption with random v, D, K_d, and a assuming ρ_{vD} = 1 and ρ_{vKd} = -1 (MODE = 7). A stochastic parameter can be made deterministic by setting its standard deviation to zero.

Table 6.1. Overview of Transport Models in CXTFIT 2.0

MODE	Model Type	Parameters	Concentration Mode
Deterministic CDE			
1	Equilibrium	v, D, R, μ or μ^z	$C_f, C_r, C_T = RC_r$
2	Nonequilibrium	$v, D, R, \beta, \omega, \mu_1, \mu_2$	$C_f, C_r, C_T = \beta RC_{1r} + (1-\beta)RC_{2r}$
Stochastic Equilibrium CDE			
3	Random v, D, and K_d with $\rho_{vD} = 1$	$\langle v \rangle, \langle D \rangle, \langle K_d \rangle, \mu$ or μ^z $\sigma_v, \sigma_D, \sigma_{Kd}, \rho_{vKd}$	$\langle C_f \rangle, \hat{C}_f = \langle vC_f \rangle / \langle v \rangle, \hat{C}_r = \langle C_r \rangle$ $\hat{C}_T = \langle RC_r \rangle$
5	Random v, D, and K_d with $\rho_{vKd} = -1$	$\langle v \rangle, \langle D \rangle, \langle K_d \rangle, \mu$ or μ^z, $\sigma_v, \sigma_D, \sigma_{Kd}, \rho_{vD}$	Same as 3
Stochastic Nonequilibrium CDE			
4	Random v, D, and K_d with $\rho_{vD} = 1$	$\langle v \rangle, \langle D \rangle, \langle K_d \rangle, \omega, \mu_1, \mu_2,$ $\sigma_v, \sigma_D, \sigma_{Kd}, \rho_{vKd}$	$\langle C_f \rangle, \hat{C}_f = \langle vC_f \rangle / \langle v \rangle, \hat{C}_r = \langle C_r \rangle$ $\hat{C}_T = \langle C_{1r} + (R-1)C_{2r} \rangle$
6	Random v, D, and K_d with $\rho_{vKd} = -1$	$\langle v \rangle, \langle D \rangle, \langle K_d \rangle, \omega, \mu_1, \mu_2,$ $\sigma_v, \sigma_D, \sigma_{Kd}, \rho_{vD}$	Same as 4
7	Random v, D, K_d, and **a** **with** $\rho_{vD} = 1$ and $\rho_{vKd} = -1$	$\langle v \rangle, \langle D \rangle, \langle K_d \rangle, \langle \alpha \rangle, \mu_1,$ $\mu_2, \sigma_v, \sigma_D, \sigma_{Kd}, \sigma_\alpha, \rho_{v\alpha}$	Same as 4

Table 6.1 also presents the mode in which the concentration is detected or predicted. Resident, flux-averaged, and total resident concentrations can be used. Although a third-type inlet condition is generally preferable [van Genuchten *and Parker,* 1994], resident concentrations are also given for a first-type inlet condition. Flux-averaged concentrations are derived from the resident concentration for a third-type inlet condition according to (2.13). Two-types of macroscopic flux-averaged concentration are available for stochastic transport, i.e., the ensemble average of the local-scale flux-averaged concentration, $\langle C_f \rangle$, and the field-scale flux concentration, $\hat{C}_f (= \langle vC_f \rangle / \langle v \rangle)$.

All analytical solutions given in Chapters 2 and 3 can be evaluated with CXTFIT 2.0. The solution of the CDE is described as the sum of (i) a boundary value problem (BVP), (ii) an initial value problem (IVP), and (iii) a production value problem (PVP). Table 6.2 summarizes the functions that are used to characterize the BVP, IVP, and PVP.

Function	Input Concentration	Initial Profile	Production Profile‡
Dirac Delta	$C_o(T) = M_B\, \delta(T)$ or $c_o(t) = \dfrac{m_B}{v}\, \delta(t)$	$C_i(Z) = M_I \delta(Z - Z_1)$ or $c_i(x) = \dfrac{m_I}{\theta} \delta(x - x_1)$	–
Stepwise	$C_o(T) = f_i \qquad T_i \le T < T_{i+1}$ $(i = 1,2,\dots,n;$ $T_1 = 0$ and $T_{n+1} = \infty)$	$C_i(Z) = U_i \qquad Z_i \le Z < Z_{i+1}$ $(i = 1,2,\dots,n;$ $Z_1 = 0$ and $Z_{n+1} = \infty)$	$\gamma(Z) = \gamma_i \qquad Z_i \le Z < Z_{i+1}$ $(i = 1,2,\dots,n;$ $Z_1 = 0$ and $Z_{n+1} = \infty)$
Exponential	$C_o(T) = f_1 + f_2 \exp(-\lambda^B T)$	$C_i(Z) = U_1 + U_2 \exp(-\lambda^I Z)$	$\gamma(Z) = \gamma_1 + \gamma_2 \exp(-\lambda^P Z)$
Arbitrary	$C_o(T)$	–	–

† f_i, U_i, γ_i are arbitrary constants.
‡ The production profiles in phases 1 and 2 can be described separately for the nonequilibrium CDE.

6.2. Input Data Instruction

The input data are read from an ASCII file. The user is prompted for the name of the input file during execution. Default names for the input and output files can be specified in the main program. The input file consists of up to eight of the following blocks:

A. Model Description

B. Inverse Problem Parameters

C. Transport Parameters

D. Boundary Value Problem

E. Initial Value Problem

F. Production Value Problem

G. Observed Data for an Inverse Problem

H. Position and Time for a Direct Problem

Blocks B and G are used for the inverse problem (INVERSE = 1) while Block H is used for the direct problem (INVERSE = 0 or -1).

All data are read in using list-directed formatting (free format) except for the case INPUTM=3 in Block G. Dummy parameter values may have to be included in the input file to maintain the proper format. Dummy comment lines are provided for each input block to identify the block and the input variables — these may be left blank but should not be omitted. All input data are to be specified in consistent units for mass [M], length [L], and time [T] (see also NREDU in Block A). The first line of the input file gives NCASE, which specifies the number of cases that are considered. Several different cases (i.e., data sets) can be handled by one input file. The distribution diskette contains all input and output files for the examples in Chapters 4 and 7. Preparation of the input file for a particular example is done most conveniently by modifying an existing input file for a similar case.

The characteristics of each input group (block) in the input file are further discussed below. Line-by-line descriptions of every block are given in Tables 6.3 through 6.11.

Block A. Model Description (Table 6.3)

This block contains the parameters that define the type of problem to be solved. The parameter INVERSE controls whether a direct (INVERSE = 0 or -1) or inverse (INVERSE = 1) problem is solved. A further distinction is made for the solution of the direct problem according to the stream tube model. CXTFIT 2.0 will only calculate field-scale mean concentrations if INVERSE = -1 while both mean concentrations and variances, the latter according to (4.20) and (4.21), are evaluated if INVERSE = 0. The parameter MODE specifies the model type while MODC denotes the concentration mode (cf. Table 6.1). The input format is different for deterministic (MODE$\leq$2) and stochastic transport (MODE$\geq$3) for some parameters. The total resident concentration is expressed as the amount of solute per unit volume of solution.

The parameter NREDU specifies whether the specified time and positions in the input and output files are dimensional or dimensionless. For dimensional times and positions (NREDU = 1) the dimensional μ and γ given by (2.5) and (2.6) should be specified for the equilibrium CDE (MODE = 1,3,5). Otherwise, dimensionless degradation and production terms as defined in Table 2.1 and 3.1 should be used. For a unit characteristic concentration, i.e., $c_o = 1$, dimensional and dimensionless

concentrations are obviously equal regardless of the value of NREDU; an exception is the adsorbed concentration in case of chemical nonequilibrium. For the nonequilibrium CDE with a random K_d, where $<s/K_d c_o> \neq <s>/(<K_d>c_o)$, the adsorbed concentration is given as $<s>$ if NREDU = 0, and as $<s/K_d>$ if NREDU $\geq$ 1.

The characteristic length, L, for nondimensional parameters is specified at the end of Block A. CXTFIT 2.0 always uses dimensionless parameters for its internal operations; all dimensional parameters, times, and positions in the input file are internally transformed to nondimensional variables using the (dummy) value for L in Block A. Depending on the value for NREDU, a transformation from the dimensionless back to the dimensional variables is carried out upon completion of all internal operations. It is recommended to use for L a value of similar magnitude as the observation scale (e.g., column length or soil profile depth).

Table 6.3. Block A - Model Description

Line	Type	Variable	Description
0	Integer	NCASE	Number of cases being considered (only for the first data set).
1	-	-	Comment line.
2,3	Char	TITLE 1,2	Descriptive title for simulation.
4			Comment Line.
5	Integer	INVERSE	Calculation control code: -**1** Direct problem (no results for variance in case of the stochastic CDE). 0 Direct problem (results for given parameters). 1 Inverse problem (parameter estimation).
5	Integer	MODE	Model code: 1 Deterministic equilibrium CDE. 2 Deterministic nonequilibrium CDE. 3 Stochastic equilibrium CDE with $f(v,K_d)$ and $\rho_{vD}=1$. 4 Stochastic nonequilibrium CDE with $f(v,K_d)$ and $\rho_{vD}=1$. 5 Stochastic equilibrium CDE with $f(v,D)$ and $\rho_{vK_d}=-1$. 6 Stochastic nonequilibrium CDE with $f(v,D)$ and $\rho_{vK_d}=-1$. 7 Stochastic nonequilibrium CDE with $f(v,\alpha)$, $\rho_{vK_d}=-1$ and $\rho_{vD}=1$.

Table 6.3. (continued)

Line	Type	Variable	Description
5	Integer	NREDU†	Input and output data code: **0** Time and position are dimensional (adsorbed concentration for the stochastic nonequilibrium CDE is $<s>$). **1** Time and position are dimensional (adsorbed concentration for the stochastic nonequilibrium CDE is $<s/K_d>$). **2** Time and position are dimensionless. **3** Dimensionless time and dimensional position.
6	-	-	Comment line.
7	Integer	MODC	Concentration mode. ***Deterministic CDE*** (MODE=1 or 2): **1,2** Flux-averaged concentration, C_f. **3** Resident concentration (third-type inlet), C_r. **4** Total resident concentration (third-type inlet), $C_T = RC_r$, or $\beta RC_{1,r} + (1-\beta)RC_{2,r}$. **5** Resident concentration (first-type inlet), C_r. **6** Total resident concentration (first-type inlet), $C_T = RC_r$, or $\beta RC_{1,r} + (1-\beta)RC_{2,r}$. ***Stochastic CDE*** (MODE≥3): **1** Ensemble-averaged flux concentration, $<C_f>$. **2** Field-scale flux-averaged concentration, $\hat{C}_f = <vC_f>/<v>$. **3** Field-scale resident concentration (third-type inlet), $\hat{C}_r = <C_r>$. **4** Field-scale total resident concentration (third-type inlet), $\hat{C}_T = <RC_r>$ or $<C_{1,r} + (R-1)C_{2,r}>$. **5** Field-scale resident concentration (first-type inlet), $\hat{C}_r = <C_r>$. **6** Field-scale total resident concentration (first-type inlet), $\hat{C}_T = <RC_r>$ or $<C_{1,r} + (R-1)C_{2,r}>$.
7	Real	ZL	Characteristic length for dimensionless parameters (see Table 2.1 and 3.1, leave blank for NREDU=1 in case of equilibrium CDE with MODE=1,3,5).

† Dimensional and dimensionless concentrations are equal if $c_o=1$ (cf. Table 2.1 and 3.1). Specify dimensional μ and γ according to (2.5) and (2.6) for the equilibrium CDE (MODE=1,3,5) when NREDU=1. Use dimensionless μ and γ (cf. Table 2.1 and 3.1) in all other cases.

Block B. Inverse Problem Parameters (Table 6.4)

This block contains data for the parameter estimation procedure. The parameter MIT specifies the maximum number of iterations. A value between 50 and 100 is recommended for MIT, a further reduction in SSQ is unlikely for MIT greater than 100. The inversion part is bypassed when MIT=0; the program then calculates concentrations for the specified initial parameters. This option is equivalent to solving the direct problem (INVERSE=l), provided that values for time and position are specified in Block G. The arrays INDEX(I) in Block C and C(1) in Block G are now read in as dummy information.

The parameter ILMT serves as a flag for parameter constraints. If the range of an estimated parameter is known, e.g., based on physical considerations or from experimental observations, maximum and minimum constraints can be specified by setting ILMT = 1. Although unrealistic parameter estimates are avoided in this manner, the rate of convergence is usually slower. If the same value is used as maximum and minimum constraint, there will be no constraint on that particular parameter during the optimization.

The input mass can be estimated along with transport parameters for either a Dirac input, step input, or pulse input by setting MASS = 1. When MASS = 1, it is necessary to give parameters for the mass estimation in Block D (ILMT, maximum and minimum constraints). This option should only be used as a last resort since a poor mass balance generally reflects discrepancies between the experiment and the conceptual transport model.

The parameter MNEQ specifies the type of nonequilibrium model being implemented. For the one-site model (MNEQ=1), β is always equal to $1/R$. This option may be useful when R is a fitting parameter. For the two-region model, no internal constraints on β are applied if MNEQ=0 ($0 < \beta \leq 0.9999$ for ILMT=O or the user can specify constraints for ILMT=1). When $\text{MNEQ} \geq 2$, internal constraints according to (5.26) or (5.27) are applied during the iteration. The user can still impose additional constraints (ILMT=l).

The relation between degradation coefficients for phase 1 (μ_1) and phase 2 (μ_2) is specified with the parameter MDEG (cf. Table 3.5). When $\text{MDEG}=0$ these coefficients are estimated independently; they are related according to Table 6.4 when MDEG>O. The fraction of mobile water, ϕ_m, should be given if MNEQ=3 or if MNEQ=O and $\text{MDEG} \geq 2$.

65

Table 6.4. Block B - Parameters for Inverse Problem

Line	Type	Variable	Description
1,2	-	-	Comment lines.
3	Integer	MIT	Maximum number of iterations (the inverse part is bypassed if MIT = 0, the program calculates concentrations at specified Z(I) and T(I) using the initial estimates as model parameters).
3	Integer	ILMT	Parameter constraint code: **0** No constraints for parameter estimation. **1** Use minimum and maximum constraints.
3	Integer	MASS	Total mass estimation code. This option is only available for the BVP in case of a Dirac, step-type, or single pulse input (see Block D; enter a dummy value or zero if MODB=0 or ≥ 4). **0** No estimation for total mass. **1** Total mass included in estimation procedure.

Omit the following lines for the equilibrium CDE (MODE=1,3,5).

Line	Type	Variable	Description
4	-	-	Comment line.
5	Integer	MNEQ	Nonequilibrium model code (MNEQ=1 for the stochastic one-site model): **0** Two-region physical nonequilibrium model ($0<\beta\leq0.9999$). **1** One-site chemical nonequilibrium model ($\beta=1/R$). **2** Two-site chemical nonequilibrium model ($1/R\leq\beta\leq0.9999$). **3** Two-region physical nonequilibrium model with internal constraints ($\phi_m/R \leq \beta \leq (\phi_m+R-1)/R$).
5	Integer	MDEG	Degradation estimation code for the nonequilibrium CDE (enter a dummy value if μ_1 and μ_2 are not fitted): **0** Solution and adsorbed phase degradation rates are independent. **1** Degradation everywhere the same ($\mu_l=\mu_s$). **2** Degradation only in the liquid phase ($\mu_l>0, \mu_s=0$). **3** Degradation only in the adsorbed phase ($\mu_l=0, \mu_s>0$).

The following lines should only be provided if MNEQ=3 or MNEQ=0 and MDEQ≥2.

Line	Type	Variable	Description
6	-	-	Comment line.
7	Real	PHIM	Mobile water fraction, $\phi_m= \theta_m/\theta$.

Block C. Transport Parameters (Tables 6.5 and 6.6)

This block contains general transport parameters. If NREDU = 1, dimensional values for μ and γ should be specified according to (2.5) and (2.6) for the equilibrium CDE (MODE = 1,3,5). If NREDU $\neq$ 1, dimensionless values for μ^E and γ^E are used in the input and output files (see Table 2.1). The degradation and production parameters are always dimensionless for the nonequilibrium CDE (MODE = 2,4,6,8).

Since K_d is used as an input parameter for the stream tube model (MODE$\geq$3), the (deterministic) value for ρ_b/θ needs to be entered for evaluating R. For nonreactive solutes ($K_d = 0$ and $R = 1$), the value for ρ_b/θ is immaterial and a dummy value can be entered. The program uses ensemble averages to generate dimensionless variables, for example:

$$T = \frac{<v>t}{L}, \qquad \omega = \frac{\alpha(<R>-1)L}{<v>} \qquad \qquad (6.1a,b)$$

We assume that the degradation coefficients in the liquid and adsorbed phases are identical ($\mu_l = \mu_s$) for stochastic equilibrium transport. Hence, $\mu = \mu_l<R>$ for a stochastic K_d.

Stochastic parameters can be made deterministic by simply setting $\sigma = 0$. If v is deterministic ($\sigma_v = 0$), any parameter that is perfectly correlated with v will become deterministic as well (D for MODE = 3,4; K_d for MODE = 5,6; and D and K_d for MODE = 8). Since the pdf is bivariate, only one parameter will remain stochastic in this case (K_d for MODE = 3,4; D for MODE = 5,6; α for MODE = 8). CXTFIT 2.0 cannot be executed if the standard deviation of each parameter in the stream tube model is zero. Instead, the deterministic CDE should be used as the transport model. If the same initial estimate is provided for the standard deviations of v and η, CXTFIT 2.0 will assume that $\sigma_v = \sigma_\eta$ throughout the optimization procedure.

Table 6.5. Block C - Transport Parameters†

Line	Type	Variable	Description
1,2	-	-	Comment lines.
			Transport parameter values.
			Deterministic CDE (MODE=1,2):
3	Real	B(1)	Initial value for each coefficient.
3	Real	B(2)	
⋮	⋮	⋮	
3	Real	B(NP)	
			Stochastic CDE (MODE≥3):
3	Real	B(1)	Initial value for each coefficient.
3	Real	B(2)	
⋮	⋮	⋮	
3	Real	B(NP)	
3	Real	RHOTH	Value for ρ_b/θ.

Omit the following if INVERSE=0 (direct problem).

Line	Type	Variable	Description
4	Integer	INDEX(1)	Parameter estimation index for B(1).
			0 Coefficient is known and kept constant during optimization.
			1 Coefficient is unknown and estimated by curve fitting the data.
4	Integer	INDEX(2)	Parameter estimation index for B(2).
⋮	⋮	⋮	⋮
4	Integer	INDEX(NP)	Parameter estimation index for B(NP).

Omit the following if ILMT=0 (no constraints).

Line	Type	Variable	Description
5	Real	BMIN(1)‡	Minimum constraint for B(1) (dummy value if INDEX(1)=0).
5	Real	BMIN(2)	Minimum constraint for B(2) (dummy value if INDEX(2)=0).
⋮	⋮	⋮	⋮
5	Real	BMIN(NP)	Minimum constraint for B(NP) (dummy value if INDEX(NP)=0).
6	Real	BMAX(1)‡	Maximum constraint for B(1) (dummy value if INDEX(1)=0).
6	Real	BMAX(2)	Maximum constraint for B(2) (dummy value if INDEX(2)=0).
⋮	⋮	⋮	⋮
6	Real	BMAX(P)	Maximum constraint for B(NP) (dummy value if INDEX(NP)=0).

† Parameters for B(I) are given in Table 6.6.
‡ No constraints will be imposed on B(I) if BMIN(I)=BMAX(I).

Table 6.6. Parameters for B(I) in Block C

MODE	NP	B(1)	B(2)	B(3)	B(4)	B(5)	B(6)	B(7)	B(8)	B(9)	B(10)	B(11) -
1	4	v	D	R	μ or μ^g	-	-	-	-	-	-	-	-
2	7	v	D	R	β	ω	μ_1	μ_2	-	-	-	-	-
3	8	$<v>$	$<D>$	$<K_d>$	μ or μ^g	σ_v	σ_{Kd}	σ_D	ρ_{vkd}	ρ_b/θ	-	-	-
4	10	$<v>$	$<D>$	$<K_d>$	ω	μ_1	μ_2	σ_v	σ_{Kd}	σ_D	ρ_{vKd}	ρ_b/θ	-
5	8	$<v>$	$<D>$	$<K_d>$	μ or μ^g	σ_v	σ_{kd}	σ_D	ρ_{vD}	ρ_b/θ	-	-	-
6	10	$<v>$	$<D>$	$<K_d>$	ω	μ_1	μ_2	σ_v	σ_{kd}	σ_D	ρ_{vD}	ρ_b/θ	-
7	11	$<v>$	$<D>$	$<K_d>$	$<\alpha>$	μ_1	μ_2	σ_v	σ_{kd}	σ_D	σ_α	$\rho_{v\alpha}$	ρ_b/θ

Block D. Boundary Value Problem (Table 6.7)

Table 6.2 lists the diirent functions that can be used for the input concentration as a function of time in the boundary value problem (BVP). The same format should be followed for the deterministic and the stream tube model. The dimension for time in the input function should be consistent with NREDU in Block A. The step (MODB = 2) and pulse (MODB = 3) input functions are special cases of the general multiple pulse input scenario (MODB = 4). The maximum number of pulses is 10. Solutions of the BVP for a user-defined input function (MODB = 6) are obtained according to (2.15) for the equilibrium CDE, and (3.13) and (3.14) for the nonequilibrium CDE. The input function needs to be specified by the user in the routine **CINPUT** in source program **USER.FOR**. The program always needs to be recompiled when the input function is being changed. This option (MODB = 6) is not available for the stream tube model (MODE = 4,6,8).

Note that INDEX, and the minimum and maximum constraints, should be specified if the total solute mass is a fitting parameter for either Dirac delta, step, or pulse input (MASS = 1 in Block B). For the stochastic CDE with a random v, the parameter MASSST specifies the mass distribution between stream tubes for a Dirac delta input and a pulse input (cf. Figures 4.3 and 4.4).

Table 6.7. Block D - Boundary Value Problem?

Line	Type	Variable	Description
1,2	-		Comment lines.

(0) Solute free water input

Line	Type	Variable	Description
3	Integer	MODB	**0**

(1) Dirac Delta input

Line	Type	Variable	Description
3	Integer	MODB	1
4	Real	PULSE(1)	m_B/v or $<m_B>/<v>$ for dimensional $\delta(t)$, M_B or $<M_B>$ for dimensionless $\delta(T)$.
4	Real	MASSST	Mass distribution index for the stochastic CDE (leave blank for the deterministic CDE, i.e., **MODE≤2**). 0 Amount of solute in each tube is proportional to v ($m_B=v<m_B>/<v>$). 1 Amount of solute in each tube is constant regardless of v ($m_B=<m_B>$).

Omit the following if INVERSE=0 (Block A) or MASS=0 (Block B).

Line	Type	Variable	Description
5	Integer	INDEX(NP+l)	Parameter estimation index for solute mass (=B(NP+l)). 0 Coefficient is known and kept constant. 1 Coefficient is assumed to be unknown and fitted to data

Omit the following if **there** are no constraints (ILMT=0, Block B).

Line	Type	Variable	Description
6	Real	BMIN(NP+1)	Minimum constraint for B(NP+1) (dummy value if INDEX(NP+1)=0).
7	Real	BMAX(NP+1)	Maximum constraint for B(NP+1) (dummy value if INDEX(NP+1)=0).

(2) Step input

Line	Type	Variable	Description
3	Integer	MODB	2
4	Real	PULSE(1)	Input concentration, f_1.

Omit the following **if** INVERSE=0 (Block A) or MASS=0 (Block B).

Line	Type	Variable	Description
5	Integer	INDEX(NP+1)	Parameter estimation index for input concentration (=B(NP+1)). 0 Coefficient is known and kept constant. 1 Coefficient is assumed to be unknown and fitted to the data.

Omit the following if **there** are no constraints (ILMT=O, Block B).

Line	Type	Variable	Description
6	Real	BMIN(NP+l)	Minimum constraint for B(NP+1) (dummy value if INDEX(NP+1) =O).
7	Real	BMAX(NP+l)	Maximum constraint for B(NP+l) (dummy value if INDEX(NP+l) =O).

Table 6.7. (continued)

Line	Type	Variable	Description

(3) Pulse input of application time, T_2

3	Integer	MODB	**3**
4	Real	PULSE(1)	Input concentration, f_1.
4	Real	TPULSE(2)	Application time, T_2 or $<T_2>$.
4	Real	MASSST	Mass distribution index for the stochastic CDE (leave blank if MODE≤2).

0 Application time, T_2, is constant for all stream tubes and the amount of solutes in each stream tube is proportional to v (MODE=5 and 6 in prior CXTFIT version as discussed in section 6.6).

1 Application time, T_2, is equal to $<T_2><v>/v$ for each stream tube. All stream tubes have the same amount of solutes (MODE=7 and 8 in prior CXTFIT version as discussed in section 6.6).

Omit the following if INVERSE=0 (Block A) or MASS=0 (Block B).

5	Integer	INDEX(NP+1)	Parameter estimation index for PULSE(1)(=B(NP+1)).

0 Coefficient is known and kept constant.
1 Coefficient is assumed to be unknown and fitted to data.

5	Integer	INDEX(NP+2)	Parameter estimation index for PULSE(2)(=B(NP+2)).

Omit the following if there are no constraints (ILMT=0, Block B).

6	Real	BMIN(NP+1)	Minimum constraint for B(NP+1) (dummy value if INDEX(NP+1)=0).
6	Real	BMIN(NP+2)	Minimum constraint for B(NP+2) (dummy value if INDEX(NP+2)=0).
7	Real	BMAX(NP+1)	Maximum constraint for B(NP+1) (dummy value if INDEX(NP+1) =0).
7	Real	BMAX(NP+2)	Maximum constraint for B(NP+2) (dummy value if INDEX(NP+2) =0).

(4) Multiple pulse input‡ (see Figure 2.1)

3	Integer	MODB	**4**
4	Integer	NPULSE	Number of pulses, n.
5	Real	PULSE(1)	Input concentration of the first pulse, f_1.
5	Real	TPULSE(1)	Starting time of the first pulse, $T_1=0$.
6	Real	PULSE(2)	Input concentration of the second pulse, f_2.
6	Real	TPULSE(2)	Starting time of the second pulse, T_2.
⋮	⋮	⋮	⋮
NPULSE+4	Real	PULSE(NPULSE)	Input concentration of the last pulse, f_n.
NPULSE+4	Real	TPULSE(NPULSE)	Starting time of the last pulse, T_n.

Table 6.7. (continued)

Line	Type	Variable	Description

(5) Exponential input concentration. $f_1 + f_2 \exp(-\lambda^\beta T)$

3	Integer	MODB	5

4	Real	PULSE(1)	Value of f_1.
4	Real	PULSE(2)	Value of f_2.
4	Real	TPULSE(1)	Value of λ^β.

(6) Arbitrary function. $C_o(T)$*

3	Integer	MODB	6

† The dimension for time in the input function should be specified according to the value of NREDU (Block A). Use dimensional time, t (i.e., d, h, min, sec) when NREDU $\leq$ 1.

‡ Step and pulse input are special cases of the multiple pulse input function.

* Specify the general $C_o(T)$ in routine **CINPUT** in source program **USER.FOR**. This option is not available for the stream tube model (MODE=4,6,8)

Block E. Initial Value Problem (Table 6.8)

Table 6.2 also lists the functions that can be used to define the initial concentration in the initial value problem (IVP). Data entry for this block is identical for the deterministic and the stream tube model. Similar to the BVP in Block D, the dimension for position in the initial distribution should be consistent with the value for NREDU specified in Block A. The maximum number of steps for a stepwise initial distribution is 10. Since a first-type inlet condition specifies the concentration at the surface, we can define a Dirac initial condition (MODI = 4) at the surface ($x_1 = 0$, $Z_1 = 0$) in case MODC is 5 or 6 (see (2.23) and (3.33)).

Table 6.8. Block E - Initial Value Problem†

Line	Type	Variable	Description
1,2	-		comment lines.

(0) Zero initial concentration

Line	Type	Variable	Description
3	Integer	MOD1	0

(1) Constant initial concentration

Line	Type	Variable	Description
3	Integer	MOD1	1
4	Real	CINI(1)	Concentration, U_1.

(2) Stepwise Initial Distribution? (see Figure 2.2)

Line	Type	Variable	Description
3	Integer	MOD1	2
4	Integer	NINI	Number of steps, n.
5	Real	CINI(1)	Concentration of the first step, U_1.
5	Real	ZINI(1)	Starting position of the first step, $Z_1=0$.
6	Real	CINI(2)	Concentration of the second step, U_2.
6	Real	ZINI(2)	Starting position of the second step, Z_2.
NINI+4	Real	CINI(NINI)	Concentration of the last step, U_n.
NINI+4	Real	ZINI(NINI)	Starting position of the last step, Z_n

(3) Exponential initial distribution. $U_1 + U_2 \exp(-\lambda^I Z)$

Line	Type	Variable	Description
3	Integer	MOD1	3
4	Real	CINI(1)	Value of U_1.
4	Real	CINI(2)	Value of U_2.
4	Real	ZINI(1)	Value of λ^I.

(4) Dirac delta initial condition. $m_I/\theta \delta(x - x_1) + U_1$, or $M_I \delta(Z - Z_1) + U_1$

Line	Type	Variable	Description
3	Integer	MOD1	4
4	Real	CINI(2)	Value of m_I/θ or M_I.
4	Real	ZINI(2)	Value of x_1 or Z_1 (x_1, Z, ≠0 when MODC=5,6).
4	Real	CINI(1)	Value of U_1.

† *The* dimension for depth in the initial condition should be specified according to the value of NREDU (Block A).

‡ Zero and constant initial concentrations are special cases of a stepwise initial distribution.

Block F. Production Value Problem (Table 6.9)

Possible mathematical expressions for the production profiles in the production value problem (PVP) are listed in Table 6.2.   The input format for the PVP is almost identical to that for the IVP (Block E). The dimension of position in the production function should again be consistent with the value of NREDU in Block A. For the equilibrium CDE with dimensional times and positions (NREDU = 0, 1), the production function given by (2.6) is also dimensional. Different production functions can be specified for phases 1 and 2 in the nonequilibrium CDE when MPRO = 1.

Table 6.9. Block F - Production Value **Problem†**

Line	Type	Variable	Description
1,2	-		Comment lines.

(0) No production term

3	Integer	MODP	0

(1) Constant   production

3	Integer	MODP	1
4	Real	GAMMA1(1)	Production value in the equilibrium phase, γ_1, or $\gamma_{1,1}$.

Omit the following for the equilibrium CDE (MODE=1,3,5).

5	Real	GAMMA2(1)	Production value in the nonequilibrium phase, $\gamma_{2,1}$.

(2) Stepwise production profile‡

3	Integer	MODP	2
3	Integer	MPRO	Production function code for a nonequilibrium phase (leave blank if MODE=1,3,or 5, i.e., the equilibrium CDE): 0 Same conditions for equilibrium and nonequilibrium phases. 1 Different conditions for equilibrium and nonequilibrium phases.
4	Integer	NPRO 1	Number of steps in an equilibrium phase, n.
5	Real	GAMMAI(1)	Production of the first step in the equilibrium phase, γ_1, or $\gamma_{1,1}$.
5	Real	ZPROI(1)	Starting position of the first step, Z_1 or $Z_{1,1}=0$.

Table 6.9. (continued)

Line	Type	Variable	Description
6	Real	GAMMA1(2)	Production of the second step in the equilibrium phase, γ_2, or $\gamma_{1,2}$.
6	Real	ZPRO1(2)	Starting position of the second step, Z_2 or $Z_{1,2}$.
⋮	⋮	⋮	⋮
NPRO1+4	Real	GAMMA1(NPRO1)	Production of the NPRO1th step in the equilibrium phase, γ_n, or $\gamma_{1,n}$.
NPRO1+4	Real	ZPRO1(NPRO1)	Starting position of the NPRO1th step, Z_n or $Z_{1,n}$.

Omit the following for the equilibrium CDE (MODE=1,3,5) or if MPRO=0.

Line	Type	Variable	Description
NPRO1+5	Integer	NPRO2	Number of steps in the nonequilibrium phase, m.
NPRO1+6	Real	GAMMA2(1)	Production of the first step for the nonequilibrium phase, $\gamma_{2,1}$.
NPRO1+6	Real	ZPRO2(1)	Starting position of the first step, $Z_{2,1}=0$.
NPRO1+7	Real	GAMMA2(2)	Production of the second step in the nonequilibrium phase, $\gamma_{2,2}$.
NPRO1+7	Real	ZPRO2(2)	Starting position of the second step, $Z_{2,2}$.
⋮	⋮	⋮	⋮
NPRO1 +NPRO2+5	Real	GAMMA2(NPRO1)	Production of the NPRO2th step in the nonequilibrium phase, $\gamma_{1,m}$.
NPRO1 +NPRO2+5	Real	ZPRO2(NPRO1)	Starting position of the NPRO2th step, $Z_{2,m}$.

(3) Exponential production profiles, $\gamma_1 + \gamma_2 \exp(-\lambda^P Z)$

Line	Type	Variable	Description
3	Integer	MODP	**3**
3	Integer	MPRO	Production function code for nonequilibrium models (leave blank if MODE=1,3, or 5, i.e., the equilibrium CDE): **0** Same conditions for equilibrium and nonequilibrium phases. **1** Different conditions for equilibrium and nonequilibrium phases.
4	Real	GAMMA1(1)	Value of γ_1 or $\gamma_{1,1}$.
4	Real	GAMMA1(1)	Value of γ_2 or $\gamma_{1,2}$.
4	Real	ZPRO1(1)	Value of λ^P or λ^P_1.

Omit the following if MPRO=0 or for the equilibrium CDE (MODE=1,3,5).

Line	Type	Variable	Description
5	Real	GAMMA2(1)	Value of $\gamma_{2,1}$.
5	Real	GAMMA2(1)	Value of $\gamma_{2,2}$.
5	Real	ZPRO2(1)	Value of λ^P_2.

† Provide dimensional γ according to (2.6) for the equilibrium CDE (MODE=1,3,5) with NREDU=1. Otherwise, use dimensionless γ as shown in Table 2.1 and 3.1 (see NREDU in Block A).

‡ Constant production is a special case of a stepwise production profile.

Block G. Observed Data for Inverse Problem (Table 6.10)

Observed data can be given in four different formats: (a) position, time, and observed concentration (INPUTM=0); (b) time and observed concentration at a particular position (INPUTM = 1); (c) position and concentration at a particular time (INPUTM = 2); and (d) similar as (a) but the data are now given in a fixed format to allow the use of input files consistent with the previous CXTFIT version (INPUTM = 3). Hence, data from breakthrough curves or concentration profiles versus depth should be described with INPUTM equal to 1 and 2, respectively. It is not necessary to specify the number of observations — the end of a data set should be marked by a line having dummy zeroes. The maximum number of observed concentrations is determined by the parameter MAXOB, which is defined at the top of the main program (the current default setting is 401).

Table 6.10 Block G - Observed Data for Inverse Problem†

Line	Type	Variable	Description
1,2	-	-	Comment lines.
3	Integer	INPUTM	Input data code: **0** $Z(I)$, $T(I)$, $C(I)$ **1** $T(I)$, $C(I)$ for a fixed depth (breakthrough curve). **2** $Z(I)$, $C(I)$ for a fixed time (concentration vs. depth). **3** $C(I)$, $Z(I)$, $T(I)$ (Fixed format, 3F10.0, for CXTFIT version 1 data).

(a) INPUTM=0

Line	Type	Variable	Description
4	-	-	Comment line.
5	Real	$Z(1)$	Position of the first observation.
5	Real	$T(1)$	Time of the first observation.
5	Real	$C(1)$	Value of the first observed concentration (dummy value if MIT=0).
6	Real	$Z(2)$	Position of the second observation.
6	Real	$T(2)$	Time of the second observation.
6	Real	$C(2)$	Value of the second observed concentration (dummy value if MIT=0).
⋮	⋮	⋮	⋮
NOB+4	Real	$Z(NOB)$	Position of the NOB^{th} observation.
NOB+4	Real	$T(MOB)$	Time of the NOB^{th} observation.
NOB+4	Real	$C(NOB)$	Value of the NOB^{th} observed concentration (dummy value if MIT=0).
NOB+5	Real	Dummy	Enter 0 to mark end of data set.
NOB+5	Real	Dummy	Enter 0 to mark end of data set.
NOB+5	Real	Dummy	Enter 0 to mark end of data set.

Table 6.10. (continued)

Line	Type	Variable	Description
(b) INPUTM=1			
4	-	-	Comment line.
5	Real	DUMTZ	Position of the breakthrough curve.
6	Real	T(1)	Time of the first observation.
6	Real	C(1)	Value of the first observed concentration (dummy value if MIT=0).
7	Real	T(2)	Time of the second observation.
7	Real	C(2)	Value of the second observed concentration (dummy value if MIT=0).
⋮	⋮	⋮	⋮
NOB+5	Real	T(MOB)	Time of the NOB[th] observation.
NOB+5	Real	C(NOB)	Value of the NOB[th] observed concentration (dummy value if MIT=0).
NOB+6	Real	Dummy	Give 0 to mark end of data set.
NOB+6	Real	Dummy	Give 0 to mark end of data set.
(c) INPUTM = 2			
4	Real	DUMTZ	Time of the solute profile.
5	-	-	Comment line.
6	Real	Z(1)	Position of the first observation.
6	Real	C(1)	Value of the first observed concentration (dummy value if MIT=0).
7	Real	Z(2)	Position of the second observation.
7	Real	C(2)	Value of the second observed concentration (dummy value if MIT=0).
⋮	⋮	⋮	⋮
NOB+5	Real	Z(NOB)	Position of the NOB[th] observation.
NOB+5	Real	C(NOB)	Value of the NOB[th] observed concentration (dummy value if MIT=0).
NOB+6	Real	Dummy	Give 0 to mark end of data set.
NOB+6	Real	Dummy	Give 0 to mark end of data set.
(d) INPUTM = 3 (Fixed format, 3F10.0, for CXTFIT version 1 data)			
4	-	-	Comment line.
5	Real	C(1)	Value of the first observed concentration (dummy value if MIT=0).
5	Real	Z(1)	Position of the first observation.
5	Real	T(1)	Time of the first observation.
6	Real	C(2)	Value of the second observed concentration (dummy value if MIT=0).
6	Real	Z(2)	Position of the second observation.
6	Real	T(2)	Time of the second observation.
⋮	⋮	⋮	⋮
NOB+4	Real	C(NOB)	Value of the NOB[th] observed concentration (dummy value if MIT=0).
NOB+4	Real	Z(NOB)	Position of the NOB[th] observation.
NOB+4	Real	T(MOB)	Time of the NOB[th] observation.
NOB+5	Real	Dummy	Give 0 to mark end of data set.
NOB+5	Real	Dummy	Give 0 to mark end of data set.
NOB+5	Real	Dummy	Give 0 to mark end of data set.

† If MIT=0 concentrations are calculated at specified Z(I) and T(I) using the initial parameter estimates.

Block H . Position and Time for Direct Problem (Table 6.11)

The concentration is calculated for a user-defined grid system of times and positions.   The maximum number of concentrations that can'be calculated in this way is given by MAXOB (= 401). If MPRINT = 1, the concentration is assumed to be given as a function of time, while for MPRINT = 2 the concentration is given versus depth.

Table 6.11. Block H - Position and Time for Direct Problem

Line	Type	Variable	Description
1,2	-		Comment lines.
3	Integer	NZ	Number of output positions.
3	Real	DZ	Spatial increment for output.
3	Real	ZI	Initial value of output position.
3	Integer	NT	Number of output times.
3	Real	DT	Time increment for output.
3	Real	TI	Initial value of output time.
3	Integer	MPRINT	Output print code:
			1 Concentration vs. time.
			2 Concentration vs. depth.

6.3. Example Input and Output Files

We will present in this section some typical examples of direct and inverse problems. All input and output files for the examples are provided on the distribution diskette.

6.3.1. Direct Problem

Tables 6.12 and 6.13 are input and output files for the deterministic nonequilibrium CDE (cf. Figure 7.6a)   Block H in the input file is used to specify the grid of times and positions for which concentrations are to be calculated.   The parameter NCASE, on the first line of the input file, specifies the number of cases considered. The output file shows the conditions for the simulation as well as calculated results for times and positions specified in Block H. The concentration is given as a function of time if MPRINT = 1 (Block H), or as a function of position (distance) if MPRINT = 2. To check the mass balance, *zeroth* time (MPRINT = 1) and depth (MPRINT = 2) moments are calculated according to:

$$\text{sum}\,(\text{C}*\text{dT}) = \sum_{i=1}^{n-1} (C_i + C_{i+1})\,\Delta T/2 \tag{6.2}$$

$$\text{Sum}\,(\text{C}*\text{dZ}) = \sum_{i=1}^{n-1} (C_i + C_{i+1})\,\Delta Z/2 \tag{6.3}$$

Table 6.12. Input File for Figure 7.6a

```
*** BLOCK A: MODEL DESCRIPTION ******************************************
Fig7-6a. Two-site CDE (Alpha=0.08,f=0.7)
 Effect of the fraction of equilibrium site, f
INVERSE     MODE        NREDU
   0           2           1
 MODC      ZL
   1        50
*** BLOCK C: TRANSPORT PARAMETERS **************************************
    V       D       R     Beta      omega    Mu1       Mu2
   20.     10.     5.0    0.44      0.56     0.0       0.0
** BLOCK D: BVP; MODB=O ZERO; =1 Dirac; =2 STEP: =3 A PULSE ************
  MODB                  =4 MULTIPLE; =5 EXPONENTIAL; =6 ARBITRARY
   1
    1.0
*** BLOCK E:  IVP; MODI=O ZERO; =1 CONSTANT;  =2 STEPWISE; =3 EXPONENTIAL **
   MODI
    0
*** BLOCK F: PVP; MODP=O ZERO; =1 CONSTANT; =2 STEPWISE; =3 EXPONENTIAL **
   MODP
    0
*** BLOCK H: POSITION AND TIME FOR DIRECT PROBLEM ********************
   NZ       DZ       ZI       NT       DT       TI       MPRINT
    1       1.0      50.0     101      0.2.     0.0       1
```

79

Table 6.13. Output File for Figure 7.6a

```
$
     ***********************************************************************
     *                                                                     *
     *      CXTFIT VERSION 2.0 (1/2/95)                                     *
     *      ANALYTICAL SOLUTIONS FOR ONE-DIMENSIONAL CDE                    *
     *      DIRECT PROBLEM                                                  *
     *                                                                     *
     *      Fig7-6a. Two-site CDE (Alpha=0.08,f=0.7)                        *
     *       Effect of the fraction of equilibrium site, f                 *
     *                                                                     *
     *      DATA INPUT FILE:  FIG7-6A.IN                                    *
     *                                                                     *
     ***********************************************************************

     MODEL DESCRIPTION
     =================
        DETERMINISTIC NONEQUILIBRIUM CDE (MODE-21
        FLUX-AVERAGED  CONCENTRATION
        REAL TIME (t), POSITION(x)
          (D AND V ARE DIMENSIONAL;
              R,beta,omega,mu, AND gamma ARE DIMENSIONLESS)
        CHARACTERISTIC LENGTH =   50.0000
          FOR  DIMENSIONLESS  PARAMETERS

     INITIAL VALUES OF COEFFICIENTS
     ================================
     NAME           INITIAL VALUE
      V........       .2000E+02
      D........       .1000E+02
      R.. .. ...      .5000E+01
      beta.....       .4400E+00
      omega....
      mu1......       .0000E+00
      mu2......       .0000E+00

     BOUNDARY,  INITIAL,  AND PRODUCTION CONDITIONS
     ==============================================
        DIRAC DELTA INPUT , MASS =   1.0000
        SOLUTE  FREE  INITIAL  CONDITION
        NO PRODUCTION TERM

$ z= 50.0000      (FLUX CONC. VS. TIME)
$ Sum(C1*dT)=          .8207,  Sum(C2*dT)=          .5062
$   TIME           C1              c2
               .00000E+00    .00000E+00
      .5000    .00000E+00    .00000E+00
     1.0000    .00000E+00    .00000E+00


    49.0000    .93484E-03    .51409E-02
    49.5000    .90217E-03    .49753E-02
    50.0000    .87064E-03    .48150E-02
```

6.3.2. Parameter Estimation

Tables 6.14 and 6.15 are input and output files for parameter optimization. Observed data were fitted with the deterministic nonequilibrium two-region model (cf. Figure 7.9b). In the input file, Block B specifies the conditions for the parameter estimation, while the observed data are given in Block G.

Table 6.14. Input File for Figure 7.9b

```
    1
*** BLOCK A: MODEL DESCRIPTION *********************************************
Fig 6.9b:BORON EFFLUENT (Exp3-1,van Genuchten,1974)
(Kd=1.04, unit, cm, d, micro g)(CXTFIT,EX.4A,Fig.5)
INVERSE    MODE       NREDU
    1        2          2
MODC       ZL
    1       30.0
*** BLOCK B: INVERSE PROBLEM **********************************************
  MIT       ILMT      MASS
  50         0          0
  MNEQ      MDEG
    0          0
*** BLOCK C: TRANSPORT PARAMETERS ****************************************
    V          D         R       Beta     omega     Mu1       Mu2
   38.5      15.5       3.9       0.5       0.2       0.        0.
    0          0          0        1         1         0         0

*** BLOCK D: BVP; MODB=0 ZERO; =1 DIRAC; =2 STEP; =3 A PULSE ***********
   MODB (Reduced Conc.& time) =4 MULTIPLE; =5 EXPONENTIAL; =6 ARBITRARY
    3
    1.0      6.494
*** BLOCK E: IVP; MODI=0 ZERO; =1 CONSTANT; =2 STEPWISE; =3 EXPONENTIAL **
   MODI
    0
*** BLOCK F: PVP; MODP=0 ZERO; =1 CONSTANT; =2 STEPWISE; =3 EXPONENTIAL **
   MODP
    0
*** BLOCK G: DATA FOR AN INVERSE PROBLEM ** *****************************
INPUTM =0; Z,T,C =1; T,C FOR SAME Z =2; Z,C FOR SAME T
    1
    1.0
         TIME        CONC      (Give "0 0 0" after last data set.)
         1.80        0.015
         1.95        0.075
          :            :
          :            :
        17.00        0.040
        18.50        0.029
        20.00        0.025
         0            0
```

81

The first part of the output file gives the conditions for the simulation and parameter estimation. The goodness of fit is described with the coefficient of determination, r^2, for the regression of observed versus fitted concentrations:

$$r^2 = 1 - \frac{\sum_{i=1}^{N}(C_i - f_i)^2}{\sum_{i=1}^{N}(C_i - \bar{C})^2} = 1 - \frac{SSQ^2}{\sum_{i=1}^{N}(C_i - \bar{C})^2} \tag{6.4}$$

where C_i and f are observed and fitted data, respectively, and $\bar{C}$ is the mean of all N observed concentrations. A value for r^2 close to unity indicates a good fit whereas values close to zero indicate a relatively poor description of the observed data by the selected model. The reliability of the parameter estimation may also be assessed with the parameter covariance matrix [*Kool and Parker*, 1988]. Once an acceptable minimum of the objective function (SSQ) has been found, a first-order approximation of the parameter covariance matrix is obtained from

$$\mathbf{C} = s^2 \mathbf{A}^{-1} \tag{6.5}$$

where s is an estimate of the variance due to error for M fitted parameters, i.e.,

$$s = \frac{SSQ}{N - M} \tag{6.6}$$

and $\mathbf{A}$ is given by (5.22). The standard error of the parameter b_j (denoted as S.E. COEFF. in the output file) is given by $(C_{jj})^{1/2}$ while the T-value is given by $b_j /(C_{jj})^{1/2}$. The values for T and the standard error provide relative and absolute measures of deviations around the mean parameter value; a high value for T is desirable. The covariance matrix, α, for the fitted parameters is obtained by simply dividing the elements of $\mathbf{C}$ by the parameter standard error:

$$\alpha_{ij} = \frac{C_{ij}}{(C_{ii})^{1/2}(C_{jj})^{1/2}} \tag{6.7}$$

In addition, the boundaries of the 95 % confidence region are calculated using the appropriate value of Student's t distribution:

$$b_{j,min} = b_{j,fit} - t_{N-M,0.975} \, (C_{jj})^{1/2} \tag{6.8}$$

$$b_{j,max} = b_{j,fit} + t_{N-M,0.975} \, (C_{jj})^{1/2} \tag{6.9}$$

where $b_{j,fit}$ is the fitted parameter value, and $t_{N-M,0.975}$ is the value of the t distribution for confidence level 0.95 with N - M degrees of freedom.

It should be noted that since (6.5), (6.8), and (6.9) are based on linear regression analysis, they hold only approximately for the nonlinear analysis as was discussed by **Kool und Parker** [1988]. However, (6.8) and (6.9) will yield reasonable approximations for individual parameter confidence intervals if no constraints are used and $b_{j,fit}$ represents the true global minimum of the objective function.

Table 6.15. Output File for Figure 7.9b

```
$
     ********************************************************************
     *                                                                  *
     *      CXTFIT VERSION 2.0 (1/2/95)                                 *
     *      ANALYTICAL SOLUTIONS FOR ONE-DIMENSIONAL CDE                *
     *      NON-LINEAR LEAST-SQUARES ANALYSIS                           *
     *                                                                  *
     *      Fig 6.9b:BORON EFFLUENT (Exp3-1,van Genuchten,1974)         *
     *      (Kd=1.04, unit, cm, d, micro g)(CXTFIT,EX.4A,Fig.5)         *
     *                                                                  *
     *      DATA INPUT FILE:  FIG7-9B.IN                                *
     *                                                                  *
     ********************************************************************

     MODEL DESCRIPTION
     =================
        DETERMINISTIC NONEQUILIBRIUM CDE (MODE=2)
        FLUX-AVERAGED  CONCENTRATION
        REDUCED TIME (T), POSITION(Z)
          (ALL PARAMETERS EXCEPT D AND V ARE DIMENSIONLESS)
        CHARACTERISTIC LENGTH =   30.0000
          FOR  DIMENSIONLESS  PARAMETERS

     INITIAL VALUES OF COEFFICIENTS
     ==============================
     NAME          INITIAL VALUE    FITTING
        V........     .3850E+02        N
        D........     .1550E+02        N
        R........     .3900E+01        N
        beta.....     .5000E+00        Y
        omega....     .2000E+00        Y
        mu1......     .0000E+00        N
        mu2......     .0000E+00        N
```

83

Table 6.15. (continued)

BOUNDARY, INITIAL, AND PRODUCTION CONDITIONS
═══

   SINGLE PULSE OF CONC. =   1.0000 & DURATION =   6.4940
   SOLUTE FREE INITIAL CONDITION
   NO PRODUCTION TERM

PARAMETER ESTIMATION MODE
═══════════════════════════

   MAXIMUM NUMBER OF ITERATIONS =   50
   TWO-REGION PHYSICAL NONEQUILIBRIUM MODEL

ITER	SSQ	beta.	omega
0	.1563E+01	.500E+00	.200E+00
1	.1628E+00	.554E+00	.564E+00
2	.8561E-01	.571E+00	.712E+00
3	.8460E-01	.576E+00	.707E+00
4	.8459E-01	.578E+00	.700E+00
5	.8459E-01	.578E+00	.700E+00

COVARIANCE MATRIX FOR FITTED PARAMETERS
═══

	beta.	omega
beta.	1.000	
omega	-.756	1.000 .

RSQUARE FOR REGRESSION OF OBSERVED VS PREDICTED = .96970540
  (COEFFICIENT OF DETERMINATION)

NON-LINEAR LEAST SQUARES ANALYSIS, FINAL RESULTS
═══

| | | | | 95% CONFIDENCE LIMITS | |
NAME	VALUE	S.E.COEFF.	T-VALUE	LOWER	UPPER
beta.	.5780E+00	.8401E-01	.6880E+01	.4059E+00	.7501E+00
omega	.6999E+00	.8401E-01	.8331E+01	.5278E+00	.8720E+00

------------------ORDERED BY COMPUTER INPUT-------------------

| | | | CONCENTRATION | | RESI- |
$ NO	DISTANCE	TIME	OBS	FITTED	DUAL
1	1.0000	1.8000	.0150	.0594	-.0444
2	1.0000	1.9500	.0750	.1253	-.0503
3	1.0000	2.1000	.1700	.2120	-.0420
4	1.0000	2.2500	.2650	.3050	-.0400
5	1.0000	2.4000	.3400	.3902	-.0502
6	1.0000	2.6000	.4300	.4794	-.0494
7	1.0000	2.8500	.5350	.5523	-.0173
⋮	⋮	⋮	⋮	⋮	⋮
25	1.0000	12.7000	.1330	.1356	-.0026
26	1.0000	14.0000	.0900	.0912	-.0012
27	1.0000	15.5000	.0540	.0573	-.0033
28	1.0000	17.0000	.0400	.0358	.0042
29	1.0000	18.5000	.0290	.0222	.0068
30	1.0000	20.0000	.0250	.0137	.0113

6.4. CXTFIT 1.0

This section outlines the difference in input format for CXTFIT 2.0 and its predecessor, version 1 [Parker and *van Genuchten, 1984]*. This information is included to quickly familiarize users of the prior CXTFIT program with the current version. All functions in CXTFIT 1 .O are also included in version 2, except for parameter estimation of the constant production term, y, in the equilibrium CDE (MODE = 1,2 in version 1). Many examples were tested using the two versions; identical results were obtained in most cases, while at times the parameter optimization was slightly better for CXTFIT 2.0.   Changes in the input structure are outlined below.

Model Type and Concentration Mode

In version 1, the parameter MODE specified model type and concentration mode. In version 2, the parameters MODE and MODC in *Block A* specify the model type and the concentration mode, respectively. The resident concentration in version 1 is identical to the resident concentration for a third-type inlet condition in version 2 (MODC = 3). Field-scale flux averaged concentrations in version 1 are specified by MODC = 2 in CXTFIT 2.0 (cf. Table 6.1).

Estimation of Solute Application Time

The pulse duration was estimated as a transport parameter in version 1. In this version, the user also needs to set MASS = 1 in *Block B* and INDEX = 1 for the application time in *Block D*.

Degradation Coefficient

The degradation coefficient μ for the deterministic CDE was always dimensional in version 1. As explained in *Block C*, μ may be dimensional or dimensionless in version 2, depending upon the value of NREDU in *Block A*.

Characteristic Length

The characteristic length L for nondimensional parameters in version 1 was defined internally as the maximum value of the independent variable, x. Instead, a value for L now has to be entered by the user in **Block A. This** modification allows greater flexibility, while nondimensional parameters, such as ω, can also be made independent from the maximum depth for a particular set of observations.

Stochastic Model with Random v

The stochastic model in version 1 consisted of a stream tube model with random pore-water velocity, v. Additional stochastic parameters can be used in version 2 as discussed in Chapter 4. The case of only a stochastic v can be modeled in CXTFIT 2.0 by setting the other standard deviations of all other parameters to zero.

Constant Local-Scale Dispersivity

In version 1 only a constant dispersivity, λ, could be used (see (4.25)). To do this in version 2, identical initial estimates for σ_v and σ_D (MODE = 3) should be entered to keep λ constant during the parameter estimation in process. The input parameter is *<D>*.

Stochastic Model for Pulse Input of Constant Duration

A constant application time for the stochastic model (MODE = 5,6 in version 1) can now be given by setting MASSST = 0 for MODB = 3 in **Block D (see** Figure 4.4).

Stochastic Model with Constant Mass

The stochastic model with constant mass (MODE = 7,8 in version 1) can be evaluated in version 2 by setting MASSST = 1 for MODB = 3 in **Block D.**

7. EXAMPLE PROBLEMS

This chapter contains several examples to illustrate the application of CXTFIT 2.0 to different transport scenarios. Both solutions of the direct and the inverse problem will be discussed for several types of boundary value (BVP), initial value (IVP), and production value (PVP) problems. A third-type inlet condition is used in all example problems, while concentrations in the examples are always normalized with respect to the input concentration or initial concentration (Tables 2.1 and 3.1). The input and output files for each example can be found on the distribution diskette.

7.1. Deterministic Equilibrium CDE (MODE = 1)

7.1.1. Direct Problem

The first two examples deal with the solution of the direct problem for the equilibrium CDE. Figure 7.1 illustrates the effect of the first-order decay constant μ, as given by (2.9, on solute
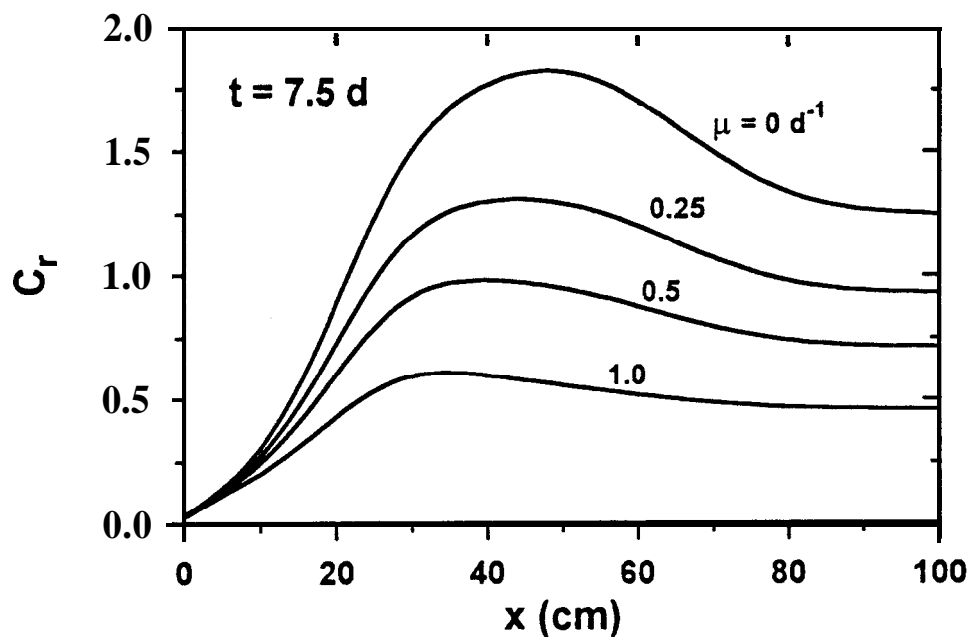
Fig. 7.1. Effect of the first-order decay constant, μ, on calculated C_r-profiles.

distributions. The resident concentration was calculated 7.5 d after applying a single pulse input at $t = 0$ with duration $t_2 = 5$ d to a solute-free soil profile assuming v = 25 cm d^{-1}, $D = 37.5$ cm^2d^{-1}, R = 3, and a constant rate of production $\gamma = 0.5$ mg kg-' d^{-1} [van *Genuchten*, 1981a]. Notice that when μ increases, the concentration decreases as a result of the rise in degradation. Concentrations were evaluated according to (2.34) for $\mu = 0$ d^{-1} while (2.33) was used for $\mu > 0$ d^{-1}.

Differences between resident (C,) and flux-averaged (C_f) concentrations for the BVP have been discussed extensively by several authors [cf. *Kreft* and *Zuber,* 1978; *Jury and Roth,* 1990; *van Genuchten and Parker,* 1984b]. We will illustrate the differences in concentration mode for the IVP [Toride *et al.,* 1993b]. Figure 7.2 shows C_r and C_f as a function of relative distance, Z, at dimensionless time $T = 0.05$ for two values of P when solute-free water is applied to a soil having a stepwise initial resident distribution as indicated by the dashed line. Dispersive transport dominates convective transport when $P = 2$, causing considerable spreading to occur in both the upstream and downstream directions (Figure 7.2a). Notice that at this small time $(T = 0.05)$, C_f is negative for $Z \approx 0.5$, and greater than unity (the initial resident concentration) for $Z \approx 1$. These somewhat odd results are a direct result of the definition of C' according to (2.13). Since the solute flux, J_s, and the water flux, J_w, *are* vectors, C_f becomes negative when the directions of these two fluxes are opposite. The negative C_f near the surface is the result of an upward dispersive solute flux in spite of a downward convective solute flux. Similarly, C_f is greater than C_r if the gradient of C_r becomes negative. For relatively large negative gradients such as those in Figure 7.2 around $Z = 1$, C_f can become greater than the initial resident concentration $C_r(Z,0)$. Notice from Figure 7.2b that the differences between C_f and C_r become smaller for an increased Peclet number, P.
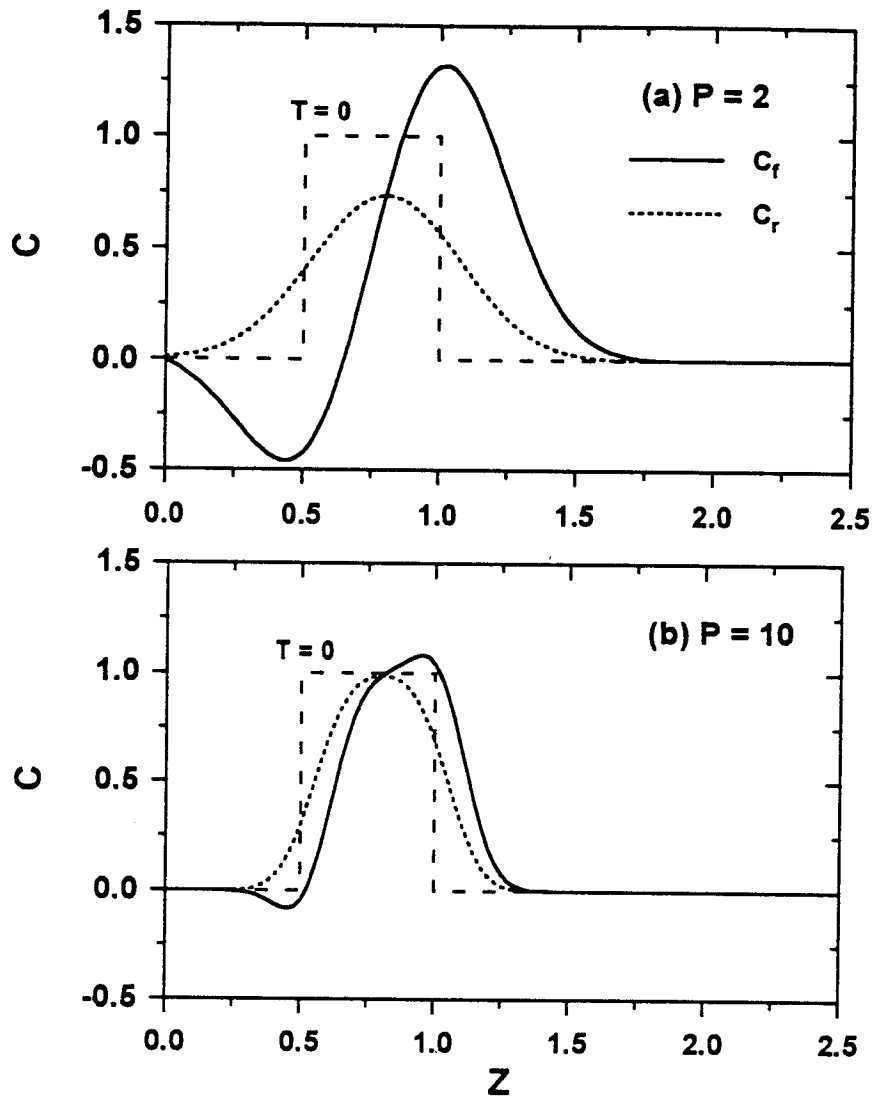
Fig. 7.2. Flux and resident concentrations versus depth at T=0.05 for a solute-free input to a stepwise initial distribution: (a) $P = 2$, and (b) $P = 10$.

7.1.2. Parameter Estimation

Figure 7.3 presents breakthrough curves (BTCs) measured by *Shiozawa* [1994, personal communication] with four-electrode EC sensors at three different depths as a result of: (a) continuous application of a 0.01 M NaCl solution to an initially solute-free saturated sand ($\theta = 0.3$), and (b) leaching with solute free water during unsaturated condition ($\theta = 0.12$). The observations were analyzed in terms of the equilibrium CDE with CXTFIT 2.0 assuming a resident mode (MODC = 3),

yielding estimates of the pore-water velocity, v, and the dispersion coefficient, D. The results are given in Table 7.1. The fitted v and D for each depth were almost identical. These results show that the CDE is an appropriate model for describing transport in this column. Note from the data in Table 7.1 that the dispersivity, λ (= D/v), is smaller for the saturated soil than for the unsaturated soil.
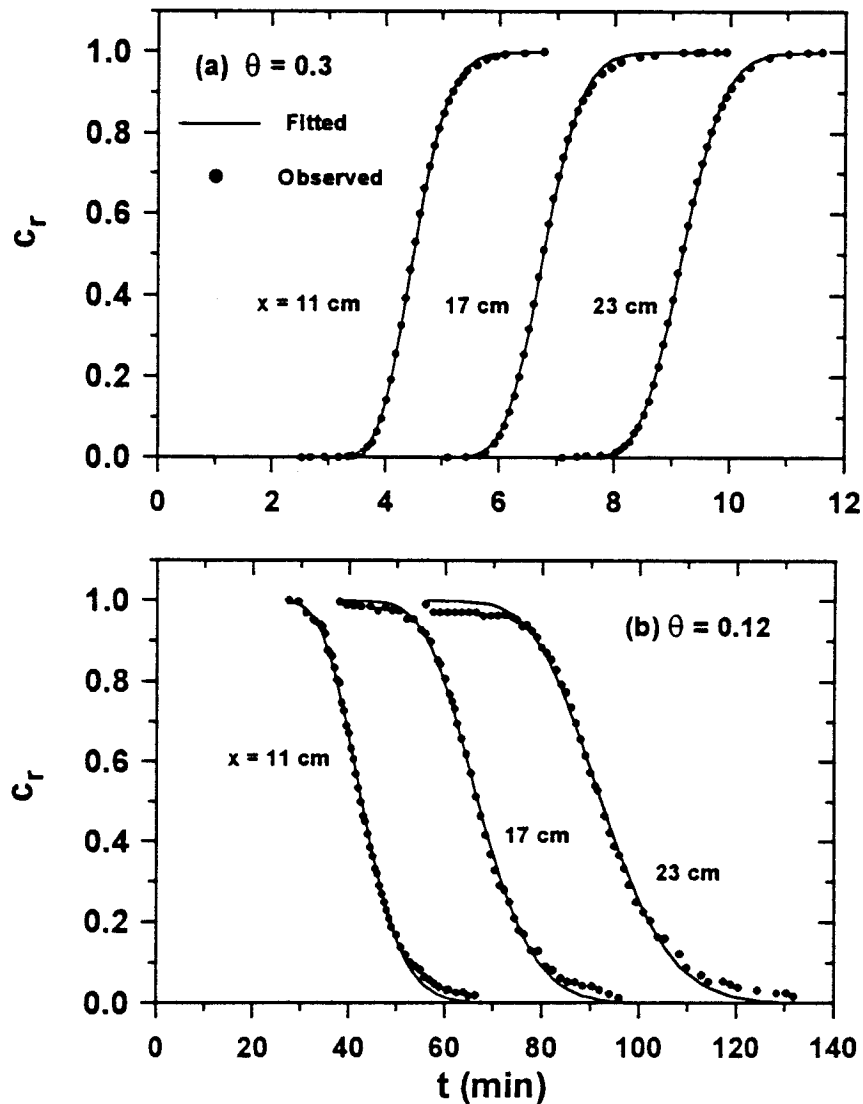
Fig. 7.3. Experimental and fitted breakthrough curves for (a) saturated ($\theta = 0.3$) and (b) unsaturated ($\theta = 0.12$) sand.

Table 7.1. Pore-Water Velocity, v, Dispersion Coeffkient, D, and
Dispersivity, I, Obtained by Fitting the Data of Figure 7.2

Depth cm	v cm d⁻¹	D cm² d⁻¹	λ cm
(a) Saturated (θ = 0.3)			
11	2.45	0.154	0.063
17	2.51	0.126	0.050
23	2.51	0.110	0.044
(b) Unsaturated (θ = 0.12)			
11	0.258	0.0357	0.14
17	0.254	0.0393	0.15
23	0.249	0.0429	0.17

The input mass can be used as a fitting parameter by setting $MASS = 1$ for a Dirac delta input and a pulse input. For a pulse input either the application time or the input concentration can be estimated. Figure 7.4 shows observations and the breakthrough curve obtained by fitting the duration of the application for a pulse input, t_2, in addition to v and D. The concentration was measured with a TDR probe at a depth of 10 cm for a pulse application of KCl solution to an undisturbed sandy soil column [Mallants et al., 1994]. The fitted parameters are v = 2.34 cm d^{-1}, D = 12.8 $cm^2 d^{-1}$, and t_2 = 0.8 h. We again note that mass balance errors are likely to have an adverse effect on the estimation of all transport parameters.
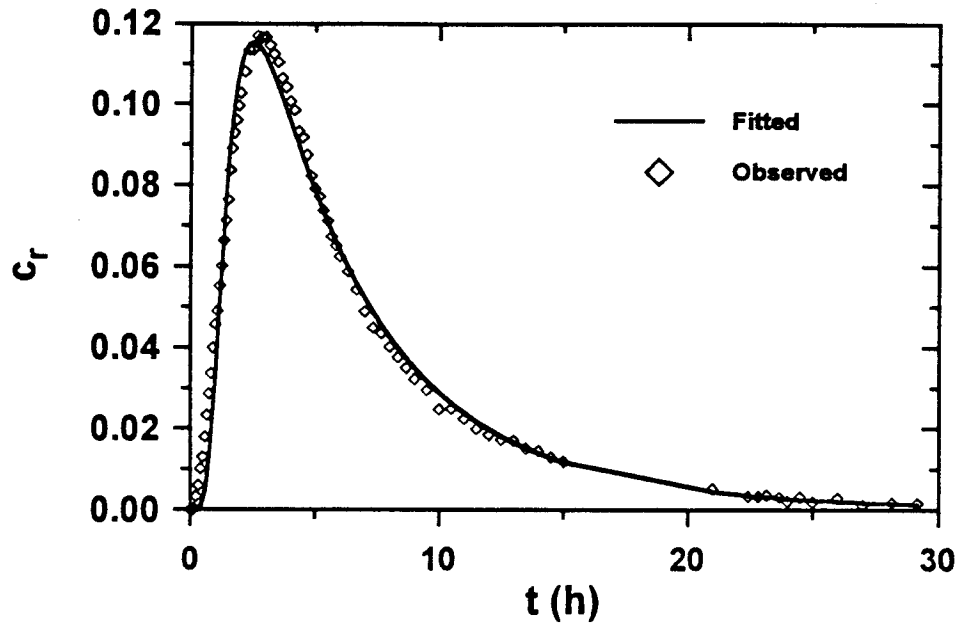
Fig. 7.4. Observed concentrations for a pulse input and breakthrough curve obtained by fitting v, D, and t_2.

7.2. Deterministic Nonequilibrium CDE (MODE = 2)

7.2.1. Direct Problem

The first two examples below are included to demonstrate differences between the one-site and two-site nonequilibrium models. The one-site model is a special case of the two-site model (cf. Section 3.1.1); it is obtained by assuming that the fraction of equilibrium adsorption sites is zero ($f = 0$). The kinetic rate coefficient, α, is then the only remaining nonequilibrium parameter in the dimensional one-site nonequilibrium model.

Figure 7.5 shows the effect of α on the BTCs in terms of the flux-averaged concentration at $x = 50$ cm, as the result of applying a Dirac delta input function to an initially solute free soil. Other parameters are $v = 20$ cm d^{-1}, $D = 10$ cm^2 d^{-1}, and $R = 5$. Note that $\beta = 0.2$, regardless of the values for α, and that the solution of the equilibrium CDE (MODE = 1) was used to predict the BTC for $\alpha \to \infty$. The effect of α may be interpreted in terms of the adsorption time scale, $1/\alpha$, a smaller α suggests slower adsorption. For equilibrium adsorption, the solute peak occurs at $t \approx 12.5$ d which corresponds closely to the value for Rx/v. As α decreases, solute spreading increases. Some of the

solutes are not readily adsorbed and move fairly quickly through the soil, while the remaining solutes move much slower since, once adsorbed, solutes will move back into the solution phase at a relatively slow pace. A concentration peak appears at $t = 2.5$ d as α decreases ($\alpha < 0.2$ d^{-1}). In the extreme case of $\alpha = 0$ (i.e., no adsorption), solute transport is described with the equilibrium CDE for nonreactive solute ($R = 1$).
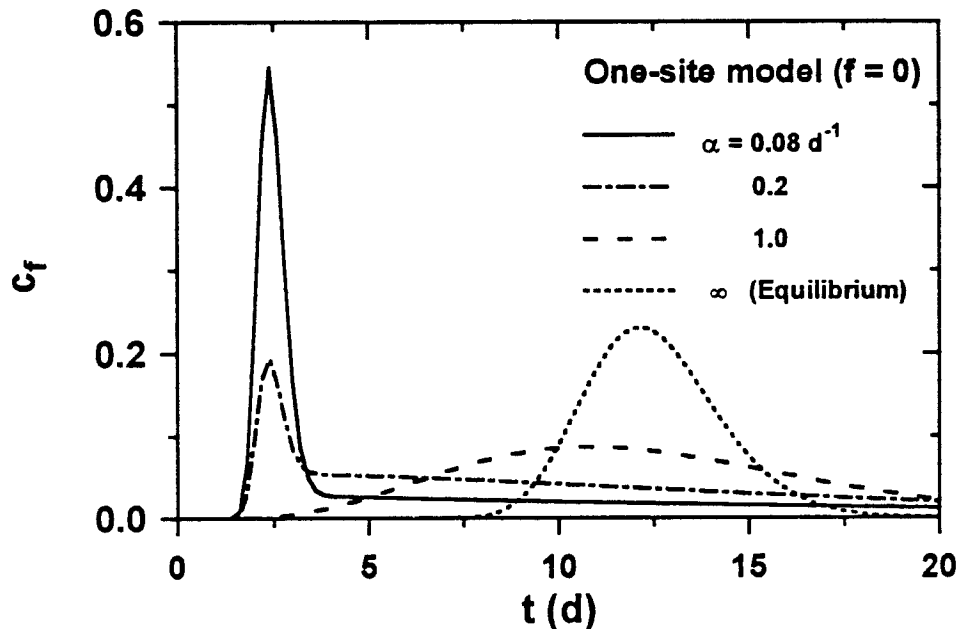
Fig. 7.5. Breakthrough curves at $x = 50$ cm for four values of α as calculated with the one-site nonequilibrium model.

Figure 7.6 presents BTCs according to the two-site nonequilibrium CDE for four values of f using the same condition as in Figure 7.5. The results for the one-site model ($f = 0$) are identical to those given in Figure 7.5. For $f = 1$ the problem is again reduced to the equilibrium CDE with $R = 5$; this case is identical to the BTC for $\alpha \to \infty$ in Figure 7.5. Notice that the concentration peak appears earlier as f decreases, while at the same time the concentration peak increases.
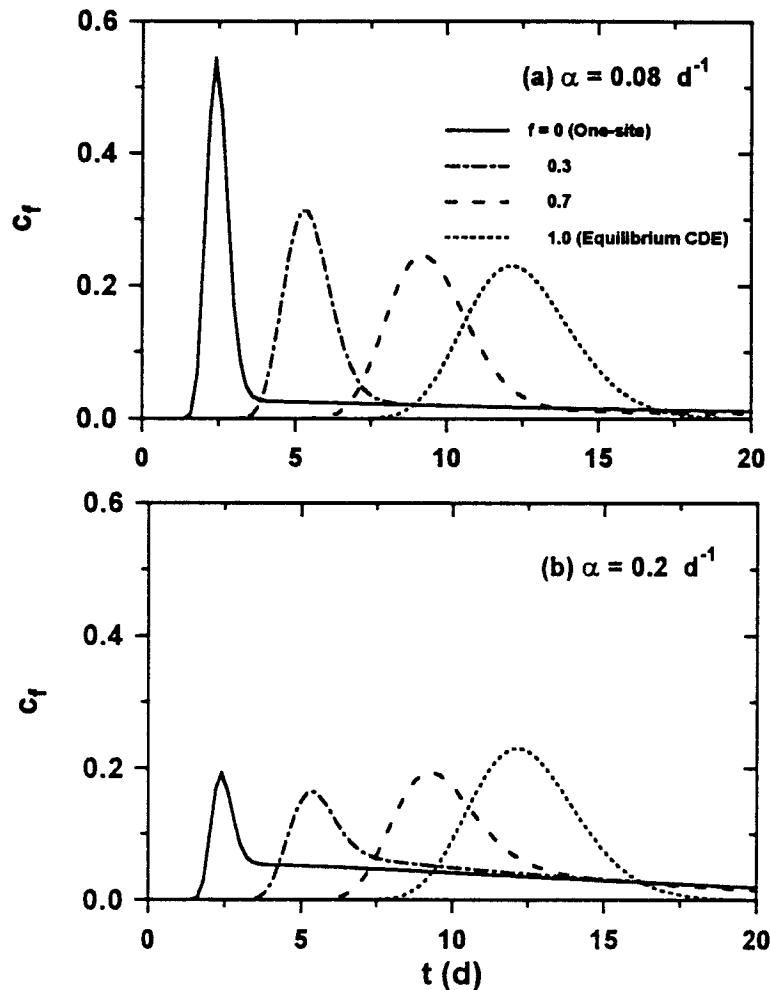
Fig. 7.6. Breakthrough curves according to the two-site nonequilibrium CDE
for four values of f assuming: (a) $\alpha = 0.08$ d^{-1} and (b) $\alpha = 0.2$ d^{-1}.

The additional nonequilibrium parameter in the two-site model, f, gives more flexibility in the estimation procedure than the one-site model. However, if R needs to be estimated in addition to the nonequilibrium parameters, α and f, it is not always possible to find a unique solution to the inverse problem. As an example, Figure 7.7a presents two breakthrough curves calculated with different values for R, α, and f. The solid line in Figure 7.7a is identical to the curves for $f = 0.3$ in Figure 7.6a. If we neglect the effects of dispersion (i.e., $P \to \infty$) and kinetic adsorption (i.e., $\omega = 0$) in equation (3.3), the product βR is equivalent to the number of pore volumes, T, at which the solute initially appears in the effluent [*Parker and van Genuchten*, 1984b]. We used $R = 10$ and $f = 0.135$ to calculate the

94

BTC given by the dashed line in Figure 7.7a — this curve has the same value of 0.22 for βR as the solid curve. Furthermore, we can adjust α to obtain the same peak concentration and an almost identical BTC with some minor differences in the tailing end of the BTC. Figure 7.7a implies that, in general, at least R (i.e., the distribution coefficient, K_d) should be estimated independently.
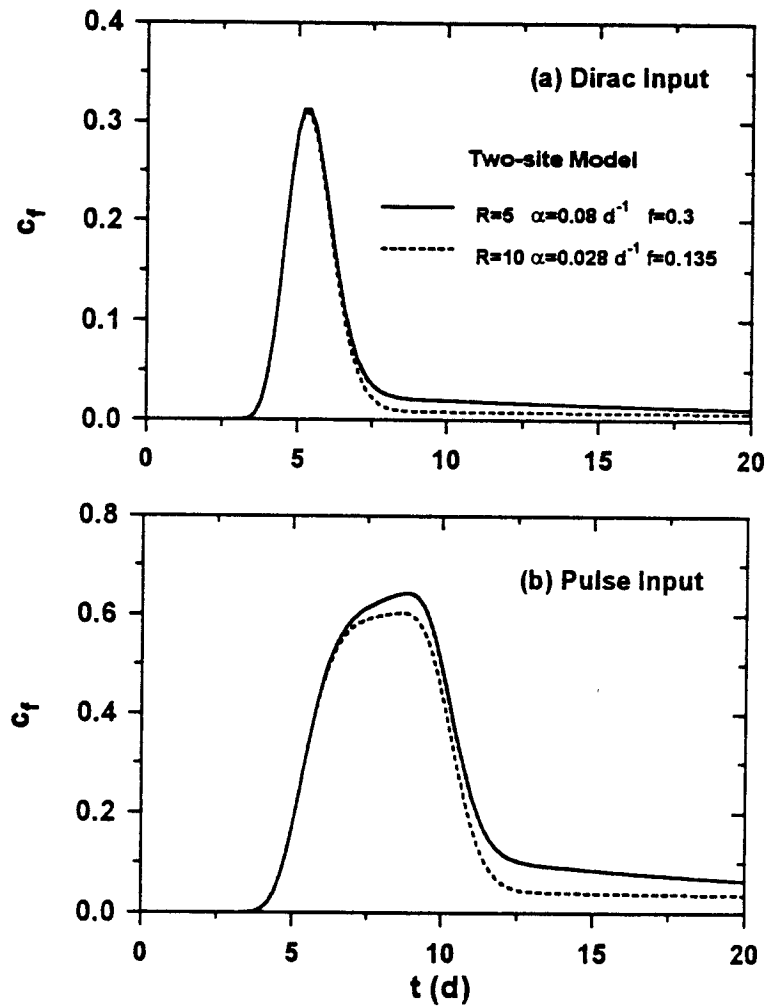
Fig. 7.7. Breakthrough curves for βR = 0.22, using different sets of R, α, and f, calculated with the two-site nonequilibrium CDE for: (a) Dirac delta input, and (b) pulse input of 5d.

Figure 7.7b presents two BTCs for a pulse input of 5 days using the same set of parameters as in Figure 7.7a. Differences between the BTCs predicted with the two different data sets are more pronounced for the pulse input than for the Dirac input. The enhanced tailing for the pulse input will likely somewhat improve the estimated transport parameters in the two-site model.

Since the two-region nonequilibrium model is mathematically identical to the two-site model (cf. Section 3.1.3), we may conclude from the above that different sets of R, α, and θ_m also may lead to nearly identical concentration profiles. For reactive solutes, the fraction, f, of adsorption sites in contact with the mobile liquid phase will cause additional uncertainty in the parameter estimation. When the BTCs for reactive solutes are analyzed in terms of the two-region model, it is best to estimate θ_m from data for a nonreactive tracer (see also Figure 7.9).

The last example involving a direct problem concerns deterministic nonequilibrium transport as described by an initial value problem (IVP). Figure 7.8 shows equilibrium (C,) and nonequilibrium (C_2) resident concentration profiles at $T = 1.0$ for three values of the partitioning coefficient β. The example involves the application of a solute-free solution to a soil with a stepwise initial solute distribution (dashed line in Fig. 7.8), assuming $P = 10$, $R = 2$, $\omega = 1$, and $\mu_1 = \mu_2 = 0.2$. Figure 7.8 shows that solutes are transported more slowly when β is relatively small, i.e., when a relatively large amount of solute resides in the nonequilibrium phase. Hence, leaching is not as effective when β is small. Notice also that the discontinuity in the nonequiiibrium concentration, C_2, persists much longer when β is small. The discontinuity persists because solute removal and subsequent leaching from the nonequilibrium phase can only occur indirectly through the equilibrium phase after the solute has kinetically desorbed from the adsorbed to the solution phase (the one- or two-site adsorption models), or has diised from immobile to mobile water (the two-region model). The nonequilibrium profiles closely resemble the equilibrium when β is large because of increased opportunity for the relatively small amount of solute in the nonequilibrium phase to move to the equilibrium phase.
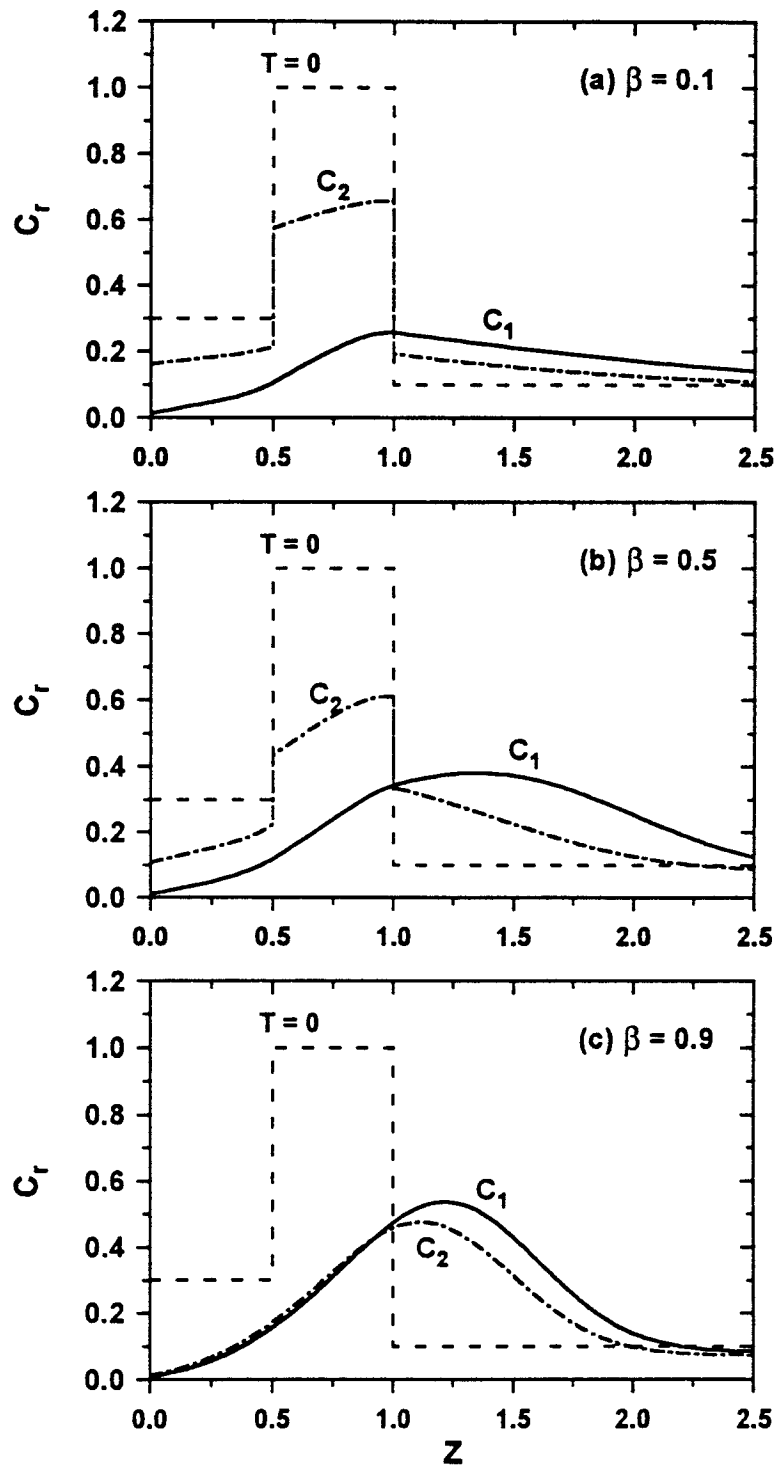
Fig. 7.8. Calculated concentration versus depth for an IVP using:
(a) $\beta = 0.1$, (b) $\beta = 0.5$, and (c) $\beta = 0.9$.

7.2.2. **Parameter Estimation**

Several examples below illustrate the use of CXTFIT **2.0** to estimate parameters involving the nonequilibrium deterministic model. The first example deals with two-region nonequilibrium transport of tritiated water through a Glendale clay loam Experiment 3-2 of van *Genuchten,* 1974]. A ^3H_2O pulse of duration T_2 = 3.102 was applied to a 30-cm long column, and the BTC was determined from the effluent. The volumetric water content, θ, was 0.454 while the pore-water velocity, v, was equal to 37.5 cm d^{-1}. Assuming that $R = 1$ for ^3H_2O, we only have to estimate β (= θ_m/θ) and ω from the measured BTC. Figure 7.9a compares the observed and fitted BTCs. The number of pore volumes, *T, was used as* the dimensionless time in this example (NREDU = 2). We emphasize that v (= $v_m \theta_m/\theta$) and D (= $D_m \theta_m/\theta$) are used as the unknown input parameters, instead of v_m and D_m, which appear in the two-region physical nonequilibrium model (Table 6.7). The fitted values were D = 15.5 $cm^2 d^{-1}$, θ_m/θ = 0.822, and ω = 0.85. These values correspond to v_m = 45.6 cm d^{-1}, D_m = 18.9 $cm^2 d^{-1}$, and α = 0.48 d^{-1}.

A pulse of boron tracer was also applied for T_2 = 6.494 pore volumes to the same column as used in Figure 7.9a [Exp. 3-l of van *Genuchten,* 1974]. The estimated parameters were v = 38.5 cm d^{-1} and R = 3.9 (K_d = 1.04 $g^{-1} cm^3$, ρ_b = 1.222 g cm^{-3}, and θ = 0.445). We assumed that D and θ_m/θ are identical for boron and ^3H_2O (Figure 7.9a). Figure 7.9b shows the observed and fitted BTCs with parameters β = 0.578 and ω = 0.70 (a= 0.40 d^{-1}). Substituting θ_m/θ = 0.822, as obtained from the ^3H_2O BTC, into the expression for β (cf. Table 3.1) yields f = 0.49 for the fraction of sorption sites in contact with the mobile phase.

The boron data are the same as those shown in Figure 5 of the previous CXTFIT manual *[Parker and van Genuchten,* 1984b] when four parameters *(D, R, β,* and ω) were estimated. Table 7.2 shows the effect of having different initial estimates and number of unknown parameter on the optimization of the boron BTC given in Figure 7-9b — similar information was previously shown in Table 3 of *Parker and van Genuchten [* 1984b]. Two different sets of initial estimates were used to estimate either two (i.e., β and ω, with D obtained by fitting the ^3H_2O BTC) or three (i.e., *D, β,* and ω) parameters. For the two-parameter estimation, β and ω converged to almost identical results regardless of the initial estimates. If D was also optimized, the final results depended greatly on the initial estimates. The results for the three-parameter estimation in Table 7.2 were quite dissimilar

although only the initial value for β was different in the two examples. Since the product βR determines the number of pore-volumes, T, at which the tracer initially appears in the effluent, it is important to provide a reasonable initial estimate for βR. If R is fitted as well — in addition to D, β, and ω such as in Table 3 in *Parker and van Genuchten* [1984b] — the likelihood that the optimization does not converge to the correct solution will increase. Figure 7.7 suggests that different parameter sets can yield very similar curves. This occurs when the response surface (i.e., the objective function, **SSQ(b))** has a flat surface near the global minimum or when multiple local minima exist.
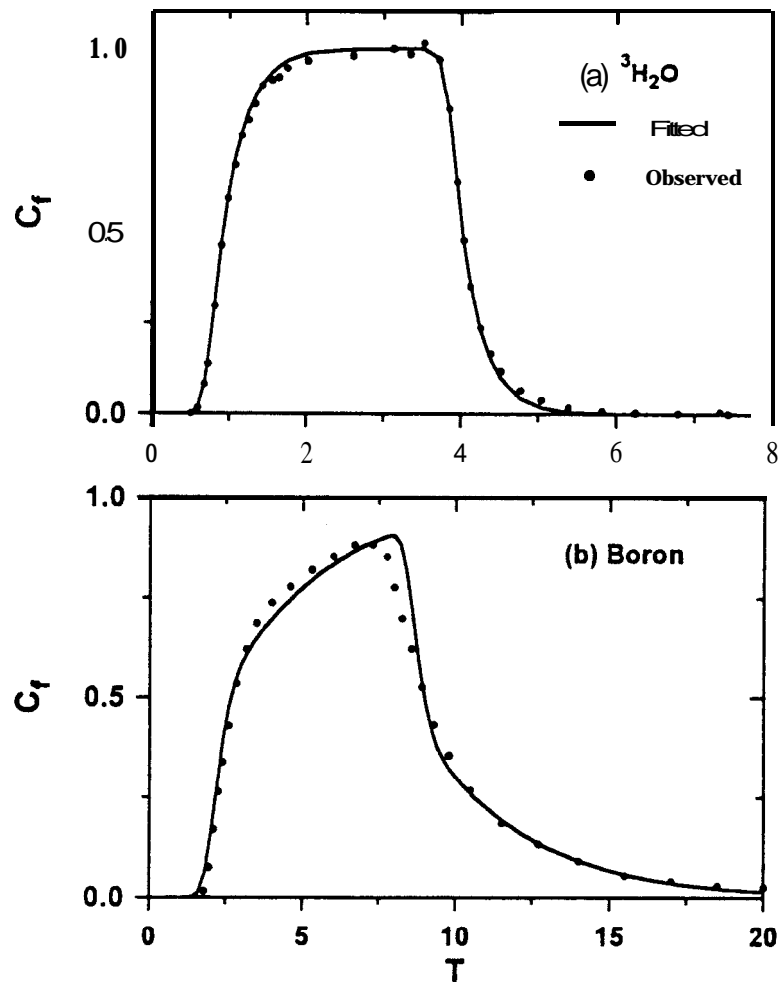
Fig 7.9. Breakthrough curves for a Glendale clay loam described by the two-region physical nonequilibrium model for nonreactive ^3H_2O and reactive boron.

Table 7.2. Fitted Parameter Values and the Coefficient of Determination,
r^2, for the Optimization of the boron BTC for
Different Sets of Initial Estimates

Example	v	D	R	β	ω	r^2
(a) Two parameter (β, ω) estimation						
Initial values	38.5	15.5	3.9	0.5	0.2	
Final values	fixed	fixed	fixed	0.58	0.70	0.970
Initial values	38.5	15.5	3.9	0.1	0.2	
Final values	fixed	fixed	fixed	0.58	0.70	0.970
(b) Three parameter (D, β, ω) estimation						
Initial values	38.5	15.5	3.9	0.5	0.2	
Final values	fixed	50.2	fixed	0.647	0.46	0.978
Initial values	38.5	15.5	3.9	0.1	0.2	
Final values†	fixed	303.6	fixed	0.9999	100.0	0.942

† β and ω reached the internal maximum constraints β=0.9999 and ω=100. The estimate for D is almost identical to that obtained by fitting the equilibrium CDE to the observed data.

In most cases β and ω will be obtained from a simultaneously fit. **Rao et al.** [1980], on the other hand, attempted to independently predict ω from the aggregate size for a medium consisting of uniform spherical aggregates. Nonequilibrium transport of a reactive solutes is probably best studied with experiments that observe the movement of reactive and nonreactive solutes (cf. Figure 7.9). As a first approximation, we can then assume that such parameters as D and θ_m are the same for both types of solute.

7.3. Stochastic CDE (MODE≥3)

7.3.1. Nonreactive Solute Transport

Direct Problem

First we consider equilibrium transport of a nonreactive solute ($R = 1$) at the local scale as discussed in Section (4.2). Figure 7.10 shows the mean, $\hat{c}_r = <c_r>$, and the variance according to (4.20) as a function of depth at $t = 3$ d for three values of σ_v as result of a 2-d solute application to a solute-free soil assuming $<v>=20$ cm d^{-1} and $<D>=20$ cm^2 d^{-1} with a constant dispersivity ($\sigma_v =\sigma_D$).
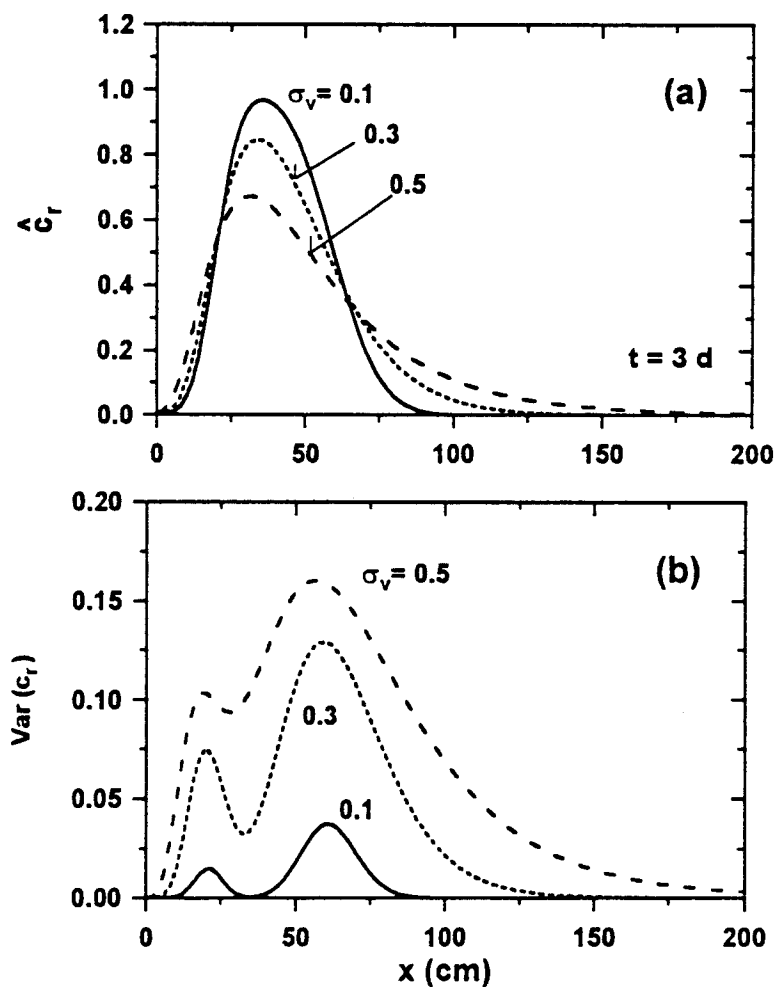
Fig. 7.10. The effect of the variability in the pore-water velocity, v, on:
(a) the field-scale resident concentration ($\hat{c}_r$) profile, and (b) the distribution of the variance for c_r in the horizontal plane.

Solute spreading in the $\hat{c}_r$-profile increased with σ_v as indicated in Figure 7.10a. Figure 7.1 Ob shows that variations in the local-scale c_r also increased with σ_v, thereby suggesting that a more heterogeneous solute distribution will occur in the horizontal plane. Because flow and transport become increasingly heterogeneous as σ_v increases, more observations are needed to reliably estimate field-scale concentrations. Note that the variance profiles have a double peak (Figure 7. 10b). The variance has a relative minimum around $x = 30$ cm where the highest concentration occurs (Figure 7. l0a). Similar bimodal behavior of the variance was observed numerically by *Burr et al. [* 1994] for transport in a three-dimensional heterogeneous medium. The variance also depends on the duration of the solute application time. As the application time increases, continued solute injection will counteract the randomness due to variations in transport properties between stream tubes.

Figure 7.11 presents BTCs for three types of field-scale concentrations ($\hat{c}_r$, $\hat{c}_f$, and $<c_f>$) as a result of a Dirac input assuming $<v> = 50$ cm d^{-1}, $<D> = 200$ cm^2 d^{-1}, and $\sigma_v = \sigma_D = 0.5$. The BTC for $\hat{c}_f$ has the highest peak at a relatively early time, while $\hat{c}_r$ and $<c_f>$ show similar distributions. The local-scale concentration mode apparently has little influence on the field-scale average when the velocity is stochastic. A relatively large value for $<D>$ *was* selected to demonstrate the difference between $\hat{c}_r$ and $<c_f>$. These two concentrations would be very similar for smaller $<D>$ *(e.g.,* 20 cm^2 d^{-1}).
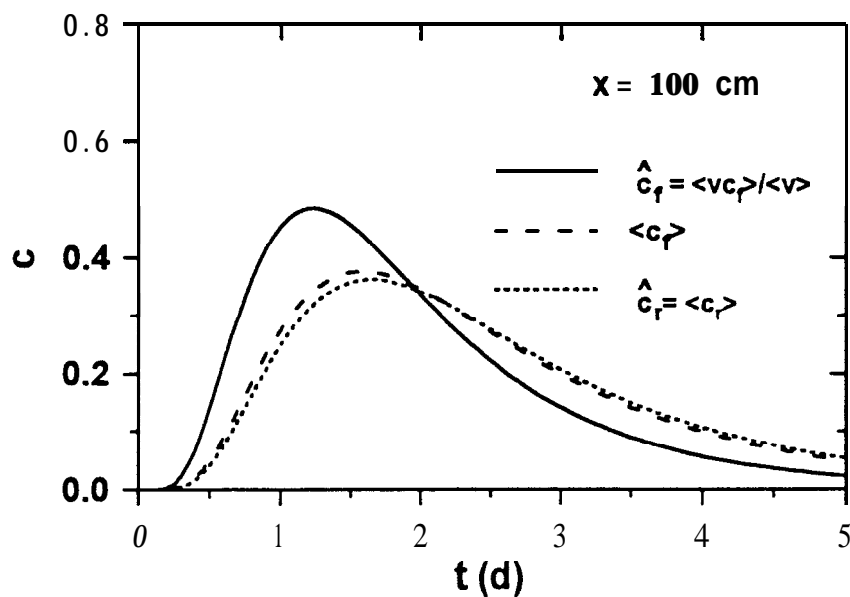
Fig. 7.11. Breakthrough curves for three types of field-scale concentration modes.

The mean breakthrough time and the amount of spreading are smaller for $\hat{c}_f$ than for $\hat{c}_r$ or $<c_r>$. All concentrations are almost identical at $t = 2$ d, which is the mean breakthrough time for $\hat{c}_f$ [*Toride and Leij*, 1995a]. Solutes will only reach $x = 100$ cm prior to $t = 2$ d if it travels in stream tubes with a velocity greater than the ensemble average, $<v>$. The velocity-weighted concentration, $\hat{c}_f$ should therefore be greater than the ensemble-averaged concentrations, $\hat{c}_r$ and $<c_r>$, during the initial stages of the displacement process ($t < 2$ d). On the other hand, $\hat{c}_f$ becomes less than $\hat{c}_r$ or $<c_r>$ at later times ($t > 2$d).

Parameter Estimation

There are very few data sets that allow solution of the inverse problem for the stream tube model. The same data as those of Figure 7a in the CXTFIT manual by *Parker and van Genuchten* [1984b] were used to demonstrate parameter estimation for the stochastic stream tube model. The example pertains to resident concentrations of a 0.64-ha field to which a bromide pulse was applied for 1.69 d followed by leaching with solute-free water [*Jury et al.*, 1982]. The stream tube model can be adapted for transient flow conditions as shown by *Parker and van Genuchten* [1984b, p. 41].
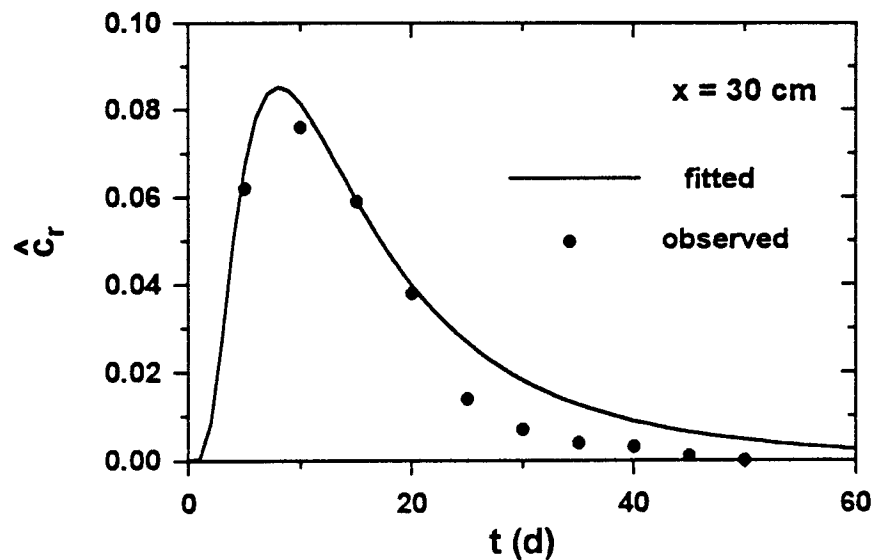
Figure 7.12. Observed and fitted values of $\hat{c}_r$ for field-scale transport of bromide (after *Jury et al.* [1982]).

The dispersivity, λ, was assumed to be constant with $\rho_{vD} = 1$; the following parameters should hence be used in the input file: MODE = 3 and $\sigma_v = \sigma_D$ (cf. Eq. (4.25) and Table 6.7). Solution of the inverse problem yielded: $<v> = 30.5$ mm d^{-1}, $<D> = 2.5$ mm^2 d^{-1}, and $\sigma_v = 0.8$ mm d^{-1}, and $\sigma_D = 0.8$ mm^2 d^{-1}. The estimates for $<v>$ and σ_v are identical to those by *Parker and van Genuchten* [1984b], whereas $<D>$ was about ten times smaller. Local dispersion typically has a minor effect on the field-scale concentration (cf. *Parker and van Genuchten* [1984b] and *Toride and Leij* [1995a]).

7.3.2. Reactive Solute Transport

Direct Problem

In addition to the variability in v and D, we may also need to consider the variability in the distribution coefficient, K_d, and the nonequilibrium rate parameter, α, when modeling the field-scale transport of reactive solutes. The effect of a stochastic v or K_d on field-scale concentrations is first demonstrated for equilibrium transport using MODE = 3. The field-scale resident concentration, $\hat{c}_r$, at $t = 5$ d resulting from a Dirac delta input at $t = 0$, is plotted versus depth in Figure 7.13 for either perfect or no correlation between v and K_d. Values of the transport parameters are: $<v> = 50$ cm d^{-1}, $D = 20$ cm^2 d^{-1}, $<K_d> = 1$ g^{-1} cm^3, $\sigma_{Kd} = 0.2$ g^{-1} cm^3, $<R> = 5$, and $\rho_b/\theta = 4$ g cm^{-3}.
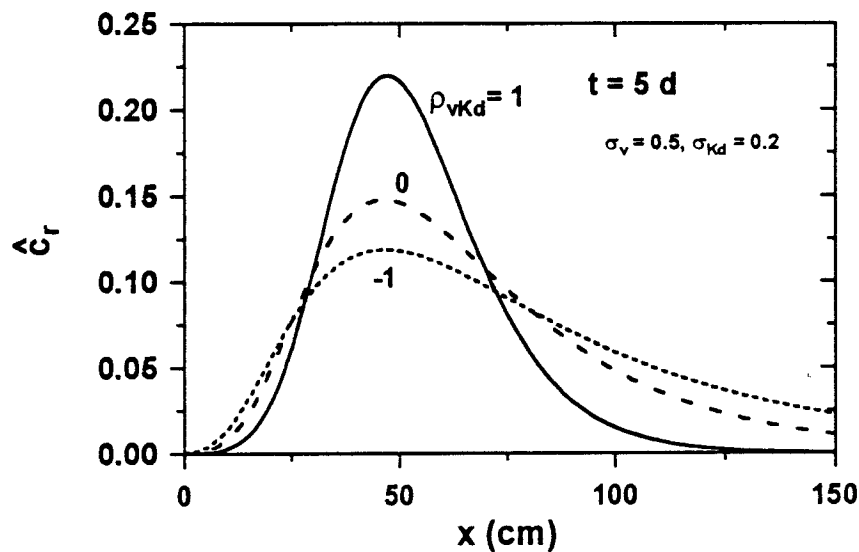
Fig. 7.13. Effect of the correlation between v and K_d on field-scale resident concentration ($\hat{c}_r$) profiles.

104

A negative correlation between v and K_d implies that R and v are inversely related; such a correlation causes additional spreading in the field-scale concentration. The effect of variability in K_d on solute spreading, as observed from the results of the relatively simple stream tube model, is quite similar as observed using more general stochastic approaches [e.g., *Bosma et al.*, 1993].

If solutes are not adsorbed instantaneously, the field-scale concentration may be predicted with the nonequilibrium transport models defined by (4.1) and (4.2). In the next example we assume that the nonequilibrium rate coefficient, α, is deterministic (MODE = 4). Figure 7.14 shows the field-scale resident ($\hat{c}_r$) and total resident ($\hat{c}_T$) concentrations versus depth at $t = 1$ d. The stochastic parameters are v and K_d, with $\rho_{Kd} = -1$, while the deterministic rate parameter (actually the dimensionless parameter, ω) is given by: (a) $\alpha = 2.5$ d^{-1}, (b) $\alpha = 0.5$ d^{-1}, and (c) $\alpha = 0.1$ d^{-1}. All other parameters were taken to be the same as those used for Figure 7.13. Differences between $\hat{c}_T$ and $\hat{c}_r$ reflect the amount of adsorbed solutes. As α decreases, some of the solute will not be readily adsorbed and hence is transported downgradient relatively quickly. On the other hand, a relatively large fraction of the solutes will be adsorbed near the surface in case of an increased α.
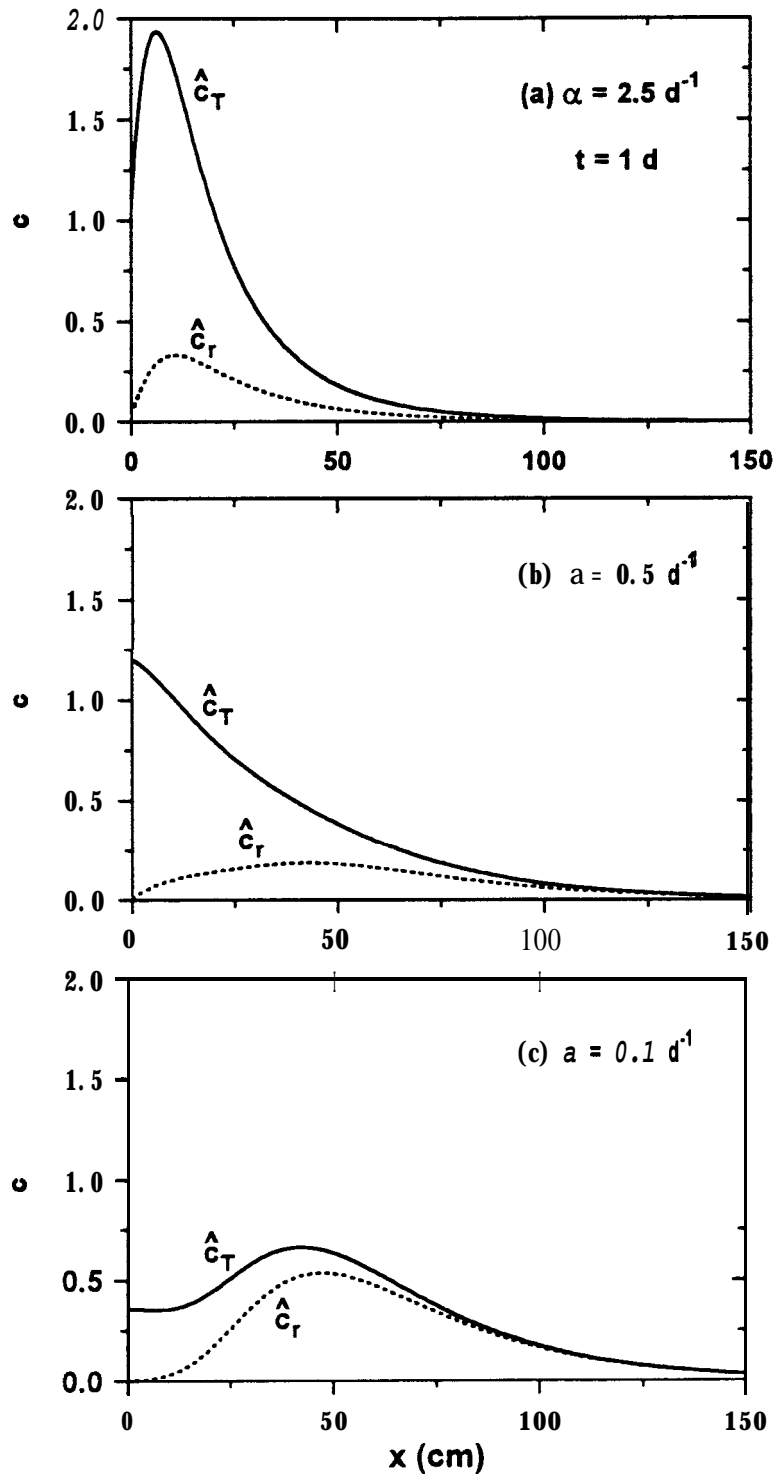
Fig. 7.14. Nonequilibrium field-scale transport for negatively correlated v and K_d.

Parameter Estimation

As for nonreactive solutes, there is a general lack of suitable data for estimating transport parameters in the stream tube model for reactive solutes. We will therefore use a hypothetical data set to illustrate the solution of the inverse problem in CXTFIT 2.0 for stochastic transport of reactive solutes. Furthermore, the solution of the inverse problem is far more complicated since both the variability in v or D as well as α or K_d [*Robin et al.*, 1991] may have to be considered. Figure 7.15 shows predicted resident concentrations, c_r, after a solute pulse is applied for one day; the following model parameters were used: $<v> = 50$ cm d^{-1}, $D = 20$ cm^2 d^{-1}, $<K_d> = 1$ g^{-1} cm^3, $\sigma_{Kd} = 0.3$ g^{-1} cm^3, $<R> = 5$, $\rho_b / \theta = 4$ g cm^{-3}, and $\rho_{vKd} = -0.8$ (MODE = 3). The standard deviation, σ_{Kd}, and the coefficient of correlation between v and K_d, ρ_{vKd}, were fitted to the hypothetical data while keeping $<v>$, σ_v, and $<K_d>$ constant at the above values. The latter parameters could also have been estimated from data for a nonreactive solute. The program converged to the correct parameter values, i.e., those that were used to generate the hypothetical data set, after just a few iterations. Unfortunately, such good results are unlikely for most practical cases since the experimental conditions in most heterogeneous fields will not conform exactly to the assumptions made for the stream tube model (cf. Chapter 4).
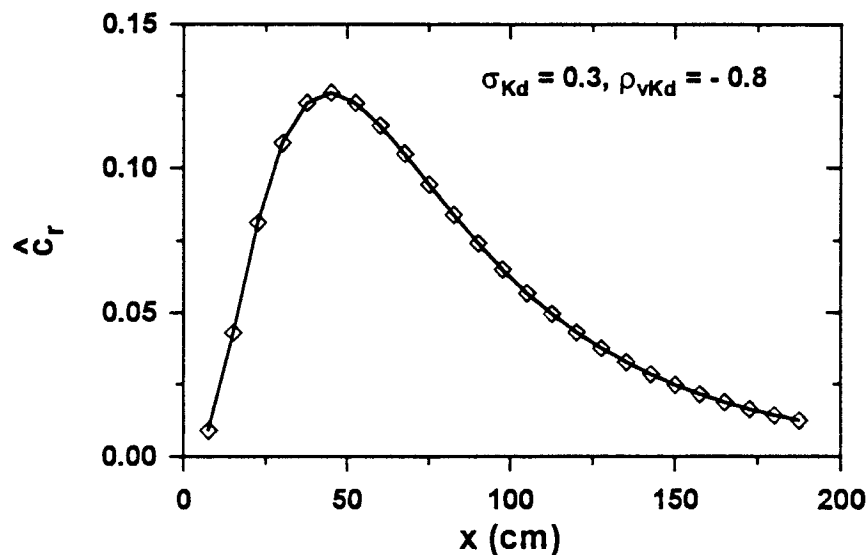
Fig. 7.15. Estimation of σ_{Kd} and ρ_{vKd}, by fitting the solution for the stream tube model to hypothetical data, generated with a stochastic v and K_d, assuming that $<v>$, σ_v, and $<K_d>$ are known.

107

8. SUMMARY AND CONCLUSIONS

The CXTFIT 2.0 program provides a convenient way of solving direct and inverse problems for one-dimensional solute transport during steady water flow. Both equilibrium and two-site/two-region type nonequilibrium transport models can be implemented — the transport equation contains terms for convection, dispersion, linear adsorption, zero-order production, and first-order decay. Analytical solutions for deterministic transport were given for a large number of boundary, initial, and production value problems. CXTFIT 2.0 also includes a stochastic transport model that views the field as an assembly of deterministic flow and transport paths; these are referred to as stream tubes for one-dimensional flow and transport. Transport in each stream tube is modeled deterministically with the convection-dispersion equation using as random parameters v and either D, K_d, or a. The random parameters are described with a bivariate lognormal probability density function. Solute concentrations across the field, in either the resident or flux-averaged mode, were obtained by averaging the concentrations of individual stream tubes.

Various transport parameters in the deterministic and stochastic transport models can be estimated by CXTFIT 2.0 by fitting the pertinent analytical solution to solute (tracer) concentrations obtained in the laboratory or field. As discussed in Chapter 5, the estimation procedure uses a nonlinear least-squares inversion method according to *Marquardt* [1963]. While the procedure has been shown to work for many examples, users should remain cognizant of potential problems involving convergence and parameter uniqueness. This is especially true when the stream tube model is used for optimizing data obtained across the field. Chapter 6 contains a detailed and schematic outline of the settings and variables for each solution of the direct or inverse problem in CXTFIT 2.0. The use of the program is further illustrated in Chapter 7, which contains a variety examples regarding the prediction of solute profiles and the analysis of experimental data to estimate parameters in deterministic and stochastic solute transport models.

9. REFERENCES

Abramowitz, M., and I. A. Stegun, *Handbook of Mathematical Functions*, Dover Publishing Co., New York, 1970.

Aharoni, C., and D. L. Sparks, Rates of Soil Chemical Processes - A theoretical treatment, in *Rates of Soil Chemical Processes*, edited by D. L. Sparks and D. L. Suarez, Special Publ. No. 27, pp. 281-302, Soil Sci. Soc. Am., Madison, WI, 1991.

Aitcheson, J., and J. A. C. Brown, *The lognormal distribution*, Cambridge University Press. London, 1963.

Bellin, A., A., Rinaldo, W. J. Bosma, S. E. A. T. M. van der Zee, and Y. Rubin, Linear equilibrium adsorbing solute transport in physically and chemically heterogeneous porous formations 1. Analytical solutions. *Water Resour. Res.*, *29*, 4019-4030, 1993.

Biggar, J. W., and D. R. Nielsen, Spatial variability of the leaching characteristics of a field soil. *Water Resour. Res.*, *12*, 78-84, 1976.

Bosma, W. J. P., A. Bellin, S. E. A. T. M. van der Zee, and A. Rinaldo, Linear equilibrium adsorbing solute transport in physically and chemically heterogeneous porous formations 2. Numerical results, *Water Resour. Res.*, *29*, 4031-4043, 1993.

Bresler, E., and G. Dagan, Solute dispersion in unsaturated heterogeneous soil at field scale: II. Applications, *Soil Sci. Soc. Am. J.*, *43*, 467-472, 1979.

Bresler, E., and G. Dagan, Convective and pore scale dispersive solute transport in unsaturated heterogeneous fields, *Water Resour. Res.*, *17*, 1683-1693, 1981.

Burr, D. T., E. A. Sudicky, and R. L. Naff, Nonreactive and reactive solute transport in three-dimensional heterogeneous porous media: Mean displacement, plume spreading, and uncertainty, *Water Resour. Res.*, *30*, 791-815, 1994.

Cameron, D. A., and A. Klute, Convective-dispersive solute transport with a combined equilibrium and kinetic adsorption model, *Water Resour. Res.*, *19*, 718-724, 1977.

Carnahan, B., H. A. Luther, and J.O. Wilkes, *Applied Numerical Methods*, John Wiley & Sons, Inc., New York, 1969.

Coats, K. H., and B. D. Smith, Dead-end pore volume and dispersion in porous media, *Soc. Petrol. Eng. J.,* 4, 73-84, 1964.

Dagan, G., Solute transport in heterogeneous porous formations, *J. Fluid Mech., 14.5,* 15 l-177, 1984.

Dagan, G., *Flow and Transport in Porous Formations,* Springer Verlag, Berlin, 1989.

Dagan, G., The Bresler-Dagan model of flow and transport: Recent theoretical developments, in *Water flow and solute transport in soils,* edited by D. Russo and G. Dagan, Springer-Verlag, Berlin, Heidelberg, 1993

Dagan, G., and E. Bresler, Solute dispersion in unsaturated heterogeneous soil at field scale: I. Theory, *Soil Sci. Soc. Am. J., 43, 461-467,* 1979.

Dagan, G., and V. Cvetkovic, Spatial moments of a kinetically sorbing solute plume in a heterogeneous aquifer, *Water Resow. Res., 29,4053-406* 1, 1993.

Danckwerts, P. V., Continuous flow systems, *Chem. Eng. Sci., 2, 1-13,* 1953.

de Marsily, G., *Quantitative Hydrogeology,* Academic Press, San Diego, 1986.

De Smedt, F., and P. J. Wierenga, A generalized solution for solute flow in soils with mobile and immobile water, *Water Resour. Res., 15,* 1137-l 141, 1979.

Destouni, G., and V. Cvetkovic, Field scale mass arrival of sorptive solute into the groundwater, *Water Resour. Res., 27, 13151325,* 1991.

Farlow, S. J., *Partial Differential Equations for Scientists and Engineers,* John Wiley & Sons, New York 1982.

Goldstein S., On the mathematics of exchange processes in fixed columns. I. Mathematical solutions and asymptotic expansions, *Proc. Roy. Soc. London., 219,* 151-185, 1953.

Jury, W. A, Simulation of solute transport using a transfer function model, *Water Resour. Res., 18, 363-368,* 1982.

Jury, W. A., and H. Flühler, Transport of chemicals through soils: Mechanism, model, and field applications, *Advances in Agronomy, 47, 14 l-20 1,* 1992.

Jury, W. A., and K. Roth., *Transfer Functions and Solute Movement through Soils: Theory and Applications,* Birkhauser, Basel, Switzerland, 1990.

Jury, W. A., L. H. Stolzy, and P. Shouse, A field test of a transfer function model for predicting solute transport, Wafer *Resour. Res.*, 18, 369-375, 1982.

Jury, W. A, and D. R Scotter, A unified approach to stochastic-convective transport problems, *Soil Sci. Soc.* Am. *J., 58.,* 1327-1336, 1994.

Kabala, Z. J., and G. Sposito, A stochastic model of reactive solute transport with time-varying velocity in a heterogeneous aquifer, *Water Resow. Res.,* 27, 341-350, 1991.

Kool, J. B., and J. C. Parker, Analysis of the inverse problem for transient unsaturated flow, *Water Resow. Res.,* 24, 817-830, 1988.

Kreft, A., and A. Zuber, On the physical meaning of the dispersion equation and its solutions for different initial and boundary conditions, *Chem.* Eng. *Sci.,* 33, 1471-1480, 1978.

Leij, F. J., N. Toride, and M. Th. van Genuchten, Analytical solutions for non-equilibrium solute transport in three-dimensional porous media, *J. Hydrol., 151,* 193-228, 1993.

Lindstrom, F. T., Pulsed dispersion of trace chemical concentration in saturated sorbing porous medium, *Water Resow. Res., 12,229-238, 1976.*

Lindstrom, F. T., and L. Boersma, Analytical solutions for convective-dispersive transport in confined aquifers with diierent initial and boundary conditions. *Water Resow. Res.,* 25, 241-255, 1989.

Lindstrom, F. T., and M. N. L. Narasimhan, Mathematical theory of a kinetic model for dispersion of previously distributed chemicals in a sorbing porous medium, *SIAM J. Appl. Math., 24, 496-5* 10, 1973.

Lindstrom, F. T., and W. M. Stone, On the start up or initial phase of linear mass transport of chemicals in a water saturated sorbing porous medium: l., *SIAM J. Appl. Math., 26, 578-591,* 1974.

Mailants, D., M. Vanclooster, M. Meddahi, and J. Feyen, Estimating solute transport parameters on undisturbed soil using time domain reflectometry, J. *Cont. Hydrol., 17,* 91-109, 1994.

Marquardt, D. W., An algorithm for least-squares estimation of nonlinear parameters, J. *Soc. Ind. Appl. Math., II, 431-441,* 1963.

Meeter, D. A, Non-linear least-squares (Gaushaus), Univ. of Wisconsin Computing Center, Program Revised 1966.

Moyer, J. R., R. J. Haque, and C. E. McKone, The effect of adsorbents on the rate of degradation of herbicides incubated with soil, Soil *Biol. Biochem., 4, 307-3* 11, 1972.

Nielsen, D. R, M. Th. van Genuchten, and Biggar, J. W., Water flow and solute transport processes in the unsaturated zone, Water *Resour. Res., 22, 89S-108S, 1986.*

Nkedi-Kizza, P., J. W. Biggar, H. M. Selim, M. Th. van Genuchten, P. J. Wierenga, J. M. Davidson, and D. R Nielsen, On the equivalence of two conceptual models for describing ion exchange during transport through an aggregated oxisol, Water *Resow. Res., 20, 1123-l 130,* 1984,

Olver, F. W. J., Bessel functions of integer order, in Abramowitz, M. and I. A. Stegun, *Handbook of Mathematical Functions,* Dover Publishing Co., New York, 355-433, 1965.

Ogram, A V., R E. Jessup, L.T. Ou, and P. S. C. Rao, Effects of sorption on biological degradation rates of (2,4-dichlorophenoxy) acetic acid in soil, *Appl. Environ. Microbiol., 49, 582-587,* 1985.

Parker, J.C., and M. Th. van Genuchten, Flux-averaged and volume-averaged concentrations in continuum approaches to solute transport, *Water Resow. Rex, 20, 866-872,* 1984a.

Parker, J. C., and M. Th. van Genuchten., Determining transport parameters from laboratory and field tracer experiments, *Bull. 84-3, Va. Agric. Exp. St.,* Blacksburg, 1984b.

Parker, J.C., and A. J. Valocchi, Constraints on the validity of equilibrium and first-order kinetic transport models in structured soils, *Water Resow. Res., 22, 399-407,* 1986.

Parlange, J. -Y., J. L. Starr, M. Th. van Genuchten, D. A. Barry, and J. C. Parker, Exit condition for miscible displacement experiments, *Soil Sci.,* 153, 165- 17 1,1992.

Press, W.H., B.P. Flannery, S.A. Teukolsky, and W.T. Vetterling, *Numerical Recipes: The Art of Scientific Computing,* 2nd ed., Cambridge University Press, New York, 1992.

Rao, P. S. C., D. E. Rolston, R. E. Jessup, and J. M. Davidson, Solute transport in aggregated porous media. Theoretical and experimental evaluation, *Soil Sci. Soc. Am. J., 44,* 1139-1146, 1980.

Robin M. J. L., E. A Sudicky, R W. Gillham, and R. G. Kachanoski, Spatial variability of Strontium distribution coefficients and their correlation with hydraulic conductivity in the Canadian forces base Borden aquifer, *Water Resour. Res., 27,2619-2632,* 1991.

Selim, H. M., J. M. Davidson, and R. S. Mansell, Evaluation of a two-site adsorption-desorption model for describing solute transport in soils, In *Proc. Summer Computer Simulation Conf.,* Washington, D.C., 1976.

Spiegel, M. R., *Schaum's outline of theory and problems of probability and statistics,* Schaum's outline series, McGraw-Hill, New York, 1992.

Sposito G., and D. A Barry, On the Dagan model of solute transport in groundwater: Foundational aspects, *Water Resow. Res., 23, 1867-1875,* 1987.

Sudicky, E. A, A natural gradient experiment on solute transport in a sand aquifer: Spatial variability of hydraulic conductivity and its role in the dispersion process. *Water Resour..Res., 22, 2069-2082,* 1986.

Toride, N., and F. J. Leij, Stochastic stream tube model for field-scale solute transport: I. Theory, *Soil Sci. Soc. Am. J.,* 1995a. (Submitted)

Toride, N., and F. J. Leij, Stochastic stream tube model for field-scale solute transport: II. Applications, *Soil Sci. Soc. Am. J.,* 1995b. (Submitted)

Toride, N., F. J. Leij, and M. Th. van Genuchten, A comprehensive set of analytical solutions for nonequilibrium solute transport with first-order decay and zero-order production, *Water Resour. Res., 29, 2167-2182,* 1993a.

Toride, N., F. J. Leij, and M. Th. van Genuchten, Flux-averaged concentrations for transport in soils having nonuniform initial solute distributions, *Soil Sci. Soc. Am., 57,* 1406- 1409, 1993b.

van der Zee, S. E. A. T. M., and W. H. van Riemsdijk, Transport of phosphate in a heterogeneous field, *Transport Porous Media, I, 339-359, 1986.*

van der Zee, S. E. A. T. M., and W. H. van Riemsdijk, Transport of reactive solute in spatially variable soil systems, *Water Resour. Res., 23,2059-2069,* 1987.

van Genuchten, M. Th., Mass transfer studies in sorbing porous media, Ph.D thesis, New Mexico State Univ., Las Cruces, 1974.

van Genuchten, M. Th., Analytical soiutions for chemical transport with simultaneous adsorption, zero-order production and first-order decay, J. *Hydrol.,* 49, 213-233, 1981a.

van Genuchten, M. Th, Non-equilibrium transport parameters from miscible displacement experiments, *Res. Rep. No.* 119, U. S. Salinity Lab., USDA, ARS, Riverside, CA, 198 lb.

van Genuchten, M. Th., and W. J. Alves, Analytical solutions of the one-dimensional convective-dispersive solute transport equation, *Tech. Bull. U. S. Dep. Agri., 1661, 1982.*

van Genuchten, M. Th., and J. C. Parker, Boundary conditions for displacement experiments through short laboratory soil columns, *Soil Sci. Soc. Am. J., 48,* 703-708, 1984.

van Genuchten, M. Th., and J. C. Parker, Reply to "Comments on 'Boundary conditions for displacement experiments through short laboratory soil columns'," *Soil Sci. Soc. Am. J.,* 58, 991-993, 1994.

van Genuchten, M. Th., and R J. Wagenet, Two-site/two-region models for pesticide transport and degradation: theoretical development and analytical solutions, *Soil Sci. Soc. Am. J.,* 53, 1303-13 10, 1989.

van Genuchten, M. Th., and P. J. Wierenga, Mass transfer studies in sorbing porous media, I, Analytical solutions, *Soil Sci. Soc. Am. J., 40,473-48* 1, 1976.

Weber, J. B., and H. D. Cole, Microbial decomposition of diquat adsorbed on montmorillonite and kaolinite clays, J. *Agric. Food Chem., 16, 475-478,* 1968.

Wehner, J. F., and R. H. Wilhelm, Boundary conditions of flow reactor, *Chem. Eng. Sci., 6, 89-93,* 1956.

APPENDIX: LIST OF SIGNIFICANT PROGRAM VARIABLES

Table A 1. List of Integer Variables

ICHEB	Integration code for Gauss Chebyshev. If ICHEB = 1, the number of integration points will increase until the result satisfies the error criterion (default is ICHEB = 1 in the subroutine **CONST1, blank** common).
ILMT	Parameter constraint code (Table 6.4).
ISKIP	Calculation control code for the evaluation of the integral limits; ISKlP = 0 to evaluate **the** limits; = l to skip evaluation (the subroutine **Model, MODAT** common).
INTM	Calculation control code for the numerical integration for the stochastic CDE in subroutine **STOCDE** (**INTM** = 1 for log-transformed Romberg; = 2 for log-transformed Gauss-Chebyshev, default is INTM = 1).
INVERSE	Calculation control code for direct and inverse problems (Table 6.3, **MODAT** common).
KP	File unit number.
MIT	Maximum number of iterations (Table 6.4, **MODAT** common).
MASS	Total mass estimation code (Table 6.4, **MODAT** common).
MASSST	Mass distribution index for the stochastic CDE (MODB = 1,3 in Table 6.7, BOUND common).
MAXTRY	Maximum number of trials to find new parameter values without a decrease in the SSQ (It is suggested that MAXTRY be in the range 10 to 50; smaller values may reduce the run time but no convergent solution may be found. Default is 50 in the subroutine **CONST1).**
MAXOB	Maximum number of data **(Main program).**
MCON	Calculation control code for concentrations (MCON = 0, Calculate equilibrium and nonequilibrium concentrations; = l only equilibrium; = 3 only nonequilibrium, blank common).
MCORR	Index for stochastic v and η defined in subroutine MODEL; MCORR = - 1 for perfect negative correlation between v and η, = 0 for uncorrelated v and η, = 1 for perfect positive correlation between v and η, = 2 for other correlation (STOCH common).
MDEG	Degradation estimation code for the nonequilibrium CDE (Table 6.4, MODAT common).
MM	Initial number of integration points for Gauss Chebyshev (default is 75 in subroutine **CONST1,** blank common).
MNEQ	Nonequilibrium model code (Table 6.4, MODAT common).
MODB	Boundary value problem code (Table 6.7, BOUND common).
MODC	Concentration mode (Table 6.3, blank common).
MODD	Index for a stochastic dispersion coefficient defined in subroutine CHECK; MODD = - 1, perfect negative correlation between v and D; = 0, deterministic D; = 1 perfect positive correlation; = 2, $\sigma_v = \sigma_D$, constant field-scale dispersivity (STOCH common)
MODE	Model code (Table 6.3, blank common).
MOD1	Initial value problem code (Table 6.8, INITI common).
MODJH	Calculation control code for step input in subroutine BOUND (MODJH = 0, evaluate (3.23) or (3.24); = 1, (3.21) or (3.22) based on Goldstein's J-function, default is MODJH = 1).
MODK	Index for a stochastic distribution coefficient defined in subroutine **CHECK;** MODK = - 2 for a. = σ_{Kd}; = - 1 for perfect negative correlation between v and K_d; = 0 for deterministic K_d; = 1 for perfect positive correlation **(STOCH** common).
MODP	Production value problem code (Table 6.9, PROD common).
MODP 1	Calculation control code for constant production for the equilibrium CDE in subroutine PRODUC (MODP1 = 0 to evaluate the integral in (2.32); = l for (2.33) or (2.34), default is MODPl= 1).

MPRINT	Output print code for direct problem (Table 6.11).
MPRO	Production function code for a nonequilibrium phase (Table 6.9).
MSD	Calculation control code for ensemble averages defined in subroutine STOCDE; MSD = 0, $<C>$; = 1, $<C^2>$, (STOCH common).
MSTOCH	Index for stochastic v and η defined in subroutine MODEL; MSTOCH = 1 for variable v and deterministic η, = 2 for deterministic v and variable η, = 3 for perfect correlation behveen v and η, = 4 for variable v and variable η (STOCH common).
NC	Number of cases considered (Table 6.3, Main **program).**
NERR	Number of errors in an input file (subroutine CHECK).
NINI	Number of steps for stepwise initial distribution (Table 6.8, INITI common).
NIT	Number of iteration trials in the least square analysis **(Main program).**
NOB	Number of observations (cannot exceed MAXOB).
NP	Number of parameters to be fitted to the data (Main **program).**
NPRO1	Number of steps for stepwise production profile in an equilibrium phase (Table 6.9, PROD common).
NPRO2	Number of steps for stepwise production profile in an nonequilibrium phase (Table 6.9, PROD common).
NPULSE	Number of pulses for multiple pulse input (Table 6.7, BOUND common).
NREDU	Data input and output code (Table 6.3, MODAT common).
NT	Number of output times for a direct problem (Table 6.11).
NTP	Number of transport parameters (subroutine DATAIN).
NTRIAL	Number of trials to decrease SSQ **(Main program).**
NU1	Value of NVAR + 1 **(Main program,** subroutine DATAIN).
NU2	Value of NVAR × 2 **(Main program,** subroutine DATAIN).
NVAR	Total number of parameters (subroutine DATAIN, MODAT common).
NZ	Number of output positions for a direct problem (Table 6.11).

A or AA	$\omega^2/(\omega+\mu_2)\beta R$ defined in subroutine **DETCDE** (blank common).
AVEV	Mean pore-water velocity, $<v>$ (subroutine **CONPROV**).
ALPHA	First-order kinetic rate coefficient, α (**STOCH** common).
ANGLE	Deviation of the correction vector from the steepest descent direction (**Main program**).
B or BB	$(\omega+\mu_2)/(1-\beta)R$ defined in subroutine **DETCDE** (blank common).
BETA	Partition coefficient, β (blank common).
BETR	Value of $\beta \times R$ (blank common).
BMASS	Mass for Dirac delta input (subroutine **BOUND**).
CBOU1	Equilibrium concentration for boundary value problem (subroutine **DETCDE**).
CBOU2	Nonequilibrium concentration for boundary value problem (subroutine **DETCDE**).
CINT1	Equilibrium concentration for initial value problem (subroutine **DETCDE**).
CINT2	Nonequilibrium concentration for initial value problem (subroutine **DETCDE**).
CORR	Correlation coefficient between v and η for stochastic model, $\rho_{v\eta}$ (**STOCH** common).
CPRO1	Equilibrium concentration for production value problem (subroutine **DETCDE**).
CPRO2	Nonequilibrium concentration for production value problem (subroutine **DETCDE**).
CX	$\omega/(\omega+\mu_2)$ defined in subroutine **DETCDE** (blank common).
D or DIS	Dispersion coefficient, D (STOCH common).
DA	$\omega\mu_2/(\omega+\mu_2)$ defined in subroutine **DETCDE** (blank common).
DK	Distribution coefficient for liner adsorption, K_d (STOCH common).
DMASS	Mass for a Dirac delta initial condition (subroutine **INITIAL**).
DMU1	First-order decay coefficient in an equilibrium phase, μ^E or μ_1, (blank common).
DMU2	First-order decay coefficient in a nonequilibrium phase, μ_2, (blank common).
DT	Time increment for output in a direct problem.
DUMTZ	Time or position for the solute profile or breakthrough for INPUTM = 1 in an inverse problem (Table 6.10).
DZ	Spatial increment for output in a direct problem.
GA	Constant for the Levenberg-Marquardt method (default is 0.01 in subroutine **CONST1**).
GD	Trial and error factor for GA for the Levenberg-Marquardt method (default is 10 in subroutine **CONST1**).
LEVEL	The maximum order for the log-transformed Romberg integration (the value will be adjusted internally depending on the Peclet number in subroutine **CONST2**, blank common).
OMEGA	Mass transfer coefficient, ω (blank common).
OMMAX	Maximum constraint for ω (default is 100 in subroutine **CONST1**).
P or PEC	Peclet number (blank common).
R or RE	Retardation factor (blank common).
PHIIM	Immobile water fraction for the physical nonequilibrium CDE, θ_{im}/θ (**MODAT** common).
PHIM	Mobile water fraction for the physical nonequilibrium CDE, $\phi_m = \theta_m/\theta$ (Table 6.4, **MODAT** common).
RHOTH	ρ_b/θ for the stochastic CDE (**STOCH** common).
SDLND	Standard deviation of ln D, σ_D (**STOCH** common).
SDLNV	Standard deviation of ln v, σ_v (**STOCH** common).
SDLNY	Standard deviation of ln η, σ_η (**STOCH** common).
SSQ	Sum of squared residuals (**Main program**).
STEP	Scale factor for the correction vector (**Main program**).
STOPCR	Iteration criterion. The curve-fitting process stops when the relative change in the ratio of all coefficients becomes less than STOPCR (default is 0.0005 in subroutine **CONST1**).

119

STOPER	Stop criterion for the log-transformed Romberg integration (inial setting is 5.E-8 and the value will be adjusted internally depending on the Peclet number in subroutine CONST2, blank common).
STSQ	Stop criterion for the iteration based on the improvement of SSQ. If the relative improvement in SSQ is less than STSQ continuously for three times, the iteration will stop (currently set to 1 .E-6 in subroutine CONST1).
TI	Initial value of output time for a direct problem.
TMAX	Modified upper integration limit for the solution for Dirac or step input (subroutine BOUND).
TMIN	Modified lower integration limit for the solution for Dirac or step input (subroutine BOUND).
TT	Time for the calculation (blank common).
V	Pore-water velocity, v (STOCH common).
XLNM	Mean of logtransformed variables in lognormal distribution (subroutine LIMIT).
XMOD	Mode for a lognormal distribution (subroutine LIMIT).
VMAX	Upper integration limit for v evaluated by subroutine LIMIT (STOCH common).
VMIN	Lower integration limit for v evaluated by subroutine LIMIT (STOCH common).
YMAX	Upper integration limit for η evaluated by subroutine LIMIT (STOCH common).
YMIN	Lower integration limit for η evaluated by subroutine LIMIT (STOCH common).
ZI	Initial value of output position for direct problem.
ZL	Characteristic length for dimensionless parameters (Table 6.3, MODAT common).
ZZ	Position for the calculation (blank common).

A(15,15)	Scaled matrix of D(15,15) (Main **program).**
B(30)	Initial values for each coefficient (Table 6.5,6.6).
BI(15)	Coefficient names.
INDEX(15)	Parameter estimation index (Table 6.5, **MODAT** common).
BMAX(15)	Maximum constraints for parameter estimation (Table 6.5).
BMIN(l5)	Minimum constraints for parameter estimation (Table 6.5).
C(MAXOB)	Observed concentrations for inverse problem (Table 6.10).
C 1 (MAXOB)	Equilibrium concentrations.
C2(MAXOB)	Nonequilibrium concentrations.
CINI(l0)	Concentration constants for IVP (Table 6.8, INITI common).
D(15,15)	Terms defined by (5.26) **(Main program).**
DERL(30)	**Constants** for evaluating derivatives given by (5.29) (currently set to 1.D-2 for all parameters in subroutine **CONST1).**
GAMMA1(10)	Production constants in equilibrium phase (Table 6.9, **PROD** common).
GAMMA2(10)	Production constants in nonequilibrium phase (Table 6.9, **PROD** common).
P(l5)	Correction vector for parameter estimation **(Main program).**
PHI(15)	Scaled vector of Q(15) **(Main program).**
PULSE(10)	Concentration constants for BVP (Table 6.7, **BOUND** common).
Q(15)	Terms defined by (5.27) **(Main program).**
T(MAXOB)	Times.
TPULSE(l0)	Time constants for BVP (Table 6.7, **BOUND** common).
VARl (MAXOB)	Variances for equilibrium concentrations.
VAR2(MAXOB)	Variances for nonequilibrium concentrations.
Z(MAXOB)	Positions.
ZINI(10)	Position constants for IVP (Table 6.8, INITI common).
ZPROl(10)	Position constants in equilibrium phase for the PVP (Table 6.9, **PROD** common).
ZPR02(10)	Position constants in nonequilibrium phase for the PVP (Table 6.9, **PROD** common).